



รายงานการวิจัย

การศึกษาอะตอมเอ็กโซติก โดยวิธีทางฟังก์ชันสเตอร์เมียน

(Study of Exotic Atoms in Sturmian Function Approach)



ได้รับทุนอุดหนุนการวิจัยจาก

มหาวิทยาลัยเทคโนโลยีสุรนารี

ผลงานวิจัยเป็นความรับผิดชอบของหัวหน้าโครงการวิจัยแต่เพียงผู้เดียว



รายงานการวิจัย

การศึกษาอะตอมเอ็กโซติก โดยวิธีทางฟังก์ชันสเตอร์เมียน (Study of Exotic Atoms in Sturmian Function Approach)

คณะผู้วิจัย

ผู้อำนวยการชุดโครงการ
ศาสตราจารย์ ดร. ประสพ สืบคำ
สาขาวิชาฟิสิกส์
สำนักวิชาวิทยาศาสตร์
มหาวิทยาลัยเทคโนโลยีสุรนารี

ผู้ร่วมวิจัย

ผู้ช่วยศาสตราจารย์ ดร. ชินรัตน์ กอบเดช
ศาสตราจารย์ ดร. ยูเป็ง แขน

ได้รับทุนอุดหนุนการวิจัยจากมหาวิทยาลัยเทคโนโลยีสุรนารี ปีงบประมาณ พ.ศ.
2548-2550

ผลงานวิจัยเป็นความรับผิดชอบของหัวหน้าโครงการวิจัยแต่เพียงผู้เดียว

สิงหาคม 2554



Study of Exotic Atoms in Sturmian Function Approach

Researchers

Head of project

Prof. Dr. Prasart Suebka

School of Physics

Institute of Science

Suranaree University of Technology

Members

Asst. Prof. Dr. Chinorat Kobdaj

Prof. Dr. Yupeng Yan

This work was supported by Suranaree University of Technology in fiscal year

2548-2550

August 2554

ACKNOWLEDGEMENTS

This work was supported by Suranaree University of Technology under Grant Nos. SUT1-105-48-36-10, SUT1-105-48-36-11 and SUT1-105-48-36-12. The authors would like to thank Mr. Chakrit Nualchimplee, Mr. Wanchaloem Poonsawat and Miss Rintarn Saengsai for their research in this project. We wish to thank Dr. Ayut Limphirat for his consistent help.



บทคัดย่อ

ชุดโครงการวิจัยนี้ประสบความสำเร็จในการศึกษาอะตอม pD พายออนเนียม และเคออนิกไฮโดรเจน โดยวิธีทางฟังก์ชันสแตรเมียน กล่าวคือคำนวณพลังงานยึดเหนี่ยว ความกว้างการสลายตัวและโดยเฉพาะฟังก์ชันคลื่นได้อย่างแม่นยำ รายละเอียดดังนี้

งานวิจัยในส่วนของอะตอม pD ได้ทำการคำนวณการเลื่อนพลังงานและความกว้างการสลายตัวของอะตอม pD ที่สถานะ $1s$ และ $2p$ ด้วยศักย์แบบ \overline{NN} และได้ผลสอดคล้องกับการทดลองเป็นอย่างดี ยกเว้นการเลื่อนพลังงานของสถานะ $2p$ ซึ่งผลการทดลองแสดงถึงระดับพลังงานเฉลี่ยเลื่อนขึ้นเนื่องจากผลของอันตรกิริยาอย่างแรงเช่นเดียวกับสถานะ $1s$ แต่ผลการคำนวณที่ได้พบว่าระดับพลังงานเฉลี่ยมีการเลื่อนลง ซึ่งหมายถึงผลของอันตรกิริยาอย่างแรงของ \overline{NN} ส่งผลกระทบต่อการศึกษาการเลื่อนพลังงานของสถานะ $2p$ นั่นคืออะตอม pD จะเป็นเครื่องมือที่สำคัญที่ช่วยปรับแต่งศักย์แบบ \overline{NN} โดยเฉพาะที่พลังงานศูนย์

งานวิจัยในส่วนของพายออนเนียม ได้ทำการศึกษาในอันตรกิริยาอย่างแรงหลากหลายรูปแบบ พบว่าอันตรกิริยาในแบบจำลองการแลกเปลี่ยนเมซอนชนิด ϵ ที่ควบคุมแบบสเกลาร์ ไม่เหมาะสมกับระบบพายออนเนียม ซึ่งมีลักษณะเฉพาะต่อการควบคุมแบบเกรเดียนต์ของการแลกเปลี่ยนเมซอนชนิด ϵ และควบคุมอย่างอ่อนต่อการแลกเปลี่ยนเมซอนชนิด ρ ใน t -channel ทั้งนี้อาจจะใช้ศักย์พายออน-พายออนจากทฤษฎีไครเรลเพอร์เทอร์เบชันซึ่งสามารถให้ผลคำนวณสอดคล้องกับการทดลองการกระเจิงของพายออนกับพายออนและพายออนเนียม และสามารถประยุกต์ใช้กับระบบสหพายออนเช่นแก๊สพายออนที่เกิดจากการชนของไอออนหนักที่พลังงานสูง

สำหรับงานวิจัยในส่วนของเคออนิกไฮโดรเจน ได้ทำการคำนวณการเลื่อนพลังงาน ความกว้างการสลายตัวและฟังก์ชันคลื่นของเคออนิกไฮโดรเจนโดยใช้ศักย์ในหลากหลายรูปแบบ พบว่าผลการคำนวณความกว้างการสลายตัวด้วยศักย์แบบ \overline{KN} เท่านั้นที่ใกล้เคียงกับการทดลอง DEAR อย่างไรก็ตามก็ตีผลการคำนวณด้วยศักย์แบบ \overline{KN} เพียงอย่างเดียว และผลการคำนวณด้วยศักย์ที่มีพื้นฐานจากสมมาตรไครเรล $SU(3)$ ต่างใกล้เคียงกับการทดลองของ KEK ทั้งนี้ผลการทดลองของ DEAR และ KEK ค่อนข้างขัดแย้งกัน จึงเป็นเรื่องยากที่จะระบุศักย์ที่เหมาะสมได้ ซึ่งต้องรอผลการทดลองของการทดลอง SIDDHARTA ที่จะให้ผลการตรวจวัดเคออนิกไฮโดรเจนที่แม่นยำกว่านี้

ABSTRACT IN ENGLISH

$\bar{p}D$ atoms, pionicium and kaonic hydrogen are successfully studied in the work in the Sturmian function approach, with binding energies, decay widths and especially wave functions evaluated accurately.

The energy shifts and decay widths of the $1s$ and $2p$ $\bar{p}D$ atomic states are calculated with $\bar{N}N$ potentials which reproduce $\bar{N}N$ scattering data well. Our theoretical predictions are not in line with experimental data for the energy shifts of the $2p$ $\bar{p}D$ atomic states. The experimental data show that the averaged energy level of the $2p$ $\bar{p}D$ atoms is pushed up by the strong interaction, the same as for the $1s$ $\bar{p}D$ atoms, but the theoretical results uniquely show the averaged energy level shifting down. The investigation of the $\bar{p}D$ atoms may provide a good platform for refining the $\bar{N}N$ interaction, especially at zero energy since the energy shifts of the $2p$ $\bar{p}D$ atomic states are very sensitive to the $\bar{N}N$ strong interactions.

The pionicium is studied in various strong interactions. It is found that the interaction in the meson-exchange model with the scalar coupling for the ε -exchange is unreasonably strong for the pionicium system. The pionicium system favors the gradient coupling for the ε -exchange, and demands a much weaker coupling for the t -channel ρ -exchange. A practical pion-pion potential may be derived from the chiral perturbation theory, which can reproduce both the pionicium and pion-pion scattering data and is applicable to other multi-pion systems, for example, the pion gas probably produced in high-energy heavy-ion collisions.

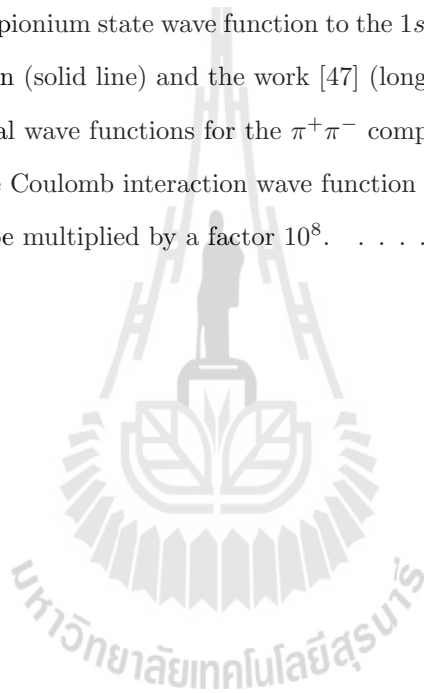
The energy shift, decay width and wave function of the kaonic hydrogen are evaluated with various potentials. We found that expect for the decay width derived the phenomenological $\bar{K}N$ potential, all other theoretical values are much larger than the DEAR data. However, the theoretical results for both the pure phenomenological potential and the chiral SU(3) symmetry based potentials are fairly consistent with the KEK measurements, considering the large error of the KEK values of the $1s$ kaonic hydrogen decay width. At this moment, however, it is difficult to conclude whether the equivalent potentials based on chiral SU(3) models are reasonable since the KEK and DEAR data are so inconsistent each other. One may have to wait for the more accurate measurement of the $1s$ kaonic hydrogen by the SIDDHARTA collaboration.

Contents

1	Introduction	1
2	Complete set of Sturmian Functions	3
3	Protonic Atoms	6
3.1	Dynamical Equation for $\bar{N}N$ Atomic States	8
3.2	$\bar{p}D$ interactions in terms of $\bar{N}N$ potentials	11
3.3	Energy shifts and decay widths of $\bar{p}D$ atoms	14
4	Pionium	17
4.1	Sturmian Function Method Applied to Pionium	18
4.2	Pionium in Realistic Interactions	20
5	Pionic and Kaonic Atoms	24
5.1	Dynamical Equations of K^-p System	25
5.2	Kaonic Hydrogen Atoms	31
6	Discussion and Conclusions	36
	Appendices	43
A	Curriculum Vitae	44
A.1	Prof. Dr. Prasart Suebka	44
A.2	Prof. Dr. Yupeng Yan	47
A.3	Asst. Prof. Dr. Chinorat Kobdaj	55
B	Publications	58

List of Figures

4.1	Ratios of the $1s$ ponium state wave function to the $1s$ hydrogen-like wave function in our calculation (solid line) and the work [47] (long-dashed line).	20
4.2	Squared $1s$ radial wave functions for the $\pi^+\pi^-$ component of ponium. For comparison the pure Coulomb interaction wave function is also plotted. All the wave functions have be multiplied by a factor 10^8	22



List of Tables

3.1	The energy shifts ΔE and decay widths of the $1s$ and $2p$ antiproton-deuteron atomic states in the approximation of undistorted deuteron core. The minus sign of the energy shifts means that the strong interaction is repulsive. The units are eV and meV for $1s$ and $2p$ states, respectively. Experimental data are taken from [25, 26].	15
4.1	Energy shift of the $1s$ ponium compared to the pure Coulomb interaction level. .	21
5.1	$1s$ kaonic hydrogen energy shift ΔE_{1s} (ΔE_{1s}^0) and decay width Γ_{1s} (Γ_{1s}^0) derived by directly solving eq. (5.21) with (without) the mass difference between the K^-p and \bar{K}^0n states considered.	32
5.2	K^-p scattering lengths a_{K^-p} derived with local single-channel potentials [75, 76] compared with the K^-p scattering lengths \tilde{a}_{K^-p} (taken from [74, 76]) derived with the multi-channel effective interactions [59, 60, 64, 66, 74].	34

Chapter 1

Introduction

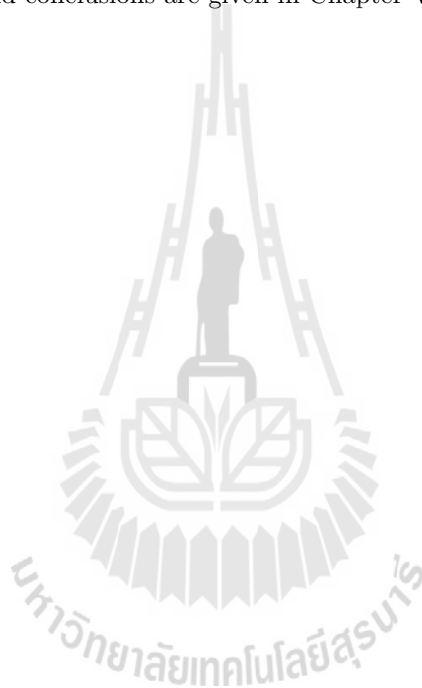
Exotic atoms are Coulomb bound states which do not exist in the nature but produced in laboratory. Among them are, for example, positronium (electron-positron bound states), protonium (proton-antiproton atomic states), pionium (pion-pion atomic states), muonic atoms (muon-nucleus atomic states), pionic atoms (pion-nucleus atomic states), and kaonic atoms (kaon-nucleus atomic states). The investigation of exotic atoms has opened up new windows in nuclear and particle physics. These atomic states allow one to study the interference of QED and QCD on the one hand, and the strong interaction (QCD) at zero-energy, with unprecedented sensitivity, on the other hand. In the last three decades muonic and pionic atoms have been the focus of much theoretical and experimental efforts at various pion factories such as LAMPF, PSI, and TRIUMF. The investigation of antiprotonic atoms, pionium and kaonic atoms has recently become of particular interest as more and more experimental data have been getting available.

In principle, one may solve an eigenstate problem through expanding the wave function in any complete set of orthonormal functions. The complete set of harmonic oscillator wave functions is widely applied to bound state problems since they have analytical forms both in coordinate and momentum spaces. Bound state problems with only the strong interaction or only the Coulomb force can be well solved in the regime of harmonic oscillator wave functions, by choosing the oscillator length being of order 1 fm or 100 fm, respectively. Detailed investigations [1], however, have shown that the harmonic oscillator wave function approach fails to describe $\bar{N}N$ atomic states which are dominated by the long-ranged Coulomb force and influenced by the short-ranged strong interaction. The reason is that two very different oscillator lengths are involved to describe the $\bar{N}N$ deep bound state *and* the atomic state.

The $\bar{N}N$ atomic problem was studied accurately in Ref. [2] the first time, employing the

Sturmian function approach, to account for both the strong *short* range nuclear potential (local and non-local) and the *long* range Coulomb force and provides directly the wave function of the protonium system and of the $\bar{N}N$ deep bound states with complex eigenvalues $E = E_R - i\frac{\Gamma}{2}$. In this work we employ the same numerical approach to investigate antiprotonic atoms, pionium and kaonic atoms.

The report is arranged as follows: In Chapter II we briefly discuss the main mathematical method, the Sturmian function approach which is applied to our evaluation of various exotic atoms. Antiprotonic atoms, pionium and kaonic atoms are respectively studied in Chapter III, IV, and V. Discussion and conclusions are given in Chapter VI.



Chapter 2

Complete set of Sturmian Functions

The Sturmian function method was first used in atomic physics to evaluate the binding energy and wave function of atoms [3, 4]. It was pointed out that the method is much more powerful than the approach using harmonic oscillator and hydrogen wave functions. Subsequently, the method was applied to various physical problems such as electromagnetic collisions [5], binding energies of nuclei [6, 7] and bound and resonant states in special potentials [8, 9]. The Sturmian functions are very similar to the hydrogen wave functions, and are, therefore, also named Coulomb-Sturmian functions. In coordinate space the Sturmians $S_{nl}(r)$, which are used in the present work, satisfy the second order differential equation [5]

$$\left(\frac{d^2}{dr^2} - \frac{l(l+1)}{r^2} + \frac{2b(n+l+1)}{r} - b^2 \right) S_{nl}(r) = 0. \quad (2.1)$$

By solving Eq. (2.1), one finds

$$S_{nl}(r) = \left[\frac{n!}{(n+2l+1)!} \right]^{\frac{1}{2}} (2br)^{l+1} \exp(-br) L_n^{2l+1}(2br), \quad (2.2)$$

where $L_n^{2l+1}(x)$ are associated Laguerre polynomials defined as

$$L_n^k(x) = (-1)^k \frac{d^k}{dx^k} [L_{n+k}(x)] \quad (2.3)$$

that is

$$L_n^{2l+1}(x) = \sum_{m=0}^n (-1)^m \frac{(n+2l+1)!}{(n-m)!(2l+1+m)!m!} x^m \quad (2.4)$$

The Sturmians are orthogonal and form a complete set with respect to the weight function $1/r$, which follows from the corresponding $1/r$ potential term in Eq. (2.1),

$$\int_0^\infty r^2 dr \frac{S_{nl}(r)}{r} \frac{1}{r} \frac{S_{n'l}(r)}{r} = \delta_{nn'}. \quad (2.5)$$

Thus radial functions $R_l(r)$ can be expanded in the complete set of the Sturmian functions $S_{nl}(r)$,

$$R_l(r) = \sum_n a_{nl} \frac{S_{nl}(r)}{r}. \quad (2.6)$$

The Sturmian functions can be defined in momentum space as

$$\begin{aligned} S_{nlm}(\vec{p}) &\equiv S_{nl}(p) Y_{lm}(\theta_p, \phi_p) \\ &= \frac{1}{(2\pi)^{3/2}} \int dr d\Omega S_{nl}(r) Y_{lm}(\theta, \phi) e^{-i\vec{p}\cdot\vec{r}} \end{aligned} \quad (2.7)$$

One can derive the momentum form analytically

$$\begin{aligned} S_{nl}(p) &= \left[\frac{2^{4l+3} (n+l+1) n! (l!)^2}{b (n+2l+1)!} \right]^{1/2} \\ &\cdot \frac{(p/b)^l}{[(p/b)^2+1]^{l+1}} C_n^{l+1} \left(\frac{(p/b)^2-1}{(p/b)^2+1} \right) \end{aligned} \quad (2.8)$$

where $C_t^s(x)$ are the Gegenbauer polynomials.

As the Sturmians have analytical forms in momentum space, one is allowed to deal with strong interactions in momentum space with the complete set of the Sturmians as easily as with the set of the harmonic oscillator wave functions. The matrix elements of the Coulomb interaction as well as the kinetic term can be evaluated analytically according to Eq. (2.1) and Eq. (2.5).

Because almost all bound-state hydrogenic wave functions are close to zero energy, the innermost zeros of the functions are insensitive to the principle quantum number. This accounts for that the bound hydrogen functions do not form a complete set; the continuum is needed to analyze the region between the origin and the limiting first zero. Unlike hydrogen functions, the first node of the Sturmian functions continues to move closer to the origin with increasing the principle number n . This is the key point why a short-ranged nuclear force can easily be taken

into account for exotic atom problems by using complete sets of the Sturmian functions.

The parameter b is the length scale entering the Sturmian functions in eqs. (2.1) and (2.2), in the same way as the corresponding parameter enters the harmonic oscillator functions. For $\bar{N}N$ (nucleon-antinucleon) deep bound states, for example, one should use $1/b$ of order 1 fm while the atomic states without strong interactions require $1/b$ of order 10^2 fm. However, for protonium accounting for both the strong interaction and the Coulomb force, one must use a $1/b$ between the two values used for the above cases. Using a complete basis of, for example, 200 Sturmian functions (100 for the $L = J - 1$ wave, and another 100 for the $L = J + 1$) with $1/b = 5 - 500$ fm, one can precisely reproduce the analytical $1s$ and $2p$ wave functions of the $\bar{N}N$ system subject to only the Coulomb interaction. Using the same basis with $1/b = 0.1 - 30$ fm, the wave functions of $\bar{N}N$ deep bound states can be precisely evaluated. The $\bar{N}N$ deep bound states can be evaluated in the complete set of the harmonic oscillator wave functions, and also in the complete set of Sturmian functions with a more suitable length parameter, for example $1/b = 1$ fm. It is found that a length parameter $1/b$ around 20 fm is suitable for the protonium problem.

We have compared our numerical method with the traditionally used method, namely the Numerov approach [10], applied to the $\bar{N}N$ atomic problem in for example the Kohno-Weise potential. The binding energies and widths presented in Ref. [10] for the states 1S_0 , 3P_0 , 3S_1 and 3SD_1 are well reproduced in the Sturmian function approach. Wave functions for these states are also compared in the two approaches. It is found that at short distance the outputs in the two approaches are quite consistent, and that the discrepancies between the wave functions evaluated in the two methods become more and more obvious as the relative distance between nucleon and antinucleon increases, especially the imaginary part of the 1S_0 and 3S_1 wave functions.

Finally, it should be pointed out that the Numerov method can not be applied to a non-local potential, for example the Bonn potential which is given in momentum space, and it is not easy to handle atomic states with higher angular momentum [11], for example the state 3PF_2 . Therefore it is essential to use a precise numerical method, applied not only to local but also to non-local potentials, to handle the $\bar{N}N$ atomic state problem from a more general point of view. In principle, there is no limit to the accuracy in the evaluation of the $\bar{N}N$ atomic states in the Sturmian function approach. One is allowed to use larger and larger complete bases of the Sturmian functions until the theoretical results converge. And the $\bar{N}N$ atomic states with higher angular momenta can be easily handled in the approach.

Chapter 3

Protonic Atoms

The simplest antiprotonic atom is the antiprotonic hydrogen atom known as protonium. In recent years several experiments have been carried out at the low-energy antiproton ring LEAR at CERN to study the properties of protonium. In these experiments low energetic antiprotons are captured into the Coulomb field of the proton via Auger electron emission, after deceleration to a kinetic energy of a few eV [12]. In the case of hydrogen, \bar{p} are captured into orbits of $n_{\bar{p}} \approx 40$ and cascade rapidly to the $1s$ and $2p$ levels (by X-ray emission), from which the $\bar{p}p$ system annihilates mostly into multi-meson final states (occasionally those multi-meson states are observed to be correlated via πf_2 , $\pi\pi f_2$ etc). The strong interaction shifts the Coulombic binding energies of the $1s$ and $2p$ states and adds a finite width describing the annihilation from this state. For a $\bar{p}p$ atom the purely Coulombic $1s$ Bohr radius is calculated to be 57.6 fm with a binding energy of $E_{1s} = 12.49$ keV. The electromagnetic energies for the Lyman $K_\alpha(2p \rightarrow 1s)$, Balmer $L_\alpha(3d \rightarrow 2p)$ and Paschen $M_\alpha(4f \rightarrow 3d)$ transitions have been calculated; they are 9.367, 1.735 and 0.607 keV, respectively. The strong interaction splits the $1s$ state into 1S_0 and 3S_1 , and the $2p$ state into 3P_0 , 3P_2 , 1P_1 and 3P_1 . In principle, these energy levels can be determined by measuring the emitted X-rays in the electromagnetic transitions. It is, however, extremely difficult to measure such small energy splittings (less than 0.5 keV). Therefore, the first experiments [13] delivered only spin-averaged data, since the experimental resolution was not sufficient to separate the transitions to the 1S_0 and 3S_1 levels. Recent measurements [14] at LEAR yielded the first information on the spin dependence of the $1s$ protonium energy shift and width.

Theoretical interest in the properties of protonium arose long before the first experiments were performed. Bryan and Phillips [15] first studied the scattering lengths of the $\bar{p}p$ annihilation

at rest in their model of $\bar{N}N$ interaction. From the scattering lengths, the energy shifts and widths of $\bar{N}N$ atoms can be derived via Truemans' formula [16]. Later, the energy shift and width of protonium states were investigated by other groups using the either original Truemans' formula [17, 18] or an improved Truemans' approach [19], or a WKB approximation [20] or an iteration technique which, however, neglected the $\bar{n}n$ component [21]. More accurate studies of the protonium properties were carried out in the matrix Numerov algorithm [10, 22]. All these theoretical predictions for the energy shifts and widths of protonium states are consistent with available experimental data. In order to quantitatively evaluate the photon and pion emission in the reaction of protonium decay to $\bar{N}N$ deep bound states, Dover *et al.* [23] explicitly worked out the wave function of the $\bar{N}N$ 1S_0 and 3S_1 atomic states in the Numerov approach. In their calculation, the coupling of the 3D_1 and 3S_1 states is neglected. Using the numerical method developed in Ref. [10], they recalculate, in a later work [24], the wave functions of $\bar{N}N$ atomic states with the tensor coupling included. However, the wave function of $\bar{N}N$ atomic states for non-local $\bar{N}N$ potentials has not yet been evaluated in an accurate numerical method which takes into account the two length scales involved, the $\bar{p}p$ and $\bar{n}n$ component coupling and the tensor coupling of the nuclear force.

The $\bar{N}N$ atomic problem was studied accurately in Ref. [2] the first time, employing the Sturmian function approach, to account for both the strong *short* range nuclear potential (local and non-local) and the *long* range Coulomb force and provides directly the wave function of the protonium system and of the $\bar{N}N$ deep bound states with complex eigenvalues $E = E_R - i\frac{\Gamma}{2}$.

The second simplest antiprotonic atom is the antiprotonic deuteron atom $\bar{p}D$, consisting of an antiproton and a deuteron bound mainly by the Coulomb interaction but distorted by the short range strong interaction. The study of the $\bar{p}D$ atom is much later and less successful than for other exotic atoms like the protonium and pionium. Experiments were carried out at LEAR just in very recent years to study the properties of the $\bar{p}D$ atom [25, 26]. Even prior to the experiments some theoretical works [27, 28, 29] had been carried out to study the $\bar{p}D$ atomic states in simplified $\bar{p}D$ interactions. Recently, a theoretical work [30] proposed a mechanism explaining the unexpected behavior, of the scattering lengths of $\bar{N}N$ and $\bar{p}D$ system, that the imaginary part of the scattering length does not increase with the size of the nucleus.

In the theoretical sector, one needs to overcome at least two difficulties in the study of the $\bar{p}D$ atom. First, the interaction between the antiproton and the deuteron core should be derived from realistic $\bar{N}N$ interactions, for example, the Paris $\bar{N}N$ potentials [31, 32, 33], the Dover-Richard $\bar{N}N$ potentials I (DR1) and II (DR2) [34, 35], and the Kohno-Weise $\bar{N}N$ potential

[36]. Even if a reliable $\bar{p}D$ interaction is in hands, the accurate evaluation of the energy shifts and decay widths (stemming for the strong $\bar{p}D$ interactions) and especially of the nuclear force distorted wave function of the atom is still a challenge. It should be pointed out that the methods employed in the works [27, 28, 29] are not accurate enough for evaluating the wave functions of the $\bar{p}D$ atoms.

3.1 Dynamical Equation for $\bar{N}N$ Atomic States

A correct treatment of $\bar{N}N$ atomic states must include the coupling of the proton-antiproton ($\bar{p}p$) and neutron-antineutron ($\bar{n}n$) configurations. We define the Hilbert spaces of proton-antiproton and neutron-antineutron as P_1 and P_2 spaces, respectively. The Hilbert space of two- and three-meson channels is defined as Q space. The corresponding projection operators P_1 , P_2 and Q satisfy the relation:

$$P_1 + P_2 + Q = 1, \quad (3.1)$$

$$P_1 P_2 = P_2 P_1 = 0, \quad (3.2)$$

$$P_1 Q = Q P_1 = 0, \quad (3.3)$$

$$P_2 Q = Q P_2 = 0. \quad (3.4)$$

The Hamilton operator of the full coupled-channel problem is given by H with the corresponding wave function $|\ \rangle$ defined in the complete Hilbert space. Analogous to the procedure of Chapter 3, we eliminate the two- and three-meson channels resulting in the coupled set of equations for the $\bar{p}p$ and $\bar{n}n$ wave function:

$$\begin{aligned} (E - P_1 H P_1) P_1 |\ \rangle &= P_1 H Q G Q H P_1 P_1 |\ \rangle \\ &+ P_1 H P_2 P_2 |\ \rangle + P_1 H Q G Q H P_2 P_2 |\ \rangle \end{aligned} \quad (3.5)$$

$$\begin{aligned} (E - P_2 H P_2) P_2 |\ \rangle &= P_2 H Q G Q H P_2 P_2 |\ \rangle \\ &+ P_2 H P_1 P_1 |\ \rangle + P_2 H Q G Q H P_1 P_1 |\ \rangle \end{aligned} \quad (3.6)$$

where E is the energy eigenvalue and G is the Greens function for two- and three-meson intermediate states, defined as:

$$G = \frac{1}{E - QHQ}. \quad (3.7)$$

The interaction terms in eq.4.3 and eq.3.6 are given as:

$$P_1HP_1 = H_0^p + V_c + V_{\bar{p}p \rightarrow \bar{p}p}, \quad (3.8)$$

$$P_2HP_2 = H_0^n + V_{\bar{n}n \rightarrow \bar{n}n}, \quad (3.9)$$

$$P_1HP_2 = P_2HP_1 = V_{\bar{p}p \rightarrow \bar{n}n}, \quad (3.10)$$

where

$$V_{\bar{p}p \rightarrow \bar{n}n} = V_{\bar{p}p \rightarrow \bar{p}p}, \quad (3.11)$$

$$H_0^p = \sqrt{m_p^2 + k^2}, \quad (3.12)$$

$$H_0^n = \sqrt{m_n^2 + k^2}, \quad (3.13)$$

$$V_{\bar{p}p \rightarrow \bar{p}p} = \frac{1}{2}(V^0 + V^1), \quad (3.14)$$

$$V_{\bar{p}p \rightarrow \bar{n}n} = \frac{1}{2}(V^0 - V^1), \quad (3.15)$$

where V_c is the Coulomb interaction, V^0 and V^1 are the potentials due to meson-exchange for the isospin $I = 0$ and 1 $\bar{N}N$ states, respectively. The mass of the proton and neutron are denoted as m_p and m_n .

$P_iHQGQHP_j$ are the optical potentials W_{ij} for $\bar{N}N$ annihilation into two and three

mesons given in the isospin basis as:

$$\begin{aligned}
W_{\bar{p}p \rightarrow \bar{p}p} &= P_1 H Q G Q H P_1 \\
&= P_2 H Q G Q H P_2 \\
&= \frac{1}{2} (W^0 + W^1),
\end{aligned} \tag{3.16}$$

$$\begin{aligned}
W_{\bar{p}p \rightarrow \bar{n}n} &= P_1 H Q G Q H P_2 \\
&= P_2 H Q G Q H P_1 \\
&= \frac{1}{2} (W^0 - W^1),
\end{aligned} \tag{3.17}$$

where W^0 and W^1 are the annihilation potentials for isospin $I = 0$ and 1 $\bar{N}N$ states in the A2 and A3 model, respectively.

As an example, we give the final equation for spin-triplet $\bar{N}N$ states in the $\{J, L, S\}$ basis as

$$\begin{pmatrix} H_{11} & H_{12} \\ H_{21} & H_{22} \end{pmatrix} \begin{pmatrix} \Psi_{\bar{p}p} \\ \Psi_{\bar{n}n} \end{pmatrix} = E_b \begin{pmatrix} \Psi_{\bar{p}p} \\ \Psi_{\bar{n}n} \end{pmatrix} \tag{3.18}$$

with

$$\begin{aligned}
H_{11} &= \begin{pmatrix} P^2/2\mu + V_c^{L_1 L_1} + V_{\bar{p}p \rightarrow \bar{p}p}^{L_1 L_1} + W_{\bar{p}p \rightarrow \bar{p}p}^{L_1 L_1} & V_{\bar{p}p \rightarrow \bar{p}p}^{L_1 L_2} \\ V_{\bar{p}p \rightarrow \bar{p}p}^{L_2 L_1} & P^2/2\mu + V_c^{L_2 L_2} + V_{\bar{p}p \rightarrow \bar{p}p}^{L_2 L_2} + W_{\bar{p}p \rightarrow \bar{p}p}^{L_2 L_2} \end{pmatrix} \\
H_{12} &= \begin{pmatrix} V_{\bar{p}p \rightarrow \bar{n}n}^{L_1 L_1} + W_{\bar{p}p \rightarrow \bar{n}n}^{L_1 L_1} & V_{\bar{p}p \rightarrow \bar{n}n}^{L_1 L_2} \\ V_{\bar{p}p \rightarrow \bar{n}n}^{L_2 L_1} & V_{\bar{p}p \rightarrow \bar{n}n}^{L_2 L_2} + W_{\bar{p}p \rightarrow \bar{n}n}^{L_2 L_2} \end{pmatrix} \\
H_{21} &= \begin{pmatrix} V_{\bar{p}p \rightarrow \bar{n}n}^{L_1 L_1} + W_{\bar{p}p \rightarrow \bar{n}n}^{L_1 L_1} & V_{\bar{p}p \rightarrow \bar{n}n}^{L_2 L_1} \\ V_{\bar{p}p \rightarrow \bar{n}n}^{L_1 L_2} & V_{\bar{p}p \rightarrow \bar{n}n}^{L_2 L_2} + W_{\bar{p}p \rightarrow \bar{n}n}^{L_2 L_2} \end{pmatrix} \\
H_{22} &= \begin{pmatrix} P^2/2\mu + 2\delta m + V_{\bar{p}p \rightarrow \bar{p}p}^{L_1 L_1} + W_{\bar{p}p \rightarrow \bar{p}p}^{L_1 L_1} & V_{\bar{p}p \rightarrow \bar{p}p}^{L_1 L_2} \\ V_{\bar{p}p \rightarrow \bar{p}p}^{L_2 L_1} & P^2/2\mu + 2\delta m + V_{\bar{p}p \rightarrow \bar{p}p}^{L_2 L_2} + W_{\bar{p}p \rightarrow \bar{p}p}^{L_2 L_2} \end{pmatrix}
\end{aligned}$$

and

$$\Psi_{\bar{p}p} = \begin{pmatrix} \Psi_{\bar{p}p}^{L_1} \\ \Psi_{\bar{p}p}^{L_2} \end{pmatrix}, \quad \Psi_{\bar{n}n} = \begin{pmatrix} \Psi_{\bar{n}n}^{L_1} \\ \Psi_{\bar{n}n}^{L_2} \end{pmatrix}, \quad (3.19)$$

where $\delta m = m_n - m_p$, $\mu = m_p/2$, $V_c = -\alpha/r$, $L_1 = J - 1$, $L_2 = J + 1$, J is the total angular momentum and $E_b = E - 2m_p$, the binding energy of $\bar{N}N$ atomic states. nucleus.

3.2 $\bar{p}D$ interactions in terms of $\bar{N}N$ potentials

We start from the Schrödinger equation of the antiproton-deuteron system in coordinate space

$$\left(\frac{P_\rho^2}{2M_\rho} + \frac{P_\lambda^2}{2M_\lambda} + V_{12}(\vec{r}_2 - \vec{r}_1) + V_{13}(\vec{r}_3 - \vec{r}_1) + V_{23}(\vec{r}_3 - \vec{r}_2) \right) \Psi(\vec{\lambda}, \vec{\rho}) = E\Psi(\vec{\lambda}, \vec{\rho}) \quad (3.20)$$

where $\vec{\lambda}$ and $\vec{\rho}$ are the Jacobi coordinates of the system, defined as

$$\vec{\lambda} = \vec{r}_3 - \frac{\vec{r}_1 + \vec{r}_2}{2}, \quad \vec{\rho} = \vec{r}_2 - \vec{r}_1 \quad (3.21)$$

$M_\rho = M/2$ and $M_\lambda = 2M/3$ are the reduced masses. Here we have assigned, for simplicity, the proton and neutron the same mass M . Eq. (3.20) can be expressed in the form, where the strong interaction is expressed in the isospin basis,

$$\left(\frac{P_\rho^2}{2M_\rho} + \frac{P_\lambda^2}{2M_\lambda} + V_S + V_C \right) \Psi(\vec{\lambda}, \vec{\rho}) = E\Psi(\vec{\lambda}, \vec{\rho}) \quad (3.22)$$

where V_S and V_C stand for the nuclear interaction and Coulomb force, respectively, and take the forms

$$V_S = V_{NN}^0(\vec{r}_2 - \vec{r}_1) + \frac{1}{4}[V_{NN}^0(\vec{r}_3 - \vec{r}_1) + V_{NN}^0(\vec{r}_3 - \vec{r}_2)] + \frac{3}{4}[V_{NN}^1(\vec{r}_3 - \vec{r}_1) + V_{NN}^1(\vec{r}_3 - \vec{r}_2)] \quad (3.23)$$

$$V_C = \frac{1}{2}[V_C(\vec{r}_3 - \vec{r}_1) + V_C(\vec{r}_3 - \vec{r}_2)] \quad (3.24)$$

V^0 and V^1 in eqs. (3.23) and (3.23) are the isospin 0 and 1 nuclear interactions, respectively. Note that we have assigned \vec{r}_{12} as the relative coordinate of the deuteron core.

One may express the interactions V_C and V_S in eq. (3.23) eq. (3.24) in terms of the

interactions of certain $\bar{N}N$ states. In the $|JM\bar{L}S\rangle$ basis of the $\bar{p}D$ states

$$|JM\bar{L}S\rangle = |(L_\rho \otimes L_\lambda)_L \otimes (S_{12} \otimes S_3)_S\rangle_{JM} \quad (3.25)$$

we derive

$$(H_0 + W_C(\lambda, \rho) + V_{NN}^0(\rho) + W_S(\lambda, \rho)) \Psi(\lambda, \rho) = E\Psi(\lambda, \rho) \quad (3.26)$$

with

$$H_0 = \frac{P_\rho^2}{2M_\rho} + \frac{P_\lambda^2}{2M_\lambda} \quad (3.27)$$

W_C and W_S in eq. (3.26) are respectively the Coulomb force and strong interaction between the antiproton and deuteron, and V_{NN}^0 the interaction between the proton and neutron in the deuteron core. W_C and W_S are derived explicitly as

$$W_C(\lambda, \rho) = \frac{1}{2} \int_{-1}^1 dx V_C(r_{13}) \quad (3.28)$$

$$W_S(\lambda, \rho) = \frac{1}{2} \int_{-1}^1 dx \sum_{Q, Q'} \langle P|Q\rangle \langle Q| V_{NN}(\vec{r}_{13}) |Q'\rangle \langle Q'|P'\rangle \quad (3.29)$$

with

$$V_{NN}(\vec{r}_{13}) = \frac{1}{2} V_{NN}^0(\vec{r}_{13}) + \frac{3}{2} V_{NN}^1(\vec{r}_{13}) \quad (3.30)$$

$$r_{13} \equiv |\vec{r}_1 - \vec{r}_3| = (\lambda^2 + \rho^2/4 - \lambda\rho x)^{1/2} \quad (3.31)$$

where $x = \cos\theta$ with θ being the angle between $\vec{\lambda}$ and $\vec{\rho}$. In eq. (3.29) $|P\rangle \equiv |JM\bar{L}S\rangle$ and $|P'\rangle \equiv |JML'S\rangle$ are as defined in eq. (3.25) while the states $|Q\rangle$ and $|Q'\rangle$ are

$$|Q\rangle = |(L_\sigma \otimes S_{13})_{J_\sigma} \otimes (L_\gamma \otimes S_2)_{J_\gamma}\rangle_{JM} \quad (3.32)$$

$$|Q'\rangle = |(L'_\sigma \otimes S_{13})_{J_\sigma} \otimes (L_\gamma \otimes S_2)_{J_\gamma}\rangle_{JM} \quad (3.33)$$

Here $\vec{\sigma}$ and $\vec{\gamma}$ are also the Jacobi coordinates of the system, defined as

$$\vec{\gamma} = \vec{r}_2 - \frac{\vec{r}_1 + \vec{r}_3}{2}, \quad \vec{\sigma} = \vec{r}_3 - \vec{r}_1 \quad (3.34)$$

So defined the states $|Q\rangle$ and $|Q'\rangle$ is based on the consideration that the $\bar{N}N$ interactions can be easily expressed in the $|J_\sigma M_\sigma L_\sigma S_{13}\rangle$ basis of the $\bar{N}N$ states. Note that $\langle P|Q\rangle$ depends on not only the quantum numbers of the states $|P\rangle$ and $|Q\rangle$, but also λ , ρ and the angle θ between $\vec{\lambda}$ and $\vec{\rho}$ resulting from the projection of the orbital angular momenta between different Jacobi coordinates. We listed the integral kernels in eq. (3.29), $\sum_{Q,Q'} \langle P|Q\rangle \langle Q| V(\vec{r}_{13}) |Q'\rangle \langle Q'|P'\rangle$, for the lowest $\bar{p}D$ states in the approximation that the deuteron core is assumed in the S-state, as follows:

$$\begin{aligned}
|P\rangle = |P'\rangle = |^2S_{1/2}\rangle : & \quad \frac{3}{4}V_{\bar{N}N}(^1S_0) + \frac{1}{4}V_{\bar{N}N}(^3S_1) \\
|P\rangle = |P'\rangle = |^4S_{3/2}\rangle : & \quad V_{\bar{N}N}(^3S_1) \\
|P\rangle = |P'\rangle = |^2P_{1/2}\rangle : & \quad F_1^2 \cdot \left[\frac{1}{12}V_{\bar{N}N}(^3P_0) + \frac{3}{4}V_{\bar{N}N}(^1P_1) + \frac{1}{6}V_{\bar{N}N}(^3P_1) \right] \\
|P\rangle = |P'\rangle = |^4P_{1/2}\rangle : & \quad F_1^2 \cdot \left[\frac{2}{3}V_{\bar{N}N}(^3P_0) + \frac{1}{3}V_{\bar{N}N}(^3P_1) \right] \\
|P\rangle = |P'\rangle = |^2P_{3/2}\rangle : & \quad F_1^2 \cdot \left[\frac{3}{4}V_{\bar{N}N}(^1P_1) + \frac{1}{24}V_{\bar{N}N}(^3P_1) + \frac{5}{24}V_{\bar{N}N}(^3P_2) \right] \\
|P\rangle = |P'\rangle = |^4P_{3/2}\rangle : & \quad F_1^2 \cdot \left[\frac{5}{6}V_{\bar{N}N}(^3P_1) + \frac{1}{6}V_{\bar{N}N}(^3P_2) \right] \\
|P\rangle = |P'\rangle = |^4P_{5/2}\rangle : & \quad F_1^2 \cdot V_{\bar{N}N}(^3P_2) \\
|P\rangle = |P'\rangle = |^4D_{3/2}\rangle : & \quad F_3^2 \cdot \left[\frac{1}{2}V_{\bar{N}N}(^3D_1) + \frac{1}{2}V_{\bar{N}N}(^3D_2) \right] \\
|P\rangle = |P'\rangle = |^2F_{3/2}\rangle : & \quad F_2^2 \cdot V_{\bar{N}N}(^3F_2) \\
|P\rangle = |P'\rangle = |^4F_{5/2}\rangle : & \quad F_2^2 \cdot \left[\frac{4}{9}V_{\bar{N}N}(^3F_2) + \frac{5}{9}V_{\bar{N}N}(^3F_3) \right] \\
|P\rangle = |^4P_{3/2}\rangle, |P'\rangle = |^4F_{3/2}\rangle : & \quad F_1F_2 \cdot \frac{1}{\sqrt{6}}V_{\bar{N}N}(^3PF_2) \\
|P\rangle = |^4P_{5/2}\rangle, |P'\rangle = |^4F_{5/2}\rangle : & \quad F_1F_2 \cdot \frac{2}{3}V_{\bar{N}N}(^3PF_2) \\
|P\rangle = |^4S_{3/2}\rangle, |P'\rangle = |^4D_{3/2}\rangle : & \quad F_3 \cdot \left[\frac{1}{\sqrt{2}}V_{\bar{N}N}(^3SD_1) + \frac{1}{\sqrt{2}}V_{\bar{N}N}(^3SD_2) \right]
\end{aligned} \quad (3.35)$$

where $|P\rangle \equiv |JM L S\rangle$ and $|P'\rangle \equiv |JM L' S\rangle$ are the $\bar{p}D$ atomic states. Both the $\bar{p}D$ and $\bar{N}N$ states in eq. (3.35) are labelled as $^{2S+1}L_J$ with S , L and J being respectively the total spin, total orbital angular momentum and total angular momentum. The potentials $V_{\bar{N}N}$, being functions of $r_{13} = \sqrt{\lambda^2 + \rho^2/4 - \rho\lambda x}$, stand for the $\bar{N}N$ interactions for various $\bar{N}N$ states as indicated in the brackets.

The F_1 , F_2 and F_3 in eq. (3.35) are functions of only λ and ρ , taking the forms

$$F_1 = \begin{cases} 1 - \frac{1}{12} \frac{\rho^2}{\lambda^2}, & \rho < 2\lambda \\ \frac{4\lambda}{3\rho}, & \rho > 2\lambda \end{cases} \quad (3.36)$$

$$F_2 = \begin{cases} \left(1 - \frac{\rho^2}{4\lambda^2}\right)^2, & \rho < 2\lambda \\ 0, & \rho > 2\lambda \end{cases} \quad (3.37)$$

$$F_3 = \begin{cases} {}_2F^1\left(1, -\frac{3}{2}, \frac{3}{2}, \frac{\rho^2}{4\lambda^2}\right), & \rho < 2\lambda \\ \frac{5}{8} - \frac{3\rho^2}{32\lambda^2} + \text{Artanh}\left(\frac{2\lambda}{\rho}\right) \left[\frac{3\lambda}{4\rho} - \frac{3\rho}{8\lambda} + \frac{3\rho^3}{64\lambda^3}\right], & \rho > 2\lambda \end{cases} \quad (3.38)$$

where ${}_2F^1(\alpha, \beta, \gamma, x)$ is the hypergeometric function and $\text{Artanh}(x)$ the inverses hyperbolic tangent function.

3.3 Energy shifts and decay widths of $\bar{p}D$ atoms

It is not a simple problem to accurately evaluate the energy shifts and decay widths, especially wave functions of exotic atoms like protonium, pionium and antiproton-deuteron atoms, which are mainly bound by the Coulomb force, but also effected by the short range strong interaction. In this work we study the $\bar{p}D$ atoms in the Sturmian function approach which has been successfully applied to our previous works [2]. Employed for the $\bar{N}N$ interactions are various realistic $\bar{N}N$ potentials, namely, the Paris $\bar{N}N$ potentials of the 1994 version [31], 1998 version [32] and 2004 version [33], the Dover-Richard $\bar{N}N$ potentials I [34] and II [35], and the Kohno-Weise $\bar{N}N$ potential [36]. In this preliminary work, we just limit our study to the approximation of undistorted deuteron core. However, one may see that the main conclusions of the work are free of this approximation.

Shown in Table I are the energy shifts and decay widths, which stem from the Paris98, DR2 and KW $\bar{N}N$ interactions, in the approximation of undistorted deuteron core. The theoretical results for other interactions like Paris84, Paris04 and DR1 are quite similar to the ones listed in Table I. The wave function of the undistorted deuteron core is evaluated in the Bonn OBEPQ potential [37]. It is found that the theoretical results for the $1s$ $\bar{p}D$ atomic states are more or less the same by all the employed $\bar{N}N$ potentials. The predicted energy shifts are roughly as twice

	Paris98		DR2		KW		Data	
	ΔE	Γ	ΔE	Γ	ΔE	Γ	ΔE	Γ
$^2S_{1/2}$	-2445	1781	-2673	2380	-2478	2450		
$^4SD_{3/2}$	-2680	2822	-2668	2390	-2503	2469		
$^2P_{1/2}$	-186	584	17	896	99	657		
$^4P_{1/2}$	265	402	47	846	101	785		
$^2P_{3/2}$	-128	515	14	897	98	643		
$^4PF_{3/2}$	282	477	21	887	97	648		
$^4PF_{5/2}$	244	814	21	877	101	660		
$\overline{\Delta E}_{1s}, \overline{\Gamma}_{1s}$	-2602	2475	-2670	2387	-2494	2463	-1050 ± 250	1100 ± 750 2270 ± 260
$\overline{\Delta E}_{2p}, \overline{\Gamma}_{2p}$	124	602	22	883	99	668	-243 ± 26	489 ± 30

Table 3.1: The energy shifts ΔE and decay widths of the $1s$ and $2p$ antiproton-deuteron atomic states in the approximation of undistorted deuteron core. The minus sign of the energy shifts means that the strong interaction is repulsive. The units are eV and meV for $1s$ and $2p$ states, respectively. Experimental data are taken from [25, 26].

large as the experimental data. However, one may expect that the predictions of the potentials in question could be improved to some extent by solving the $\bar{p}D$ dynamical equation in eq. (3.26) without any approximation. A better treatment of the deuteron core will yield lower $1s$ $\bar{p}D$ atomic states, hence smaller energy shifts. The theoretical results for the decay widths of the $1s$ $\bar{p}D$ atoms are also larger than the experimental data though not as far from the data as for the energy shifts. The predictions for the decay widths are also expected to be improved by treating the deuteron core more properly.

The theoretical predictions for the energy shifts of the $2p$ $\bar{p}D$ atomic states are totally out of line for all the \overline{NN} potentials employed. The experimental data show that the averaged energy level of the $2p$ $\bar{p}D$ atoms is pushed up by the strong interaction, the same as for the $1s$ $\bar{p}D$ atoms, but the theoretical results uniquely show the averaged energy level shifting down. It is unlikely to improve, by treating the deuteron core more accurately, the theoretical predictions of the \overline{NN} potentials in question for the $2p$ $\bar{p}D$ energy shifts since a more accurate treatment of the deuteron core will lead to deeper $2p$ $\bar{p}D$ atomic states.

All the \overline{NN} potentials employed in the work reproduce \overline{NN} scattering data reasonably, but badly fail to reproduce the energy shifts of the $2p$ $\bar{p}D$ atoms. The investigation of the $\bar{p}D$ atoms may provide a good platform for refining the \overline{NN} interaction, especially at zero energy since the energy shifts of the $2p$ $\bar{p}D$ atomic states are very sensitive to the \overline{NN} strong interactions.

The research here is just a preliminary work, where a frozen, S-state deuteron is employed. The work may be improved at two steps, considering that the numerical evaluation is time-consuming. One may, at the first step, solve the $\bar{p}D$ dynamical equation in eq. (3.26) by

expanding the $\bar{p}D$ wave function in a bi-wave basis of the Sturmian functions, where a realistic nucleon-nucleon potential is employed but the deuteron core is assumed to be at the S-state. Such an evaluation is still manageable at a personnel computer but it may take a week or longer. We may compare the results of the improved work with the results here to figure out how important an unfrozen deuteron core is.

One may also consider, at the second step, to solve the $\bar{p}D$ dynamical equation in eq. (3.26) by expanding the $\bar{p}D$ wave function in a bi-wave basis of the Sturmian functions without any approximation, where realistic nucleon-nucleon and nucleon-antinucleon potentials are employed and the deuteron core is allowed to be at both the S- and D-waves. It is certain that the numerical calculation will take longer time but, anyway, we will do it after we complete the first-step improvement.



Chapter 4

Pionium

Pionium is an exotic atom of π^+ and π^- , bound mainly by the Coulomb force. The strong interaction between the two pions also play a role, leading to an energy shift from the Coulomb energy ($E = -1.86$ keV) and distorting the hydrogen-like wave function at short distance (a few fm). Pionium decays predominantly into $\pi^0\pi^0$ via strong interaction, which probes the low energy interactions of the pions. It has been believed that pionium might be employed to test more accurately the predictions of chiral perturbation theory. The investigation of pionium is the only mean to study the pion-pion strong interaction at zero energy.

The investigation of pionium has recently become of particular interest due to the pionium DIRAC experiment [38, 39, 40]. The aim of the DIRAC experiment at CERN is to measure the lifetime of $1s$ pionium with 10% precision. Such a measurement would yield a precision of 5% on the value of the S-wave $\pi\pi$ scattering lengths combination $|a_0 - a_2|$. The DIRAC spectrometer was commissioned at the end of 1998, and the first results [40] have been published recently based on part of the collected data. The preliminary result of the pionium lifetime is $\tau_{1S} = 2.91^{+0.49}_{-0.62} \times 10^{-15}$ seconds.

The nonrelativistic formula of the pionium lifetime in the lowest order of electromagnetic interactions was first evaluated by Deser et al. [41] and later reanalyzed by others [42]. It reads

$$\Gamma_0 = \frac{2}{9} \frac{64\pi p}{M^3} |\psi(0)|^2 |a_0 - a_2|^2 \quad (4.1)$$

where M is the mass of the $\pi\pi$ system, p is the center-of-mass momentum of the π^0 in the pionium system, $\psi(0)$ is the pionium S-wave function at the origin ($r = 0$), and a_0 and a_2 are the S-wave $\pi\pi$ scattering lengths for isospin $I = 0$ and 2 respectively. In the approximation of

the pionium wave function in eq. (4.1) to the hydrogen-like wave function, one derives the chiral perturbation result at leading order [42]

$$\Gamma = \frac{2}{9}\alpha^3 p |a_0 - a_2|^2 \quad (4.2)$$

where α is the fine structure constant.

An evaluation of the relativistic, strong interaction and higher-order electromagnetic corrections to the nonrelativistic formula in eq. (4.1) has recently been done in the frameworks of quantum field theory and chiral perturbation theory. These works have led to similar estimates, of the order of 6%, of these corrections [43, 44, 45, 46]. The strong interaction of the pion-pion system with respect to the bound state wave equation has been treated perturbatively though the methods employed in these works are quite different.

However, it is arguable to treat the pion-pion strong interaction as a small perturbation as well as to approximate in the lowest order the pionium wave function to the hydrogen-like one at small distance. In the work we tackle this issue by evaluating accurately the pionium wave functions in realistic pion-pion strong interactions.

4.1 Sturmian Function Method Applied to Ponium

Any reasonable prediction of the pionium lifetime in the potential model (or say, in the quantum mechanics regime) must be based on accurate knowledge of the wave function of the pionium state. The evaluation of the pionium wave function has been a challenge to numerical methods. Required is an approach, which is able to overcome the longstanding problem, that is, accounting for both the strong short-range interaction and the long-range Coulomb force. The pionium problem is more difficult than the more popular protonium problem in term of evaluating the wave functions since the Bohr radius of pionium is much larger than the one of protonium. In this section we verify the Sturmian function approach, which has been successfully applied to the protonium problem [2], is powerful to handle the pionium problem.

A correct treatment of pionium must include the coupling of the $\pi^+\pi^-$ and $\pi^0\pi^0$ configurations. The dynamical equations of the $(\pi^+\pi^-, \pi^0\pi^0)$ system take the form

$$\begin{aligned} (E - H_{\pi^+\pi^-}^0) \pi^+\pi^- &= (V_c + V_{11}) \pi^+\pi^- + V_{12} \pi^0\pi^0 \\ (E - H_{\pi^0\pi^0}^0) \pi^0\pi^0 &= V_{22} \pi^0\pi^0 + V_{21} \pi^+\pi^- \end{aligned} \quad (4.3)$$

where E is the energy of the $(\pi^+\pi^-, \pi^0\pi^0)$ system, $H_{\pi^+\pi^-}^0$ and $H_{\pi^0\pi^0}^0$ are respectively the free energies of the π^\pm and π^0 , V_c is the coulomb interaction between π^+ and π^- , and V_{ij} are the strong interactions of the system. The strong interactions take, for example, for pionium in S-waves the form in the isospin basis

$$V = \begin{pmatrix} \frac{2}{3} V^0 + \frac{1}{3} V^2 & \frac{\sqrt{2}}{3} (V^2 - V^0) \\ \frac{\sqrt{2}}{3} (V^2 - V^0) & \frac{1}{3} V^0 + \frac{2}{3} V^2 \end{pmatrix} \quad (4.4)$$

where V^0 and V^2 are respectively the isospin 0 and 2 strong interactions of the $\pi\pi$ system. In principle, one could solve Eq. (4.4) through expanding the pionium wave functions $\pi^+\pi^-$ and $\pi^0\pi^0$ in any complete set of orthonormal functions.

To guarantee the accuracy of the numerical method employed here, we have followed in our numerical calculations the procedures as follows:

- (1) Employ a hadronic potential to the pionium problem. The interaction should be strong enough to provide at least one deep bound state for the $\pi\pi$ system. Solve the pionium problem in any numerical method (for example, expanding the pionium wave function in the complete basis of the harmonic oscillator functions or Sturmian functions) to obtain the binding energy and wave function of the deep bound states of the $\pi\pi$ system.
- (2) Solve the pure Coulomb pionium problem in the complete basis of Sturmian functions, with the length parameter b as large as possible, to numerically reproduce the analytical hydrogen-like wave functions in high accuracy.
- (3) Solve the pionium problem in (1) in the complete basis of Sturmian functions employed in (2). The binding energy and wave function in (1) must be accurately reproduced in the present basis, or one has to employ a larger basis with larger b in (2).

A basis worked out by following the steps mentioned above enables one to accurately evaluate the binding energy and wave function of pionium. For comparison we have resolved the simplified pionium problem in Ref. [47] where the $\pi^0\pi^0$ component is ignored and the strong interaction is simply a Yakawa form. It is quite an easy job to solve such a simplified pionium problem in the Sturmian function method. The relative correction to the binding energy of the pionium ground state due to strong interaction is derived in our work as

$$\eta = \frac{E - E_0}{E_0} = 0.0021543718. \quad (4.5)$$

where E and E_0 are respectively the ground state binding energies of the pionium and the $\pi\pi$

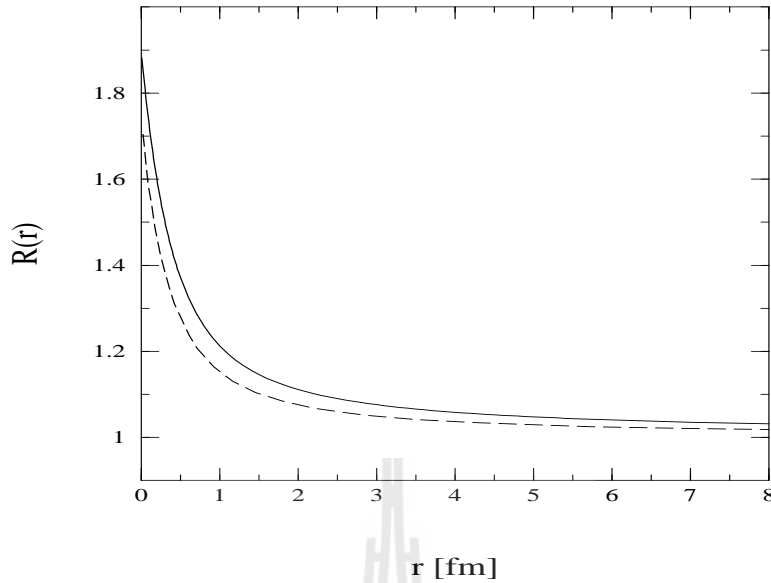


Figure 4.1: Ratios of the $1s$ pionium state wave function to the $1s$ hydrogen-like wave function in our calculation (solid line) and the work [47] (long-dashed line).

system with only the Coulomb interaction. The pionium $1s$ energy level is slightly shifted lower compared to the pure Coulomb interaction. The approach employed here is so powerful that the binding energy of the pionium ground state can be evaluated to an accuracy better than 10^{-8} . The relative correction derived in Ref. [47] is $\eta = 0.0020256$ [?]. We would say that the method employed in Ref. [47] needs to be improved since an accuracy of 10^{-4} guaranteed in Ref. [47] is not good enough for the pionium problem. But, as realized by the authors [47], the calculation of the pionium wave functions is not a simple problem.

Shown in Fig. 1 are the ratios $\pi^+\pi^-(r)/c(r)$, derived respectively in our calculation and Ref. [47], of the $1s$ pionium state wave function to the $1s$ hydrogen-like wave function. The pionium ground state wave function in our work is a little bit higher than that in Ref. [47] at short distances, which is consistent with that our binding energy of the pionium ground state is larger.

4.2 Pionium in Realistic Interactions

Since Pionium has a small $\pi^0\pi^0$ component, the coupling of the $\pi^+\pi^-$ and $\pi^0\pi^0$ configurations must be properly treated. The dynamical equations of the $(\pi^+\pi^-, \pi^0\pi^0)$ system may take the general form as shown in eq. (4.3). As the pion mesons are finite, we describe the charge

distribution of π^+ and π^- by the form factor

$$F(q) = \frac{1}{1 + q^2/a^2}, \quad (4.6)$$

with $a = 0.77$ GeV.

The pionium problem is more difficult than other exotic problems, for example, the protonium problem in term of evaluating the wave function of exotic atoms since the Bohr radius of pionium is much larger than the one of protonium. Here we solve the pionium dynamical equation in eq. (4.3) by expanding the pionium wave function Ψ in the complete basis of Sturmian functions.

Table 4.1: Energy shift of the $1s$ pionium compared to the pure Coulomb interaction level.

	Model B	Model C	Model D	Model E	Data
$\Delta E(eV)$	-1.36	-2.97	-3.93	-2.87	–
$\tau(10^{-15}s)$	1.10	2.68	2.59	2.24	$2.91^{+0.49}_{-0.62}$

Studied first in the work is the pion-pion interactions in the work [48], which are worked out in the meson-exchange model and reproduce well the pion-pion phase shift data. The work considers the contributions of the ρ -exchange in the t -channel and the exchanges of ρ , f_2 and ε (a scalar meson) in the s -channel for the very low energy pion-pion scattering. For the ε exchange both the scalar coupling and the gradient coupling are studied. For our convenience, we may call the interaction with the ε scalar coupling Model A and the one with the ε gradient coupling Model B. It is found that the pion-pion potential in Model A supports a number of pion-pion deep bound states which have never been observed. The deep bound states stem mainly from the large contribution of the ε scalar coupling at zero energy. The predictions for the energy shift and the pionium lifetime in Model B are shown in Table 5.1 while the pionium S-wave function is plotted in Fig. 4.2 as the dash-dotted curve. The lifetime in Model B and also in other models below is evaluated using eq. (4.1) with the scattering length a_0 and a_2 taken from [49]. Although Model B does not support any deep bound state, it is obvious that the interaction in the model is also too strong at zero energy. The main contributor to the pion-pion interaction at zero energy in Model B is the t -channel ρ -exchange. The pion-pion potentials in both Model A and B reproduce very well the pion-pion scattering data, but both of them fail to give reasonable predictions for the pionium properties.

The pion-pion interaction has been studied intensively in the chiral perturbation theory (ChPT) and considerable successes have been achieved in the regime. However, the ChPT success

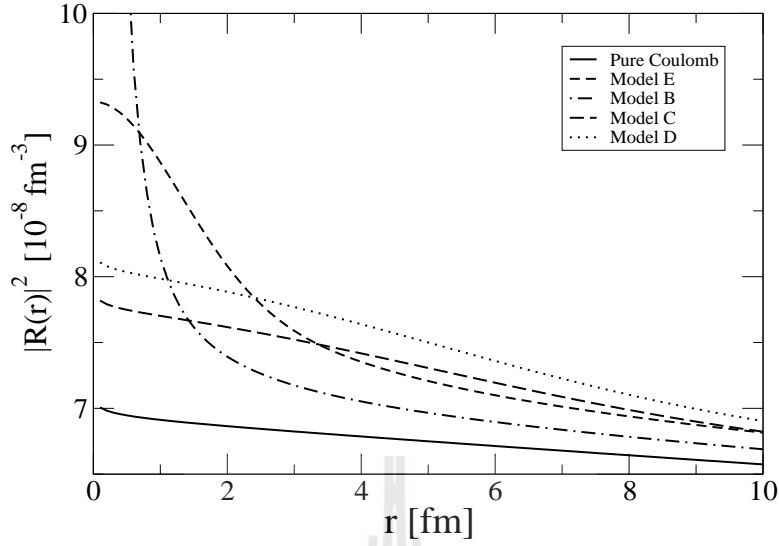


Figure 4.2: Squared $1s$ radial wave functions for the $\pi^+\pi^-$ component of pionium. For comparison the pure Coulomb interaction wave function is also plotted. All the wave functions have been multiplied by a factor 10^8 .

in reproducing pion-pion experimental data does not necessarily guarantee a practical potential which is applicable to, for example, the pionium problem where the off-shell effects have to be considered. In this work we apply the pion-pion potentials derived in the chiral Lagrangian to the pionium problem. In analogy to the works [50], where meson-meson potentials provided by the lowest order chiral Lagrangian combined with Lippmann-Schwinger equations are applied to study the reactions of $\gamma\gamma$ to two mesons and two mesons to two mesons, and the derivation of the nucleon-nucleon interaction in chiral perturbation theory [51], we impose a cutoff of the momentum on the pion-pion potentials derived in the chiral perturbation theory. Devoted to Model C is the potential derived from the tree diagram of the leading order Lagrangian \mathcal{L}_2 in [52] with the cutoff $\Lambda = 0.1$ GeV for all momenta and to Model D is the potential derived from the tree diagrams of the chiral Lagrangian $\mathcal{L}_{eff} = \mathcal{L}_2 + \mathcal{L}_4 + \mathcal{L}_6$ in [52] with the same cutoff. Shown in Table 5.1 are the predictions of Model C and D for the energy shifts and lifetimes of pionium, and the long dashed and dotted curves in Fig. 4.2 are the pionium S-wave functions. All the parameters of the potentials are taken from the works [52]. It is found that the predictions of Model C and D are fair good with a reasonable cutoff $\Lambda = 0.1$ GeV, hence it is possible to construct a pion-pion potential in the framework of the chiral perturbation theory. Of course, to get a practical pion-pion potential one needs to reproduce not only the pionium data but also the pion-pion scattering data by solving Lippmann-Schwinger equations for both bound and scattering problems.

The last model interaction we study here is a simple, local potential which has been widely

employed for studying the influence of the hadronic interaction on ponium wave functions [53]. The potential is independent of both the energy of the ponium system and pion masses, and reproduce very well the phase shifts given by two-loop chiral perturbation theory [52]. For convenience, we may call the pion-pion interaction here Model E. In consistence with the works [53], we solve for the $(\pi^+\pi^-, \pi^0\pi^0)$ system here the coupled Schrödinger equations employed in the works [53].

The predictions of Model E for the energy shift and lifetime of the $1s$ ponium state are listed in Table 5.1 while the evaluated $1s$ radial wave functions for the $\pi^+\pi^-$ component of ponium is plotted in Fig. 4.2 as the dashed curve. It is clear that the ground state ponium wave function in Model E is considerably different from the hydrogen-like one at small distances, and the $1s$ ponium lifetime is much shorter than the experimental value.

The ponium has been studied in various strong interactions, which may lead us to some points. The interaction in the meson-exchange model with the scalar coupling for the ε -exchange is unreasonably strong for the ponium system. The ponium system favors the gradient coupling for the ε -exchange, and demands a much weaker coupling for the t -channel ρ -exchange. A practical pion-pion potential may be derived from the chiral perturbation theory, which can reproduce both the ponium and pion-pion scattering data and is applicable to other multi-pion systems, for example, the pion gas probably produced in high-energy heavy-ion collisions. The local pion-pion potential, which has been widely applied to the ponium system, is indeed too strong at zero energy though it reproduces well the pion-pion phase shift data.

Chapter 5

Pionic and Kaonic Atoms

The simplest pionic atom is the pionic hydrogen, a bound state of negatively charged pion and the proton combined mainly by Coulomb interaction and effected also by the short ranged strong interaction. Due to the hadronic interaction the electromagnetic ground state ($1s$) of this atom is shifted in energy and is unstable: it can decay into an uncharged pion and a neutron. The finite life time due to this decay and the energy shift can give information on the hadronic interaction between pions and nucleons [54]. The measurement of the pion-nucleon scattering lengths constitutes a high-precision test of the methods of Chiral Perturbation Theory, which is the low-energy approach of QCD. The pion-nucleon s -wave scattering lengths are related to the strong-interaction shift and width of the s -states of the pionic hydrogen atom. Shift and width are determined from the measured energies and line widths of X-ray transitions to the $1s$ ground state when compared to the calculated electromagnetic values. A new experiment [55], set up at the Paul-Scherrer-Institut, has completed a first series of measurements and the primary analysis yields $\varepsilon_{1s} = +7.120 \pm 0.017$ eV. The result is consistent with the previous precision experiment [56] with $\varepsilon_{1s} = +7.108 \pm 0.047$ eV and $\Gamma_{1s} = 0.868 \pm 0.078$ eV. To extract the pion-nucleon scattering lengths from the experimental energy shift ε_{1s} and width Γ_{1s} of the pionic hydrogen, one needs the accurate knowledge of its wave function. However, the wave function of the pionic hydrogen has not yet been evaluated for non-local potentials, for example, the interaction derived in the Chiral Perturbation Theory, which is in momentum space and non-local.

Kaonic hydrogen is mainly the Coulomb bound state of a K^- and a proton but is affected by the strong interaction at small distances. The strong interaction couples the K^-p state to the \bar{K}^0n , $\pi\Sigma$, $\pi\Lambda$, $\eta\Sigma$ and $\eta\Lambda$ channels and results in the $\pi\Sigma$ and $\pi\Lambda$ decaying modes. It is believed that the study of kaonic hydrogen effectively probes the low-energy, especially zero energy strong

kaon-nucleon interaction. Inspired by the recent precise determination of the energy and decay width by the DEAR Collaboration [57], kaonic hydrogen has been extensively studied in the theoretical sector, mainly in effective field theory [58, 59, 60, 61, 62, 63, 64, 65, 66].

The kaonic hydrogen may be formed with a much shorter time than the lifetime of the charged kaons which is 1.24×10^{-8} seconds with the main decay mode:

$$K^- \rightarrow \mu^- + \bar{\nu}_\mu \quad (5.1)$$

$$K^- \rightarrow \pi^- + \pi^0 \quad (5.2)$$

$$K^- \rightarrow \pi^- + \pi^- + \pi^+. \quad (5.3)$$

The involved time scales for the formation of the kaonic hydrogen are; first for slowing a kaon down and capturing it into an atomic orbit about 10^{-12} to 10^{-19} s, then for Coulomb de-excitation and Auger processes about 10^{-12} to 10^{-15} s and finally, for radiative transitions about 10^{-15} to 10^{-17} s. Thus the charged kaon in the kaonic hydrogen atom can be considered a practically stable particle. Despite its short lifetime, kaonic hydrogen can be considered as a quasi-stable bound state, because the charged kaon travels many times around the proton before decaying.

5.1 Dynamical Equations of K^-p System

A correct treatment of kaonic hydrogen atomic states must include the couplings of the K^-p , \bar{K}^0n , $\pi^0\Lambda$, $\pi^0\Sigma$, $\pi^-\Sigma^+$ and $\pi^+\Sigma^-$ configurations. We define the Hilbert spaces of the K^-p , \bar{K}^0n , $\pi^0\Lambda$, $\pi^0\Sigma$, $\pi^-\Sigma^+$ and $\pi^+\Sigma^-$ configurations as P_1 , P_2 , P_3 , P_4 , P_5 and P_6 spaces, respectively. The Hilbert space of other channels is defined as Q space. The corresponding projection operators P_1 , P_2 , P_3 , P_4 , P_5 , P_6 and Q satisfy the completeness relation

$$P_1 + P_2 + P_3 + P_4 + P_5 + P_6 + Q = 1 \quad (5.4)$$

$$P_i^2 = P_i, \quad Q^2 = Q \quad (5.5)$$

as well as orthogonality

$$P_i P_j (i \neq j) = 0, \quad P_i Q = Q P_i = 0. \quad (5.6)$$

The Hamilton operator of the full coupled-channel problem is given by H with the corre-

sponding wave function $|\Psi\rangle$ defined in the complete Hilbert space. To construct the dynamical equations of kaonic hydrogen atoms, we start from the Schrödinger equation

$$(E - H)|\Psi\rangle = 0. \quad (5.7)$$

Starting from the K^-p channel, we get

$$EP_1|\Psi\rangle - P_1H|\Psi\rangle = 0$$

$$EP_1|\Psi\rangle - P_1H(P_1 + P_2 + P_3 + P_4 + P_5 + P_6 + Q)|\Psi\rangle = 0$$

$$\begin{aligned} EP_1|\Psi\rangle - P_1HP_1|\Psi\rangle - P_1HP_2|\Psi\rangle - P_1HP_3|\Psi\rangle - P_1HP_4|\Psi\rangle \\ - P_1HP_5|\Psi\rangle - P_1HP_6|\Psi\rangle - P_1HQ|\Psi\rangle = 0. \end{aligned}$$

By using the properties of the projection operators above, we can write

$$\begin{aligned} EP_1|\Psi\rangle - P_1HP_1P_1|\Psi\rangle - P_1HP_2P_2|\Psi\rangle - P_1HP_3P_3|\Psi\rangle - P_1HP_4P_4|\Psi\rangle \\ - P_1HP_5P_5|\Psi\rangle - P_1HP_6P_6|\Psi\rangle - P_1HQQ|\Psi\rangle = 0. \end{aligned}$$

Hence, the dynamical equation of the K^-p channel is

$$\begin{aligned} (E - P_1HP_1)P_1|\Psi\rangle = (P_1HP_2)P_2|\Psi\rangle + (P_1HP_3)P_3|\Psi\rangle + (P_1HP_4)P_4|\Psi\rangle \\ + (P_1HP_5)P_5|\Psi\rangle + (P_1HP_6)P_6|\Psi\rangle + (P_1HQ)Q|\Psi\rangle \end{aligned} \quad (5.8)$$

with $P_1|\Psi\rangle = \Psi_{K^-p}$, $P_2|\Psi\rangle = \Psi_{K^0n}$, $P_3|\Psi\rangle = \Psi_{\pi^0\Lambda}$, $P_4|\Psi\rangle = \Psi_{\pi^0\Sigma}$, $P_5|\Psi\rangle = \Psi_{\pi^-\Sigma^+}$ and $P_6|\Psi\rangle = \Psi_{\pi^+\Sigma^-}$. E is the energy eigenvalue and G is the Greens function for all possible intermediate states, defined as:

$$G = \frac{1}{E - QHQ} \quad (5.9)$$

By using the same method, we derive the dynamical equations

$$\begin{aligned} (E - P_2HP_2)P_2|\Psi\rangle = (P_2HP_1)P_1|\Psi\rangle + (P_2HP_3)P_3|\Psi\rangle + (P_2HP_4)P_4|\Psi\rangle \\ + (P_2HP_5)P_5|\Psi\rangle + (P_2HP_6)P_6|\Psi\rangle + (P_2HQ)Q|\Psi\rangle, \end{aligned} \quad (5.10)$$

for the $\bar{K}^0 n$ channel,

$$(E - P_3 H P_3) P_3 |\Psi\rangle = (P_3 H P_1) P_1 |\Psi\rangle + (P_3 H P_2) P_2 |\Psi\rangle + (P_3 H P_4) P_4 |\Psi\rangle \\ + (P_3 H P_5) P_5 |\Psi\rangle + (P_3 H P_6) P_6 |\Psi\rangle + (P_3 H Q) Q |\Psi\rangle, \quad (5.11)$$

for the $\pi^0 \Lambda$ channel,

$$(E - P_4 H P_4) P_4 |\Psi\rangle = (P_4 H P_1) P_1 |\Psi\rangle + (P_4 H P_2) P_2 |\Psi\rangle + (P_4 H P_3) P_3 |\Psi\rangle \\ + (P_4 H P_5) P_5 |\Psi\rangle + (P_4 H P_6) P_6 |\Psi\rangle + (P_4 H Q) Q |\Psi\rangle, \quad (5.12)$$

for the $\pi^0 \Sigma$ channel,

$$(E - P_5 H P_5) P_5 |\Psi\rangle = (P_5 H P_1) P_1 |\Psi\rangle + (P_5 H P_2) P_2 |\Psi\rangle + (P_5 H P_3) P_3 |\Psi\rangle \\ + (P_5 H P_4) P_4 |\Psi\rangle + (P_5 H P_6) P_6 |\Psi\rangle + (P_5 H Q) Q |\Psi\rangle, \quad (5.13)$$

for the $\pi^- \Sigma^+$ channel,

$$(E - P_6 H P_6) P_6 |\Psi\rangle = (P_6 H P_1) P_1 |\Psi\rangle + (P_6 H P_2) P_2 |\Psi\rangle + (P_6 H P_3) P_3 |\Psi\rangle \\ + (P_6 H P_4) P_4 |\Psi\rangle + (P_6 H P_5) P_5 |\Psi\rangle + (P_6 H Q) Q |\Psi\rangle, \quad (5.14)$$

for the $\pi^+ \Sigma^-$ channel and

$$(E - Q H Q) Q |\Psi\rangle = (Q H P_1) P_1 |\Psi\rangle + (Q H P_2) P_2 |\Psi\rangle + (Q H P_3) P_3 |\Psi\rangle \\ + (Q H P_4) P_4 |\Psi\rangle + (Q H P_5) P_5 |\Psi\rangle + (Q H P_6) P_6 |\Psi\rangle. \quad (5.15)$$

for all other channels. Eq. (5.15) may be written formally as

$$Q |\Psi\rangle = \frac{1}{E - Q H Q} (Q H P_1) P_1 |\Psi\rangle + \frac{1}{E - Q H Q} (Q H P_2) P_2 |\Psi\rangle \\ + \frac{1}{E - Q H Q} (Q H P_3) P_3 |\Psi\rangle + \frac{1}{E - Q H Q} (Q H P_4) P_4 |\Psi\rangle \\ + \frac{1}{E - Q H Q} (Q H P_5) P_5 |\Psi\rangle + \frac{1}{E - Q H Q} (Q H P_6) P_6 |\Psi\rangle \\ = G(Q H P_1) P_1 |\Psi\rangle + G(Q H P_2) P_2 |\Psi\rangle \\ + G(Q H P_3) P_3 |\Psi\rangle + G(Q H P_4) P_4 |\Psi\rangle \\ + G(Q H P_5) P_5 |\Psi\rangle + G(Q H P_6) P_6 |\Psi\rangle \quad (5.16)$$

By eliminating the Q channel, we derive the dynamical equations for the coupled channels $K^- p$,

$\bar{K}^0 n$, $\pi^0 \Lambda$, $\pi^0 \Sigma$, $\pi^- \Sigma^+$ and $\pi^+ \Sigma^-$,

$$E P_i |\Psi\rangle = \sum_{j=1}^6 (P_i H P_j) P_j |\Psi\rangle + \sum_{j=1}^6 (P_i H Q) G (Q H P_j) P_j |\Psi\rangle \quad (5.17)$$

with $i = 1, \dots, 6$. $P_i |\Psi\rangle$ are the wave function of the P_i channel, that is, $P_1 |\Psi\rangle = \Psi_{K^- p}$, $P_2 |\Psi\rangle = \Psi_{\bar{K}^0 n}$, $P_3 |\Psi\rangle = \Psi_{\pi^0 \Lambda}$, $P_4 |\Psi\rangle = \Psi_{\pi^0 \Sigma}$, $P_5 |\Psi\rangle = \Psi_{\pi^- \Sigma^+}$ and $P_6 |\Psi\rangle = \Psi_{\pi^+ \Sigma^-}$.

The factor $P_i H P_i$ in Eq. (5.17) includes the free energy and the direct interaction of the P_i channel, taking the forms

$$\begin{aligned} P_1 H P_1 &= H_0^p + H_0^{K^-} + V_c + V_{K^- p \rightarrow K^- p} \\ P_2 H P_2 &= H_0^n + H_0^{\bar{K}^0} + V_{\bar{K}^0 n \rightarrow \bar{K}^0 n} \\ P_3 H P_3 &= H_0^{\pi^0} + H_0^\Lambda + V_{\pi^0 \Lambda \rightarrow \pi^0 \Lambda} \\ P_4 H P_4 &= H_0^{\pi^0} + H_0^\Sigma + V_{\pi^0 \Sigma \rightarrow \pi^0 \Sigma} \\ P_5 H P_5 &= H_0^{\pi^-} + H_0^{\Sigma^+} + V_c + V_{\pi^- \Sigma^+ \rightarrow \pi^- \Sigma^+} \\ P_6 H P_6 &= H_0^{\pi^+} + H_0^{\Sigma^-} + V_c + V_{\pi^+ \Sigma^- \rightarrow \pi^+ \Sigma^-} \end{aligned} \quad (5.18)$$

where V_c is the Coulomb interaction. $H_0^p = \sqrt{m_p^2 + \vec{k}^2}$, $H_0^n = \sqrt{m_n^2 + \vec{k}^2}$, $H_0^\Lambda = \sqrt{m_\Lambda^2 + \vec{k}^2}$, $H_0^{K^-} = \sqrt{m_{K^-}^2 + \vec{k}^2}$, $H_0^{\bar{K}^0} = \sqrt{m_{\bar{K}^0}^2 + \vec{k}^2}$, $H_0^{\pi^0} = \sqrt{m_{\pi^0}^2 + \vec{k}^2}$, $H_0^{\pi^-} = \sqrt{m_{\pi^-}^2 + \vec{k}^2}$, $H_0^{\pi^+} = \sqrt{m_{\pi^+}^2 + \vec{k}^2}$, $H_0^\Sigma = \sqrt{m_\Sigma^2 + \vec{k}^2}$, $H_0^{\Sigma^-} = \sqrt{m_{\Sigma^-}^2 + \vec{k}^2}$, and $H_0^{\Sigma^+} = \sqrt{m_{\Sigma^+}^2 + \vec{k}^2}$ are the free energies of the proton, neutron, lambda, negatively charge kaon, neutral antikaon, neutral pion, negatively charge pion, sigma, positively charge sigma and negatively charge sigma, respectively. The masses of the proton, neutron, lambda, negatively charge kaon, neutral antikaon, neutral pion, negatively charge pion, sigma, positively charge sigma and negatively charge sigma are denoted as m_p , m_n , m_Λ , m_{K^-} , $m_{\bar{K}^0}$, m_{π^0} , m_{π^-} , m_{π^+} , m_Σ , m_{Σ^-} and m_{Σ^+} , respectively.

$P_i H P_j$ ($i \neq j$) in Eq. (5.17) stand for the exchange interactions between two different

channels, taking the forms

$$\begin{aligned}
P_1HP_2 &= P_2HP_1 = V_{K^-p \rightarrow \bar{K}^0n} \\
P_1HP_3 &= P_3HP_1 = V_{K^-p \rightarrow \pi^0\Lambda} \\
P_1HP_4 &= P_4HP_1 = V_{K^-p \rightarrow \pi^0\Sigma} \\
P_1HP_5 &= P_5HP_1 = V_{K^-p \rightarrow \pi^-\Sigma^+} \\
P_1HP_6 &= P_6HP_1 = V_{K^-p \rightarrow \pi^+\Sigma^-} \\
P_2HP_3 &= P_3HP_2 = V_{\bar{K}^0n \rightarrow \pi^0\Lambda} \\
P_2HP_4 &= P_4HP_2 = V_{\bar{K}^0n \rightarrow \pi^0\Sigma} \\
P_2HP_5 &= P_5HP_2 = V_{\bar{K}^0n \rightarrow \pi^-\Sigma^+} \\
P_2HP_6 &= P_6HP_2 = V_{\bar{K}^0n \rightarrow \pi^+\Sigma^-} \\
P_3HP_4 &= P_4HP_3 = V_{\pi^0\Lambda \rightarrow \pi^0\Sigma} \\
P_3HP_5 &= P_5HP_3 = V_{\pi^0\Lambda \rightarrow \pi^-\Sigma^+} \\
P_3HP_6 &= P_6HP_3 = V_{\pi^0\Lambda \rightarrow \pi^+\Sigma^-} \\
P_4HP_5 &= P_5HP_4 = V_{\pi^0\Sigma \rightarrow \pi^-\Sigma^+} \\
P_4HP_6 &= P_6HP_4 = V_{\pi^0\Sigma \rightarrow \pi^+\Sigma^-} \\
P_5HP_6 &= P_6HP_5 = V_{\pi^-\Sigma^+ \rightarrow \pi^+\Sigma^-}
\end{aligned} \tag{5.19}$$

$(P_iHQ)G(QHP_j)$ in Eq. (5.17) are optical potentials, stemming from annihilations to other channels represented by Q . We express the optical potentials for various channels explicitly

as follows:

$$\begin{aligned}
W_{K^-p \rightarrow K^-p} &= (P_1HQ)G(QHP_1) \\
W_{\bar{K}^0n \rightarrow \bar{K}^0n} &= (P_2HQ)G(QHP_2) \\
W_{\pi^0\Lambda \rightarrow \pi^0\Lambda} &= (P_3HQ)G(QHP_3) \\
W_{\pi^0\Sigma \rightarrow \pi^0\Sigma} &= (P_4HQ)G(QHP_4) \\
W_{\pi^+\Sigma^- \rightarrow \pi^+\Sigma^-} &= (P_5HQ)G(QHP_5) \\
W_{\pi^-\Sigma^+ \rightarrow \pi^-\Sigma^+} &= (P_6HQ)G(QHP_6) \\
W_{K^-p \rightarrow \bar{K}^0n} &= (P_1HQ)G(QHP_2) = (P_2HQ)G(QHP_1) \\
W_{K^-p \rightarrow \pi^0\Lambda} &= (P_1HQ)G(QHP_3) = (P_1HQ)G(QHP_1) \\
W_{K^-p \rightarrow \pi^0\Sigma} &= (P_1HQ)G(QHP_4) = (P_4HQ)G(QHP_1) \\
W_{K^-p \rightarrow \pi^-\Sigma^+} &= (P_1HQ)G(QHP_5) = (P_5HQ)G(QHP_1) \\
W_{K^-p \rightarrow \pi^+\Sigma^-} &= (P_1HQ)G(QHP_6) = (P_6HQ)G(QHP_1) \\
W_{\bar{K}^0n \rightarrow \pi^0\Lambda} &= (P_2HQ)G(QHP_3) = (P_3HQ)G(QHP_2) \\
W_{\bar{K}^0n \rightarrow \pi^0\Sigma} &= (P_2HQ)G(QHP_4) = (P_4HQ)G(QHP_2) \\
W_{\bar{K}^0n \rightarrow \pi^-\Sigma^+} &= (P_2HQ)G(QHP_5) = (P_5HQ)G(QHP_2) \\
W_{\bar{K}^0n \rightarrow \pi^+\Sigma^-} &= (P_2HQ)G(QHP_6) = (P_6HQ)G(QHP_2) \\
W_{\pi^0\Lambda \rightarrow \pi^0\Sigma} &= (P_3HQ)G(QHP_4) = (P_4HQ)G(QHP_3) \\
W_{\pi^0\Lambda \rightarrow \pi^-\Sigma^+} &= (P_3HQ)G(QHP_5) = (P_5HQ)G(QHP_3) \\
W_{\pi^0\Lambda \rightarrow \pi^+\Sigma^-} &= (P_3HQ)G(QHP_6) = (P_6HQ)G(QHP_3) \\
W_{\pi^0\Sigma \rightarrow \pi^-\Sigma^+} &= (P_4HQ)G(QHP_5) = (P_5HQ)G(QHP_4) \\
W_{\pi^0\Sigma \rightarrow \pi^+\Sigma^-} &= (P_4HQ)G(QHP_6) = (P_6HQ)G(QHP_4) \\
W_{\pi^-\Sigma^+ \rightarrow \pi^+\Sigma^-} &= (P_5HQ)G(QHP_6) = (P_6HQ)G(QHP_5)
\end{aligned} \tag{5.20}$$

For the kaonic atom problem, one may further eliminate the $\pi^0\Lambda$, $\pi^0\Sigma$, $\pi^-\Sigma^+$ and $\pi^+\Sigma^-$ channels by substituting $P_3|\Psi\rangle$, $P_4|\Psi\rangle$, $P_5|\Psi\rangle$ and $P_6|\Psi\rangle$ formally derived in Eqs. (5.11), (5.12), (5.13) and (5.14) into Eqs. (5.8) and (5.10).

5.2 Kaonic Hydrogen Atoms

The success of the effective field theory applied to kaonic hydrogen makes it possible to construct equivalent local $\bar{K}N$ potentials which may be conveniently applied to computations of K -nuclear few body systems and hyper-nucleus productions [67]. The solution of the Schrödinger or Lippmann-Schwinger equation with such an equivalent potential should approximate as closely as possible the scattering amplitude derived from the full coupled-channel calculation of the effective field theory.

In the work we study kaonic hydrogen with local potentials which are purely phenomenological or based on chiral SU(3) models. After eliminating the $\pi^0\Lambda$, $\pi^0\Sigma$, $\pi^-\Sigma^+$ and $\pi^+\Sigma^-$ channels in Eq. (5.17), one derives the dynamical equations for the K^-p and \bar{K}^0n system, with the radial part of such equations taking the form,

$$\left[-\frac{1}{r^2} \frac{d}{dr} \left(r^2 \frac{d}{dr} \right) + \frac{l(l+1)}{r^2} - \mathbf{Q}^2 + \mathbf{f} \mathbf{V} \right] \mathbf{R}(r) \quad (5.21)$$

with

$$\mathbf{Q}^2 = \begin{pmatrix} q_c^2 & 0 \\ 0 & q_0^2 \end{pmatrix}, \quad \mathbf{f} = \begin{pmatrix} f_c & 0 \\ 0 & f_0 \end{pmatrix}, \quad (5.22)$$

$$\mathbf{V} = \mathbf{V}^{em} + \mathbf{V}^h, \quad (5.23)$$

$$\mathbf{V}^{em} = \begin{pmatrix} V^{em} & 0 \\ 0 & 0 \end{pmatrix}, \quad (5.24)$$

$$\mathbf{V}^h = \begin{pmatrix} \frac{1}{2}(V_1^h + V_0^h) & \frac{1}{2}(V_1^h - V_0^h) \\ \frac{1}{2}(V_1^h - V_0^h) & \frac{1}{2}(V_1^h + V_0^h) \end{pmatrix}, \quad (5.25)$$

$$\mathbf{R}(r) = \begin{pmatrix} R_{K^-p}(r) \\ R_{\bar{K}^0n}(r) \end{pmatrix}, \quad (5.26)$$

$$q_c^2 = \frac{[E^2 - (M_p - M_{K^-})^2][E^2 - (M_p + M_{K^-})^2]}{4E^2}, \quad (5.27)$$

$$q_0^2 = \frac{[E^2 - (M_n - M_{\bar{K}^0})^2][E^2 - (M_n + M_{\bar{K}^0})^2]}{4E^2}, \quad (5.28)$$

$$f_c = \frac{E^2 - M_p^2 - M_{K^-}^2}{E}, \quad (5.29)$$

$$f_0 = \frac{E^2 - M_n^2 - M_{\bar{K}^0}^2}{E} \quad (5.30)$$

Table 5.1: $1s$ kaonic hydrogen energy shift ΔE_{1s} (ΔE_{1s}^0) and decay width Γ_{1s} (Γ_{1s}^0) derived by directly solving eq. (5.21) with (without) the mass difference between the K^-p and \bar{K}^0n states considered.

	ΔE_{1s}^0 [eV]	Γ_{1s}^0 [eV]	ΔE_{1s} [eV]	Γ_{1s} [eV]
AY [75]	-268	312	-384	288
ORB [76]	-255	534	-348	646
HNJH [76]	-248	527	-336	648
BNW [76]	-220	544	-288	674
BMN [76]	-197	517	-297	622

where V^{em} is the electromagnetic potential, V_0^h and V_1^h are respectively the isospin $I = 0$ and 1 strong interactions of the $\bar{K}N$ system, $R_{K^-p}(r)$ and $R_{\bar{K}^0n}(r)$ are respectively the K^-p and \bar{K}^0n components of the radial wave function of the $\bar{K}N$ system. Eq. (5.21) embeds into the Schrödinger equation the relativistic effect and the mass difference between the K^-p and \bar{K}^0n components. The relativistic modification of the Schrödinger equation to eq.(5.21) has been discussed in the works [68, 69, 70, 71, 72, 73]. The strong interactions V_0^h and V_1^h are complex, taking into account the contributions of the direct interactions of the $\bar{K}N$ system and the couplings of the $\bar{K}N$ system to the channels $\pi^0\Lambda$, $\pi^0\Sigma$, $\pi^-\Sigma^+$ and $\pi^+\Sigma^-$ which are eliminated during the derivation of the above equations.

The local potentials considered here in the work are the phenomenological $\bar{K}N$ potential taken from the work [74, 75] and the various effective potentials which are worked out in Ref. [76]. The interaction [74, 75] is constructed by fitting the free $\bar{K}N$ scattering data [77], the KpX data of kaonic hydrogen by the KEK Collaboration [78] and the binding energy and decay width of $\Lambda(1405)$, which is regarded as an isospin $I = 0$ bound state of $\bar{K}N$.

In Ref. [76] an effective local potential in coordinate space is constructed such as the solution of the Schrödinger or Lippmann-Schwinger equation with such a potential approximates as closely as possible the scattering amplitude derived from the full chiral coupled-channel calculation. Four versions of effective potentials referred to as ORB, HNJH, BNW, BMN have been constructed in Ref. [76], based respectively on the chiral SU(3) models [59, 60, 64, 66].

The accurate evaluation of energy shifts, decay widths and especially wave functions of exotic atoms has been a challenge to numerical methods [72, 79]. An approach is required, which is able to account accurately for both the strong short-range interaction and the long-range Coulomb force. The numerical approach based on Sturmian functions [5] has been found effective and accurate. In this work we use the numerical method which has been carefully studied and discussed in [5, 2, 80] to study kaonic hydrogen.

The $1s$ kaonic hydrogen energy shift ΔE_{1s} and decay width Γ_{1s} shown in Table 5.1 are derived by solving eq. (5.21) in the above mentioned Sturmian function approach [5, 2, 80], with the mass difference between the K^-p and \bar{K}^0n channels treated as shown in eqs. (5.21) to (5.30). The negative energy shift in Table 5.1 means that the $1s$ energy level is effectively pushed up by the strong interaction since there exists one deep bound state, the $\Lambda(1405)$. Shown in Table 5.1 are also the energy shift ΔE_{1s}^0 and decay width Γ_{1s}^0 in the isospin symmetry limit, where the mass of proton is applied for both the proton and neutron and the mass of K^- for both the K^- and \bar{K}^0 .

It is found from Table 5.1 that the theoretical results in the approximation of the isospin symmetry limit are rather different from the full results where the mass difference between the K^-p and \bar{K}^0n channels is properly treated as shown in eqs. (5.21) to (5.30). Except for the decay width for the phenomenological $\bar{K}N$ potential [74, 75], the isospin symmetry approximation largely underestimates both the energy shift and decay width of the $1s$ kaonic hydrogen. On average, the theoretical result for the energy shift in the isospin symmetry limit is smaller by a factor of about 28% than the full result. For the equivalent local potentials referred to as ORB, HNJH, BNW, BMN in Table 5.1 which are constructed in the work [76], based respectively on the chiral SU(3) models [59, 60, 64, 66], the isospin symmetry approximation for the decay width of the $1s$ kaonic hydrogen is about 18% smaller than the result where the mass difference between the K^-p and \bar{K}^0n channels is considered.

The most recent experimental values on the energy shift and decay width of the ground state of kaonic hydrogen are respectively

$$\Delta E_{1s} = -193 \pm 37 \text{ (stat)} \pm 6 \text{ (syst)} \text{ eV} \quad (5.31)$$

and

$$\Gamma_{1s} = 249 \pm 111 \text{ (stat)} \pm 30 \text{ (syst)} \text{ eV} \quad (5.32)$$

obtained by the DEAR Collaboration [57], by a factor of almost 2 smaller than the experimental values measured by the KEK Collaboration [78]

$$\Delta E_{1s} = -323 \pm 63 \text{ (stat)} \pm 11 \text{ (syst)} \text{ eV} \quad (5.33)$$

and

$$\Gamma_{1s} = 407 \pm 208 \text{ (stat)} \pm 100 \text{ (syst)} \text{ eV} \quad (5.34)$$

Table 5.2: K^-p scattering lengths a_{K^-p} derived with local single-channel potentials [75, 76] compared with the K^-p scattering lengths \tilde{a}_{K^-p} (taken from [74, 76]) derived with the multi-channel effective interactions [59, 60, 64, 66, 74].

	a_{K^-p} [fm]	\tilde{a}_{K^-p} [fm]
AY [75]	$-0.678 + i0.506$	$-0.70 + i0.53$
ORB [59]	$-0.586 + i0.844$	$-0.617 + i0.861$
HNJH [60]	$-0.566 + i0.829$	$-0.608 + i0.835$
BNW [64]	$-0.487 + i0.838$	$-0.532 + i0.833$
BMN [66]	$-0.426 + i0.788$	$-0.410 + i0.824$

It is clear that except for the decay width derived with the phenomenological \overline{KN} potential referred to as AY in Table 5.1, all other theoretical values are much larger than the DEAR data. However, the theoretical results shown in Table 5.1 for both the pure phenomenological potential and the chiral SU(3) symmetry based potentials are fairly consistent with the KEK measurements, considering the large error of the KEK values of the $1s$ kaonic hydrogen decay width.

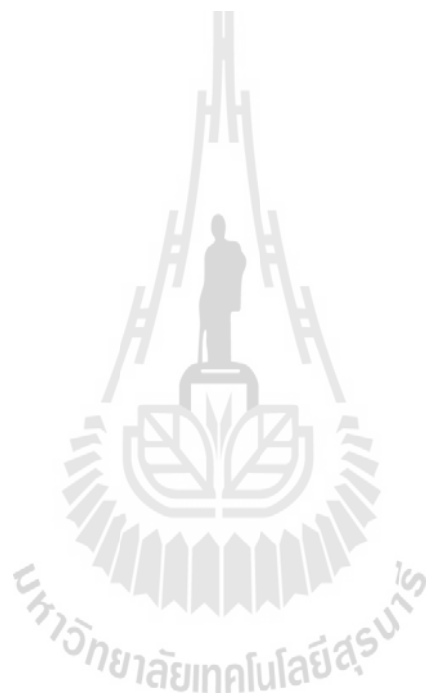
It is difficult to conclude whether the equivalent potentials based on chiral SU(3) models are reasonable since the KEK and DEAR data are so inconsistent each other. One may have to wait for the more accurate measurement of the $1s$ kaonic hydrogen by the SIDDHARTA collaboration.

One may argue that the theoretical results of the $1s$ kaonic hydrogen energy shifts and decay widths derived in the work with the the local, equivalent single-channel potentials may not reflect well the original equivalent interactions. To clear this issue, we compare the K^-p scattering lengths derived with the effective multi-channel interactions [59, 60, 64, 66, 74] with the ones evaluated with the local single-channel potentials [75, 76] using

$$a_{K^-p} = \frac{1}{2} (a_{I=0} + a_{I=1}) \quad (5.35)$$

in the isospin symmetry limit where the mass of proton is applied for both the proton and neutron and the mass of K^- for both the K^- and \bar{K}^0 . Shown in Table 5.2 are the K^-p scattering lengths a_{K^-p} derived with the local single-channel potentials [75, 76] which are employed here in this work to evaluate the energy shifts and decay widths of the $1s$ kaonic hydrogen and the K^-p scattering lengths \tilde{a}_{K^-p} derived with the multi-channel effective interactions [59, 60, 64, 66, 74]. It is found that the average discrepancy between a_{K^-p} and \tilde{a}_{K^-p} is less than 5%, much smaller than the effect resulted from the mass difference between the K^-p and \bar{K}^0n channels. One

may conclude that the local single-channel potentials [75, 76] applied to the KN system well approximate the original multi-channel effective interactions.



Chapter 6

Discussion and Conclusions

$\bar{p}D$ atoms, pionium and kaonic atoms are successfully studied in the work in the Sturmian function approach, with binding energies, decay widths and especially wave functions accurately evaluated. We summarize the main points of the work as follows:

The theoretical predictions for the energy shifts of the $2p \bar{p}D$ atomic states are totally out of line for all the $\bar{N}N$ potentials employed. The experimental data show that the averaged energy level of the $2p \bar{p}D$ atoms is pushed up by the strong interaction, the same as for the $1s \bar{p}D$ atoms, but the theoretical results uniquely show the averaged energy level shifting down. It is unlikely to improve, by treating the deuteron core more accurately, the theoretical predictions of the $\bar{N}N$ potentials in question for the $2p \bar{p}D$ energy shifts since a more accurate treatment of the deuteron core will lead to deeper $2p \bar{p}D$ atomic states. All the $\bar{N}N$ potentials employed in the work reproduce $\bar{N}N$ scattering data reasonably, but badly fail to reproduce the energy shifts of the $2p \bar{p}D$ atoms. The investigation of the $\bar{p}D$ atoms may provide a good platform for refining the $\bar{N}N$ interaction, especially at zero energy since the energy shifts of the $2p \bar{p}D$ atomic states are very sensitive to the $\bar{N}N$ strong interactions. The research here is just a preliminary work, where a frozen, S-state deuteron is employed. The work may be improved at two steps, considering that the numerical evaluation is time-consuming. One may, at the first step, solve the $\bar{p}D$ dynamical equation by expanding the $\bar{p}D$ wave function in a bi-wave basis of the Sturmian functions, where a realistic nucleon-nucleon potential is employed but the deuteron core is assumed to be at the S-state. Such an evaluation is still manageable at a personnel computer but it may take a week or longer. We may compare the results of the improved work with the results here to figure out how important an unfrozen deuteron core is. One may also consider, at the second step, to solve the $\bar{p}D$ dynamical equation by expanding the $\bar{p}D$ wave function in a bi-wave basis of the Sturmian

functions without any approximation, where realistic nucleon-nucleon and nucleon-antinucleon potentials are employed and the deuteron core is allowed to be at both the S- and D-waves. It is certain that the numerical calculation will take longer time but, anyway, we will do it after we complete the first-step improvement.

The ponium has been studied in various strong interactions, which may lead us to some points. The interaction in the meson-exchange model with the scalar coupling for the ε -exchange is unreasonably strong for the ponium system. The ponium system favors the gradient coupling for the ε -exchange, and demands a much weaker coupling for the t -channel ρ -exchange. A practical pion-pion potential may be derived from the chiral perturbation theory, which can reproduce both the ponium and pion-pion scattering data and is applicable to other multi-pion systems, for example, the pion gas probably produced in high-energy heavy-ion collisions. The local pion-pion potential, which has been widely applied to the ponium system, is indeed too strong at zero energy though it reproduces well the pion-pion phase shift data.

It is clear that except for the decay width derived with the phenomenological $\bar{K}N$ potential, all other theoretical values are much larger than the DEAR data. However, the theoretical results for both the pure phenomenological potential and the chiral SU(3) symmetry based potentials are fairly consistent with the KEK measurements, considering the large error of the KEK values of the $1s$ kaonic hydrogen decay width. However, it is difficult to conclude whether the equivalent potentials based on chiral SU(3) models are reasonable since the KEK and DEAR data are so inconsistent each other. One may have to wait for the more accurate measurement of the $1s$ kaonic hydrogen by the SIDDHARTA collaboration.

Bibliography

- [1] Y. Yan, Ph.D. Thesis, Universität Tübingen, 1994.
- [2] Y. Yan, R. Tegen, T. Gutsche and A. Faessler, Phys. Rev. C **56** (1997) 1596.
- [3] E. Holoien, Phys. Rev. **104**, 1301 (1965).
- [4] H. Schull and P.-O. Löwdin, J. Chem. Phys. **30**, 617 (1959).
- [5] M. Rotenberg, Adv. At. Mol. Phys. **6**, 233 (1970).
- [6] E. Truhlik, Nucl. Phys. **A296**, 134 (1978).
- [7] B. Gyarmati, A.T. Kruppa and J. Révai, Nucl. Phys. **A326**, 119 (1979); B. Gyarmati and A.T. Kruppa, Nucl. Phys. **A378**, 407 (1982).
- [8] B. Gyarmati, A.T. Kruppa, Z. Papp and G. Wolf, Nucl. Phys. **A417**, 393 (1984).
- [9] K.F. Pál, J. Phys. A **18**, 1665 (1985).
- [10] J. Carbonell, G. Ihle and J.-M. Richard, Z. Phys. **A334**, 329 (1989).
- [11] J. Carbonell, Private Communication.
- [12] J.S. Cohen and N.T. Padial, Phys. Rev. **A41**, 3460 (1990).
- [13] S. Ahmad, *et al.*, Phys. Lett. **157B**, 333 (1985); M. Ziegler, *et al.*, Phys. Lett. **206B**, 151 (1988); C.W.E. Van Eijk, *et al.*, Nucl. Phys. **A486**, 604 (1988); C.A. Baker, *et al.*, Nucl. Phys. **A483** 631 (1988); R. Bacher, *et al.*, Z. Phys. **A334**, 93 (1989).
- [14] K. Heitlinger, *et al.*, Z. Phys. **A342**, 359 (1992)
- [15] R.A. Bryan and R.J.N. Phillips, Nucl. Phys. **B5**, 201 (1968).
- [16] T.L. Trueman, Nucl. Phys. **26**, 57 (1961).

- [17] A.M. Green and S. Wycech, Nucl. Phys. **A377**, 441 (1982).
- [18] W. Schweiger, J. Haidenbauer and W. Plessas, Phys. Rev. C **32**, 1261 (1985).
- [19] J. Thaler, J. Phys. G **9**, 1009 (1983).
- [20] W.B. Kaufmann and H. Pilkuhn, Phys. Rev. C **17**, 215 (1978); W.B. Kaufmann, Phys. Rev. C **19**, 440 (1979).
- [21] M.A. Alberg, *et al.*, Phys. Rev. D **27**, 536 (1983).
- [22] B. Moussallam, Z. Phys. A **325**, 1 (1986).
- [23] C.B. Dover, J.M. Richard and J. Garbonell, Ann, Phys. (N.Y.) **130**, 70 (1980)
- [24] C.D. Dover, J.-M. Richard and J. Carbonell, Phys. Rev. C **44**, 1281 (1991).
- [25] M. Augsburger, *et al.*, Phys. Lett. B 461 (1999) 417.
- [26] D. Gotta, *et al.*, Nucl. Phys. A 660 (1999) 283.
- [27] S. Wycech, A.M. Green, and J.A. Niskanen, Phys. Lett. B 152 (1985) 308.
- [28] G.P. Latta, and P.C. Tandy, Phys. Rev. C 42 (1990) R1207.
- [29] G.Q. Liu, J.-M. Richard, and S. Wycech, Phys. Lett. B 2602 (1991) 15.
- [30] V.A. Karmanov, K.V. Protasov, and A.Yu. Voronin, Eur. Phys. J. A 8, 429 (2000).
- [31] M. Pignone, M. Lacombe, B. Loiseau, and R. Vinh Mau, Phys. Rev. C 50 (1994) 2710.
- [32] B. El-Bennich, M. Lacombe, B. Loiseau, and R. Vinh Mau, Phys. Rev. C 59 (1998) 2313.
- [33] S. Wycech, B. Loiseau, AIP Conference Proceedings, Volume 796 (2005) 131.
- [34] C.B. Dover, and J.M. Richard, Phys. Rev. C 21, 1466 (1980).
- [35] J.M. Richard, and M.E. Sainio, Phys. Lett. B 110, 349 (1982)
- [36] M. Kohno, and W. Weise, Nucl. Phys. A 454, 429 (1986).
- [37] R. Machleidt, K. Holinde and Ch. Elster, Phys. Rep. 149, 1 (1987).
- [38] B. Adeva, *et al.*, Proposal to the SPSLC, CERN/SPSLC 95-1 (1995).
- [39] J. Schacher *et al.* (DIRAC Collaboration), "Results from DIRAC", Proc. 4th Int. Workshop on Chiral Dynamics 2003: Theory and Experiment, 08-13 September 2003, Bonn.

- [40] Phys. Lett. B619, 50 (2005)
- [41] S. Deser, M. L. Goldberger, K. Baumann and W. Thirring, Phys. Rev. 96 (1954) 774.
- [42] J. L. Uretsky and T. R. Palfrey, Jr., Phys. Rev. 121 (1961) 1798; T. L. Trueman, Nucl. Phys. 26 (1961) 57.
- [43] H. Jallouli and H. Sazdjian, Phys. Rev. D58 (1998) 014011.
- [44] M. A. Ivanov, V. E. Lyubovitskij, E. Z. Lipartia and A. G. Rusetsky, Phys. Rev. D 58 (1998) 094024.
- [45] A. Gall, J. Gasser, V. E. Lyubovitskij and A. Rusetsky, Phys. Lett. B 462 (1999) 335; J. Gasser, V. E. Lyubovitskij and A. Rusetsky, Phys. Lett. B 471 (1999) 244; J. Gasser, V. E. Lyubovitskij, A. Rusetsky and A. Gall, Phys. Rev. D64 (2001) 016008.
- [46] H. Sazdjian, Phys. Lett. B490 (2000) 203.
- [47] I. Amirkhanov, I. Puzynin, A. Tarasov, O. Voskresenskaya and O. Zeinalova, Phys. Lett. B452 (1999) 155.
- [48] D. Lohse, J.W. Durso, K. Holinde and J. Speth, Nucl. Phys. **A516** (1990) 513.
- [49] S. Pislak *et al.*, Phys. Rev. Lett. **87** (2001) 221801.
- [50] J. A. Oller, E. Oset, Nucl. Phys. **A620** (1997) 438; **A629** (1998) 739.
- [51] D. R. Entem and R. Machleidt, Phys. Lett. **B524** (2002) 93.
- [52] J. Bijnens, G. Colangelo, G. Ecker, J. Gasser, M. E. Sainio, Nucl. Phys. **B508** (1997) 263.
- [53] A. Gashi, G. Rasche and W. S. Woolcock, Phys. Lett. **B513** (2001) 269; A. Gashi, G. C. Oades, G. Rasche, W. S. Woolcock, Nucl. Phys. **A699** (2002) 732.
- [54] G. Rasche and W.S. Woolcock, Nucl. Phys. A381 (1982) 405.
- [55] P. Indelicato, L. Simons, D. Gotta, and D. Anagnostopoulos, Phys. Rev. Lett. **91**, 240801 (2003).
- [56] H.-Ch. Schröder, *et al.*, Eur. Phys. J. C21, 433 (2001).
- [57] G. Beer *et al.* [DEAR Collaboration], Phys. Rev. Lett. **94**, 212302 (2005); M. Gargnelli *et al.* [DEAR Collaboration], Int. J. Mod. Phys. A **20**, 341-348 (2005).

- [58] J. A. Oller and U.-G. Meißner, Phys. Lett. B **500** (2001) 263.
- [59] E. Oset, A. Ramos, C. Bennhold, Phys. Lett. B **527** (2002) 99.
- [60] T. Hyodo, S.I. Nam, D. Jido, A. Hosaka, Phys. Rev. C **68** (2003) 018201.
- [61] U. -G. Meißner, U. Raha, and A. Rusetsky, Eur. Phys. J. C **35** (2004) 349; Eur. Phys. J. C **41** (2005) 213; Eur. Phys. J. C **47** (2006) 473.
- [62] A. N. Ivanov, M. Cargnelli, M. Faber, J. Marton, N.I. Troitskaya and J. Zmeskal, Eur. Phys. J. A **21** (2004) 11.
- [63] A. N. Ivanov, M. Cargnelli, M. Faber, H. Fuhrmann, V. A. Ivanova, J. Marton, N. I. Troitskaya and J. Zmeskal, Eur. Phys. J. A **25**, (2005) 329.
- [64] B. Borasoy, R. Nißler and W. Weise, Phys. Rev. Lett. **94** (2005) 213401; Eur. Phys. J. A **25** (2005) 79.
- [65] J. A. Oller, J. Prades and M. Verbeni, Phys. Rev. Lett. **95** (2005) 172502.
- [66] B. Borasoy, U.-G. Meißner and R. Nißler, Phys. Rev. C **74** (2006) 055201.
- [67] A. Limphirat, C. Kobdaj, M. Bleicher, Y. Yan and H. Stoecker, J. Phys. G: Nucl. Part. Phys. **36** (2009) 064049.
- [68] P.R. Auvil, Phys. Rev. D **4** (1971) 240.
- [69] B.C. Pearce, B.K. Jennings, Nucl. Phys. A **528** (1991) 655.
- [70] W.R. Gibbs, Li Ai, W.B. Kaufmann, Phys. Rev. C **57** (1998) 784.
- [71] A. Gashi, E. Matsinos, G. C. Oades, G. Rasche, W. S. Woolcock, Nucl. Phys. A **686** (2001) 463.
- [72] A. Gashi, G. Rasche, W.S. Woolcock, Phys. Lett. B **513** (2001) 269.
- [73] A. Gashi, G.C. Oades, G. Rasche, W.S. Woolcock, Nucl. Phys. A **699** (2002) 732.
- [74] Y. Akaishi, T. Yamazaki, Phys. Rev. C **65** (2002) 044005.
- [75] T. Yamazaki, Y. Akaishi, Phys. Rev. C **76** (2007) 045201.
- [76] T. Hyodo, W. Weise, Phys. Rev. C **77** (2008) 035204.
- [77] A. D. Martin, Nucl. Phys. B **179** (1981) 33.

- [78] M. Iwasaki *et al.* [KEK Collaboration], Phys. Rev. Lett. **78** (1997) 3067.
- [79] I. Amirkhanov, I. Puzynin, A. Tarasov, O. Voskresenskaya, O. Zeinalova, Phys. Lett. B **452** (1999) 155.
- [80] P. Suebka, Y. Yan, Phys. Rev. C **70** (2004) 034006.



Appendices



Appendix A

Curriculum Vitae

A.1 Prof. Dr. Prasart Suebka

School of Physics, Suranaree University of Technology

Nakhon Ratchasima 30000, Thailand

e-mail: prasart@sut.ac.th

EDUCATION

Ph.D.(Physics), 1984

Arizona State University, U.S.A.

M. S. (Physics), 1979

Indiana University, U.S.A.

M. Sc. (Physics), 1974

Chulalongkorn University, Thailand

B. Ed. (Hons.), 1972

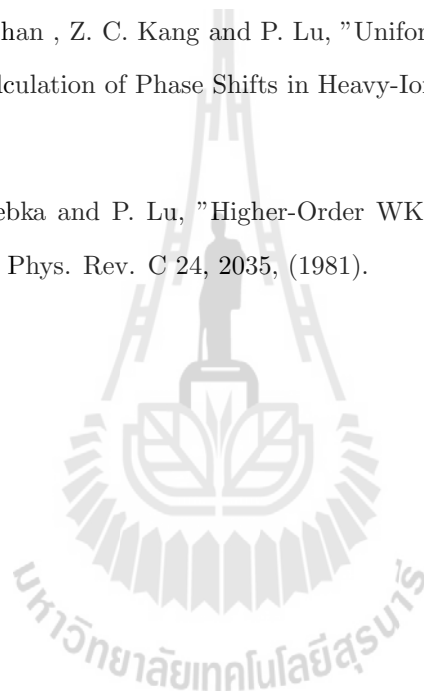
Sri Nakharinwirote University, Thailand

SELECTED PUBLICATIONS

1. Ayut Limphirat, Chinorat Kobdaj, Prasart Suebka and Yupeng Yan, "Decay width of ground and excited Ξ_b baryons in non-relativistic quark model" Phys. Rev. C 82, 055201 (2010).

2. Amand Faessler, K. Khosonthongkee, C. Kobdaj, A. Limphirat, P. Suebka and Y. Yan, "Low-lying baryon decays in 3P0 quark model", accepted for publication in *J. Phys. G: Nucl. Part. Phys.* **37**, 115002 (2010).
3. Y. Yan, W. Poonsawat, K. Khosonthongkee, C. Kobdaj, P. Suebka, "Kaonic hydrogen atoms with realistic potentials", *Phys. Rev. C* **81**, 065208 (2010).
4. Y. Yan, K. Khosonthongkee, C. Kobdaj, P. Suebka, " $e^+e^- \rightarrow N\bar{N}$ at Threshold and Proton Form Factor", *J. Phys. G: Nucl. Part. Phys.* **37**, 075007 (2010).
5. C. Nualchimplee, P. Suebka, Y. Yan and Amand Faessler, "Accurate evaluation of the 1s wave functions of kaonic hydrogen", *Hyperfine Interact* **193**, 97 (2009).
6. Y. Yan, C. Nualchimplee, P. Suebka, C. Kobdaj and K. Khosonthongkee, "Accurate evaluation of wave functions of ponium and kaonium", *Modern Physics Letters A* **24**, 901 (2009).
7. K. Kittimanapun, K. Khosonthongkee, C. Kobdaj, P. Suebka and Y. Yan, " $e^+e^- \rightarrow \omega\pi$ reaction and $\rho(1450)$ and $\rho(1700)$ mesons in a quark model", *Phys. Rev. C* **79** 025201 (2009).
8. Y. Yan, K. Khosonthongkee, C. Kobdaj, P. Suebka, Th. Gutsche, Amand Faessler and V.E. Lyubovitskij, " $\bar{p}D$ atoms in realistic potentials", *Physics Letter B* **659**, 555 (2008).
9. P. Suebka, C. Kobdaj and Y. Yan, "Reaction in non-relativistic quark model", *International Journal of Modern Physics E*, Vol. 14, No. 7 pp. 987-994 (2005).
10. Y. Yan, C. Kobdaj, P. Suebka, Y.M. Zheng, Amand Faessler, Th. Gutsche and V.E. Lyubovitskij, "Electron-positron annihilation into hadron-antihadron pairs", *Phys. Rev. C* **71** 025204 (2005).
11. J. E. Lowther, P. Manyum, and P. Suebka, "Electronic and structural properties of orthorhombic KTiOPo_4 and related isomorphic materials" *Physica Status Solidi (B) Basic Research* **242** (7), pp. 1392-1398 (2005).
12. P. Suebka and Y. Yan, "Accurate evaluation of ponium wave functions", *Phys. Rev. C* **70**, 034006 (2004).
13. E. B. Manoukian, N. Jearnkulprasert, and P. Suebka, "Photon number emission in Synchrotron radiation: Systematics for high-energy particles", *Nuovo Cimento della Societa Italiana di Fisica B*. **119** (1) pp. 9-15 (2004).

14. P. Suebka, "Atom in Paris Potential", *Mod. Phys. Lett. A.* 18, Nos. 2 -6, 402, (2003).
15. P. Lu , and P. Suebka, "Mechanism of Anomalous of Increase of Specific Heat Of He II near the λ - point", *Phys. Rev. B* 36, 760, (1987).
16. P. Lu and P. Suebka, "On the Calculated Cross Section of Fusion Reaction", *Letter A1 Nuovo Cimento* 42, 145, (1985).
17. P. Suebka and Pao Lu, "The T-Dependence Spectrum of He II", *Phys. Rev.* B31, 1603, (1985).
18. P. Suebka, C. K. Chan , Z. C. Kang and P. Lu, "Uniformly Approximated WKB Method as Used for the Calculation of Phase Shifts in Heavy-Ion Collision Problems", *Phys. Rev. C* 29, 844, (1984).
19. C. K Chan, P. Suebka and P. Lu, "Higher-Order WKB Phase Shifts for the Heavy-Ion Optical Potential", *Phys. Rev. C* 24, 2035, (1981).



A.2 Prof. Dr. Yupeng Yan

School of Physics, Suranaree University of Technology

Nakhon Ratchasima 30000, Thailand

e-mail: yupeng@sut.ac.th

PROFESSIONAL EXPERIENCE

Professor (February 2007 - present)

School of Physics, Suranaree University of Technology, Thailand

Associate Professor (September 2002 - February 2007)

School of Physics, Suranaree University of Technology, Thailand

Assistant Professor (June 1999 - September 2002)

School of Physics, Suranaree University of Technology, Thailand

Lecturer (June 1997 - June 1999)

School of Physics, Suranaree University of Technology, Thailand

Research Officer (January 1996 - June 1997)

Department of Physics, University of the Witwatersrand, South Africa

FRD Post Doctoral Fellow (Foundation for Research Development of South Africa) (January 1995 - December 1995) Department of Physics, University of the Witwatersrand, South Africa

Lecturer (September 1987 - April 1990)

Department of Physics, Nankai University, P. R. China

DAAD Senior Visiting Researcher (Deutscher Akademischer Austauschdienst)

(November 2001 - December 2001);

DAAD Senior Visiting Researcher (October 2000 - November 2000);

DAAD Visiting Researcher (April 1998 to June 1998,)

Institute for Theoretical Physics, Tuebingen University, Germany.

FRD Senior Research Officer (December 1999)

Department of Physics, University of the Witwatersrand, South Africa

Research Associate (July 1994 - December 1994),

Research Assistant (April 1990 - June 1994)

Institute for Theoretical Physics, Tuebingen University, Germany.

EDUCATION

Ph.D. in Physics (awarded on August 2, 1994)

Institute for Theoretical Physics, Tuebingen University, Germany.

Field of Study: Nuclear and Particle Theory

Title of Thesis: Nucleon-Antinucleon Bound States in Nonrelativistic Quark Models

Supervisor: Amand Faessler

Master of Science (awarded July 1987)

Department of Physics, Nankai University, P. R. China

Field of Study: Nuclear and Particle Theory

Title of Thesis: Vacuum Contribution to Nucleon-Nucleon Interaction

Supervisor: Guozu He

Bachelor of Science (awarded in July 1984)

Department of Physics, Nankai University, P. R. China

Field of Study: Electro-Optics

Title of Thesis: Design of Color-TV Bending Coil.

Supervisor: Shouqian Ding

AWARDS and RESEARCH GRANTS

ThEP Fund (2009-present) Project: Study of strong interactions through exotic atoms, chiral perturbation theory and heavy ion collisions

CHE Fund (2007-2009) Project: Theoretical Physics

NRCT Fund (2006) Project: Dynamical Studies of Intermediate and High Energy Heavy Ion

SUT Fund (Oct. 2005 - Sep. 2007) Project: Study of Protonium Atoms in Sturmian Function Approach

NRCT Fund (NRCT: National Research Council of Thailand) (Oct. 2001 - Sep. 2003) Project: Heavy Ion Reactions at Ultra-Relativistic Energies

RGJ Grant (RGJ: Royal Golden-Jubilee Ph.D. Project of Thailand, for more information see <http://rgj.trf.or.th/eng.htm>) (Oct. 2001 - Sep. 2006) Project: Low-Energy Pion-Proton Processes in Chiral Quark Models

RGJ Grant (October 2001 - September 2006) Project: Two-Pion and Two-Kaon Bound States in Chiral Quark Models

RGJ Grant (October 1998 - September 2003) Project: Baryon Weak and Electromagnetic Decays in Chiral Quark Models

RGJ Grant (October 1998 - September 2003) Project: Nucleon-Nucleon and Nucleon-Antinucleon Interactions

TRF Research Fund (Thailand Research Foundation) (Oct. 1997 - Sept. 1999) Suranaree University of Technology, Thailand

FRD Post Doctoral Fellowship (January 1995 - December 1995) (Foundation for Research Development of South Africa) University of the Witwatersrand, South Africa

Graduate Fellowship of Baden-Wuerttemberg of Germany (January 1992 - August 1994) Tuebingen University, Germany

INVITED LECTURES and TALKS:

The 9th conference on frontier topics of the interdisciplinary sciences of particle physics, nuclear physics and cosmology (July 20 - 24, 2010)

Talk: Decay widths of $X(1835)$ as $N\bar{N}$ bound state

Autumn School on Medium Energy Nuclear and Hadron Physics (October 8 - November 5, 2009)

Lectures: Antinucleon-nucleon interactions

International Workshop on the Physics of Excited Nucleon: NSTAR 2009 (April 19-22, 2009)

Talk: Electron-positron annihilation to nucleon-antinucleon pairs at low energies

The Fourth Asia-Pacific Conference on Few Body Problems in Physics (August 19-23, 2008)

Talk: Accurate evaluation of wave functions of ponium, kaonium and kaonic atom

The Third Asia-Pacific Conference on Few Body Problems in Physics (July 26-30, 2005)

Talk: Accurate Evaluation of Antiproton-Deuteron Atoms

CCAST World Laboratory Workshop (April 2-6, 2001)

China Center of the Advanced Science and Technology (CCAST), Beijing, P. R. China

Lectures: Proton-antiproton annihilation into two and three mesons (10 hours)

Nucleon-antinucleon atomic states (4 hours)

Quantum object is merely particle (4 hours)

(CCAST directed by T.D. Lee invites every year one outstanding young Chinese scholar working in each field abroad to give a series of lectures in Beijing)

Germany-East Asia Symposium of Nuclear and Particle Physics (May, 1998)

Talk: Proton-antiproton annihilation to two pions and two kaons

SELECTED PUBLICATIONS

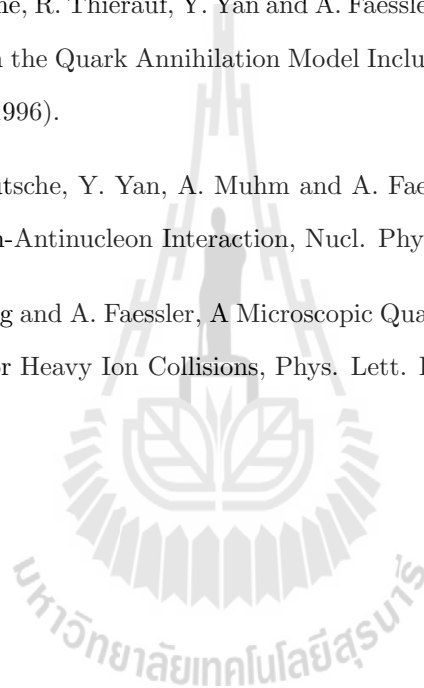
1. Xuzhong Kang, Shuifa Shen et al., "Study of the Multiphonon γ -Vibrational Bands in Even-Even $^{176-190}\text{Pt}$ Isotopes", Journal of the Physical Society of Japan 80, 044201 (2011).
2. Dai-Mei Zhou, Ayut Limphirat, Yu-Liang Yan, Xiao-Mei Li, Yu-Peng Yan, Ben-Hao Sa, "Impact of parton rescattering on analysis of p+p collision data at LHC energies", Phys. Lett. B 694, 435 (2011).
3. Nopmanee Supanam, Harold W. Fearing, Yupeng Yan, "Baryon chiral perturbation theory with virtual photons and leptons", JHEP 11, 124 (2010).
4. Ayut Limphirat, Chinorat Kobdaj, Prasart Suebka and Yupeng Yan, "Decay width of ground and excited Ξ_b baryons in non-relativistic quark model" Phys. Rev. C 82, 055201 (2010).
5. Amand Faessler, K. Khosonthongkee, C. Kobdaj, A. Limphirat, P. Suebka and Y. Yan, "Low-lying baryon decays in 3P0 quark model", accepted for publication in J. Phys. G: Nucl. Part. Phys. 37, 115002 (2010).

6. P. Srisawad, Y. M. Zheng, C. Fuchs, Amand Faessler, Y. Yan, C. Kobdaj and Y. Z. Xing, "Sigma meson production in proton-nucleus collisions", *International Journal of Modern Physics E* 19, 1843 (2010).
7. Shuifa Shen et al., "High spin states and level structure in ^{84}Rb ", *Phys. Rev. C* 82, 014306 (2010).
8. Y. Yan, W. Poonsawat, K. Khosonthongkee, C. Kobdaj, P. Suebka, "Kaonic hydrogen atoms with realistic potentials", *Phys. Rev. C* 81, 065208 (2010).
9. Y. Yan, K. Khosonthongkee, C. Kobdaj, P. Suebka, " $e^+e^- \rightarrow N\bar{N}$ at Threshold and Proton Form Factor", *J. Phys. G: Nucl. Part. Phys.* 37, 075007 (2010).
10. Y. Z. Xing, Y. M. Zheng, P. Srisawad and Y. Yan, "Influence of the Lorentz force on the centrality dependence of the kaon flow in heavy-ion collisions", *Europhysics Letters*, 90, 12002 (2010).
11. Y. Z. Xing, Y. M. Zheng, P. Srisawad and Y. Yan, "Transverse momentum dependence of differential directed flow of Λ hyperon within kaon covariant dynamics", *Sci. China Phys. Mech. Astron. (Sci. China Ser. G)* 53, 331 (2010).
12. P. Srisawad, Y. M. Zheng, Y. Yan and Y. Z. Xing, "Collective flow of K^+ meson within covariant Kaon dynamics", *Nuclear Physics A* 834, 590c (2010).
13. C. Nualchimplee, P. Suebka, Y. Yan and Amand Faessler, "Accurate evaluation of the 1s wave functions of kaonic hydrogen", *Hyperfine Interact* 193, 97 (2009).
14. Ayut Limphirat, Chinorat Kobdaj, Marcus Bleicher, Yupeng Yan and Horst Stoecker, "Strange and non-strange particle production in antiproton-nucleus collisions in the UrQMD model", *J. Phys. G: Nucl. Part. Phys.* 36, 064049 (2009).
15. Y. Yan, C. Nualchimplee, P. Suebka, C. Kobdaj and K. Khosonthongkee, "Accurate evaluation of wave functions of ponium and kaonium", *Modern Physics Letters A* 24, 901 (2009).
16. Pornrad Srisawad, Yu-Ming Zheng, Yupeng Yan, Chinorat Kobdaj and Yong-Zhong Xing, "Collective flow in heavy-ion collisions for $E_b = 0.25 - 1.15$ GeV/nucleon", *Modern Physics Letters A* 24, 1063 (2009).

17. K. Kittimanapun, K. Khosonthongkee, C. Kobdaj, P. Suebka and Y. Yan, " $e^+e^- \rightarrow \omega\pi$ reaction and $\rho(1450)$ and $\rho(1700)$ mesons in a quark model", Phys. Rev. C79 025201 (2009).
18. Y. Z. Xing, Y. M. Zheng, P. Srisawad, Y. Yan and C. Kobdaj, "Differential Directed Flow of K^+ Meson within Covariant Kaon Dynamics", Chinese Phys. Lett. 26, 022501 (2009).
19. Y. M. Zheng, C. Fuchs, P. Srisawad, A. Faessler, Y. Yan, C. Kobdaj and Y. Z. Xing, "Sigma meson production in nuclear reactions", Commun. Theor. Phys. 50, 725 (2008).
20. Y. Yan, K. Khosonthongkee, C. Kobdaj, P. Suebka, Th. Gutsche, Amand Faessler and V.E. Lyubovitskij, " $\bar{p}D$ atoms in realistic potentials", Physics Letter B 659, 555 (2008).
21. P. Srisawad, Y. M. Zheng, C. Fuchs, A. Faessler, Y. Yan, C. Kobdaj and Y.Z. Xing, "Sigma meson production in heavy ion collisions at intermediate energies", International Journal of Modern Physics A 22, 6219 (2007).
22. Y. Yan, P. Suebka, C. Kobdaj and K. Khosonthogkee, "Strong interaction in pionium", Nuclear Physics A 790, 402c (2007).
23. K. Khosonthogkee, N. Supanam, Y. Yan, Th. Gutsche and Amand Faessler, " $N^*(1440)$ decays in a hybrid baryon model", Nuclear Physics A 790, 518c (2007).
24. K. Pumsa-ard, W. Uchai and Y. Yan, "Meson exchange theory for high energy proton-proton scattering", International Journal of Modern Physics E, Vol. 15, No. 1 pp. 109-119 (2006).
25. P. Suebka, C. Kobdaj and Y. Yan, " $\pi\pi$ Reaction in non-relativistic quark model", International Journal of Modern Physics E, Vol. 14, No. 7 pp. 987-994 (2005).
26. Y. Yan, C. Kobdaj, P. Suebka, Y.M. Zheng, Amand Faessler, Th. Gutsche and V.E. Lyubovitskij, "Electron-positron annihilation into hadron-antihadron pairs", Phys. Rev. C71 025204 (2005).
27. P. Suebka and Y. Yan, "Accurate evaluation of pionium wave functions", Phys. Rev. C 70, 034006 (2004).
28. Yu-Ming Zheng, C. Fuchs, Amand Faessler, K. Shekhter, Yu-Peng Yan and Chinorat Kobdaj, "Covariant kaon dynamics and kaon flow in heavy ion collisions" Phys. Rev. C 69, 034907 (2004).

29. Ben-Hao Sa, Zhong-Qi Wang, Xu Cai, Dai-Mei Zhou, C. Kobdaj and Yu-Peng Yan, "Energy dependence of string fragmentation function and ϕ meson production" Commun. Theor. Phys. 41, 291 (2004).
30. Y. M. Zheng, C. Fuchs, Amand Faessler, K. Shekhter, P. Srisawad, Y. Yan and C. Kobdaj, "Influence of Chiral Mean Field on Kaon In-plane Flow in Heavy Ion Collisions" Commun. Theor. Phys. 41, 746 (2004).
31. K. Khosonthongkee, V.E. Lyubovitskij, Th. Gutsche, Amand Faessler, K. Pumsa-ard, S. Cheedket and Y. Yan, Axial form factor of the nucleon in the perturbative chiral quark model, J. Phys. G: Nucl. Part. Phys. 30, 793 (2004).
32. S. Cheedket, V.E. Lyubovitskij, Th. Gutsche, Amand Faessler, K. Pumsa-ard and Y. Yan, Electromagnetic form factors of the baryon octet in the perturbative chiral quark model, Eur. Phys. J. A. 20, 317 (2004).
33. Y. Yan, K. Pumsa-ard, R. Tegen, Th. Gutsche, V.E. Lyubovitskij and Amand Faessler, Nucleon-Nucleon High-Energy Scattering, Int. J. Mod. Phys. E 12, 367 (2003).
34. Y. Yan, C. Kobdaj, W. Uchai, A. Faessler, T. Gutsche and Y.M. Zheng, Electron-Positron Annihilation into Nucleon-Antinucleon Pairs, Mod. Phys. Lett. A18, 370 (2003).
35. Y.M. Zheng, Z.L. Chu, C. Fuchs, A. Faessler, W. Xiao, D.P. Hua, Y. Yan, Transverse Flow of Kaons in Heavy-Ion Collisions, Chin. Phys. Lett. 19, 926 (2002).
36. Y. Yan, Baryon Structure and Baryon Interaction, CCAST (World Laboratory) Workshop Series: Volume 129 (2001).
37. Y. Yan and R. Tegen, On the Quark Substructure of the Hydrogen Nucleus, Suranaree Journal of Science and Technology Vol. 7, 42 (2000).
38. Y. Yan and R. Tegen, Proton-Antiproton to two Pions and two Kaons in Baryon Exchange and Meson Pole Diagrams, Nucl. Phys. A648, 89 (1999).
39. Y. Yan and R. Tegen, Scale Invariance of g_A/g_V in Dirac-scalar and Dirac-vector Quark Confining Potentials, ISMPE 13 (1998).
40. Y. Yan, T. Gutsche, R. Thierauf, A. Muhn and A. Faessler, Quasinuclear Nucleon-Antinucleon Bound States in the Quark Annihilation Model, J. Phys. G23, 605 (1997).

41. Y. Yan, R. Tegen, T. Gutsche and A. Faessler, Nucleon-Antinucleon Bound States and Sturmian Function Method, *Phys. Rev. C*56, 1596 (1997).
42. E. Bauer, T. Gutsche, A. Muhm, R. Thierauf, Y. Yan, A. Faessler and R.V. Mau, The Rho Parameter of Low-Energy Proton-Antiproton Scattering in the 3P0 Quark Model, *Phys. Lett. B*386, 50 (1996).
43. Y. Yan and R. Tegen, Role of Tensor Meson Pole and Delta Exchange Diagrams in Proton-Antiproton to two Pions, *Phys. Rev. C*54, 1441 (1996).
44. A. Muhn, T. Gutsche, R. Thierauf, Y. Yan and A. Faessler, Proton-Antiproton Annihilation into Two Mesons in the Quark Annihilation Model Including Final State Interaction, *Nucl. Phys. A*598, 285 (1996).
45. R. Thierauf, T. Gutsche, Y. Yan, A. Muhm and A. Faessler, The Non-Relativistic Quark Model and Nucleon-Antinucleon Interaction, *Nucl. Phys. A*588, 783 (1995).
46. Y. Yan, S.W. Huang and A. Faessler, A Microscopic Quark Model of Pion Nucleon to Kaon Sigma Reactions for Heavy Ion Collisions, *Phys. Lett. B*354, 24 (1995).



A.3 Asst. Prof. Dr. Chinorat Kobdaj

School of Physics, Suranaree University of Technology

Nakhon Ratchasima 30000, Thailand

e-mail: kobdaj@g.sut.ac.th

EDUCATION

Ph.D. (Theoretical Physics), 1995

University of London, UK

Master of Science (Mathematical Physics), 1990

University of London, UK

Bachelor of Science (Physics), 1989

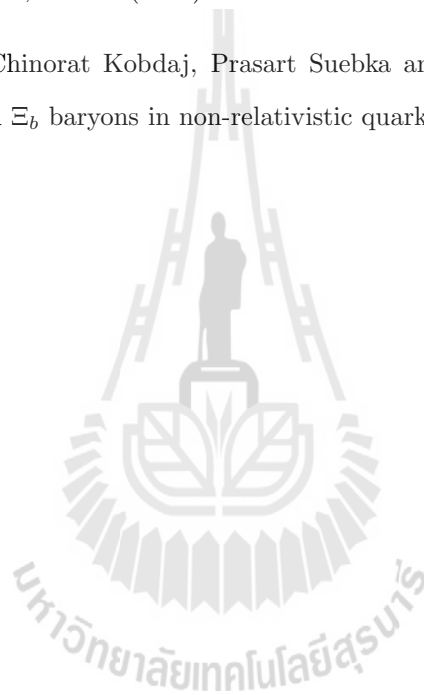
Chulalongkorn University, Thailand

SELECTED PUBLICATIONS

1. C. Kobdaj and S. Thomas, "Nonabelian Vortices" Nucl. Phys. B 413, [FS] 689 (1994).
2. C. Kobdaj and S. Thomas "Screening in two-dimensional nonabelian vortex systems" Nucl. Phys. B 438, [FS] 607 (1995).
3. Y. Yan, C. Kobdaj, W. Uchai, Amand Faessler, T. Gutsche and Y. M. Zheng, " e^+e^- Annihilation in to $\bar{N}N$ Pairs" Mod. Phys. Lett. A 18, 370 (2003).
4. Ben-Hao Sa, Zhong-Qi Wang, Xu Cai, Dai-Mei Zhou, C. Kobdaj and Yu-Peng Yan, "Energy dependence of string fragmentation function and ϕ meson production" Commun. Theor. Phys. 41, 291 (2004).
5. Yu-Ming Zheng, C. Fuchs, Amand Faessler, K. Shekhter, Yu-Peng Yan and Chinorat Kobdaj, "Covariant kaon dynamics and kaon flow in heavy ion collisions" Phys. Rev. C 69, 034907 (2004).
6. Y. M. Zheng, C. Fuchs, Amand Faessler, K. Shekhter, P. Srisawad, Y. Yan and C. Kobdaj, "Influence of Chiral Mean Field on Kaon In-plane Flow in Heavy Ion Collisions" Commun. Theor. Phys. 41, 746 (2004).

7. Y. Yan, C. Kobdaj, P. Suebka, Y.M. Zheng, Amand Faessler, Th. Gutsche and V.E. Lyubovitskij, "Electron-positron annihilation into hadron-antihadron pairs", Phys. Rev. C71, 025204 (2005).
8. P. Suebka, C. Kobdaj and Y. Yan, "Reaction in non-relativistic quark model", International Journal of Modern Physics E, Vol. 14, No. 7 pp. 987-994 (2005).
9. Y. Yan, P. Suebka, C. Kobdaj and K. Khosonthongkee, "Strong interaction in pionium", Nuclear Physics A 790, 402c (2007).
10. P. Srisawad, Y. M. Zheng, C. Fuchs, A. Faessler, Y. Yan, C. Kobdaj and Y.Z. Xing, "Sigma meson production in heavy ion collisions at intermediate energies", International Journal of Modern Physics A 22, 6219 (2007).
11. Y. Yan, K. Khosonthongkee, C. Kobdaj, P. Suebka, Th. Gutsche, Amand Faessler and V.E. Lyubovitskij, " $\bar{p}D$ atoms in realistic potentials", Physics Letter B 659, 555 (2008).
12. Y. M. Zheng, C. Fuchs, P. Srisawad, A. Faessler, Y. Yan, C. Kobdaj and Y. Z. Xing, "Sigma meson production in nuclear reactions", Commun. Theor. Phys. 50, 725 (2008).
13. Y. Z. Xing, Y. M. Zheng, P. Srisawad, Y. Yan and C. Kobdaj, "Differential Directed Flow of K^+ Meson within Covariant Kaon Dynamics", Chinese Phys. Lett. 26, 022501 (2009).
14. K. Kittimanapun, K. Khosonthongkee, C. Kobdaj, P. Suebka and Y. Yan, " $e^+e^- \rightarrow \omega\pi$ reaction and $\rho(1450)$ and $\rho(1700)$ mesons in a quark model", Phys. Rev. C79 025201 (2009).
15. Pornrad Srisawad, Yu-Ming Zheng, Yupeng Yan, Chinorat Kobdaj and Yong-Zhong Xing, "Collective flow in heavy-ion collisions for $E_b = 0.25 - 1.15$ GeV/nucleon", Modern Physics Letters A 24, 1063 (2009).
16. Y. Yan, C. Nualchimplee, P. Suebka, C. Kobdaj and K. Khosonthongkee, "Accurate evaluation of wave functions of pionium and kaonium", Modern Physics Letters A 24, 901 (2009).
17. Ayut Limphirat, Chinorat Kobdaj, Marcus Bleicher, Yupeng Yan and Horst Stoecker, "Strange and non-strange particle production in antiproton-nucleus collisions in the UrQMD model", J. Phys. G: Nucl. Part. Phys. 36, 064049 (2009).
18. Y. Yan, K. Khosonthongkee, C. Kobdaj, P. Suebka, " $e^+e^- \rightarrow N\bar{N}$ at Threshold and Proton Form Factor", J. Phys. G: Nucl. Part. Phys. 37, 075007 (2010).

19. Y. Yan, W. Poonsawat, K. Khosonthongkee, C. Kobdaj, P. Suebka, "Kaonic hydrogen atoms with realistic potentials", *Phys. Rev. C* 81, 065208 (2010).
20. P. Srisawad, Y. M. Zheng, C. Fuchs, Amand Faessler, Y. Yan, C. Kobdaj and Y. Z. Xing, "Sigma meson production in proton-nucleus collisions", *International Journal of Modern Physics E* 19, 1843 (2010).
21. Amand Faessler, K. Khosonthongkee, C. Kobdaj, A. Limphirat, P. Suebka and Y. Yan, "Low-lying baryon decays in 3P0 quark model", accepted for publication in *J. Phys. G: Nucl. Part. Phys.* 37, 115002 (2010).
22. Ayut Limphirat, Chinorat Kobdaj, Prasart Suebka and Yupeng Yan, "Decay width of ground and excited Ξ_b baryons in non-relativistic quark model" *Phys. Rev. C* 82, 055201 (2010).



Appendix B

Publications

1. P. Suebka, C. Kobdaj and Y. Yan, “ $\pi\pi$ Reaction in non-relativistic quark model”, International Journal of Modern Physics E, Vol. 14, No. 7 pp. 987-994 (2005).
2. Y. Yan, P. Suebka, C. Kobdaj and K. Khosonthogkee, “Strong interaction in pionium”, Nuclear Physics A 790, 402c (2007).
3. Y. Yan, K. Khosonthongkee, C. Kobdaj, P. Suebka, Th. Gutsche, Amand Faessler and V.E. Lyubovitskij, “ $\bar{p}D$ atoms in realistic potentials”, Physics Letter B 659, 555 (2008).
4. Y. Yan, C. Nualchimplee, P. Suebka, C. Kobdaj and K. Khosonthongkee, “Accurate evaluation of wave functions of pionium and kaonium”, Modern Physics Letters A 24, 901 (2009).
5. C. Nualchimplee, P. Suebka, Y. Yan and Amand Faessler, “Accurate evaluation of the 1s wave functions of kaonic hydrogen”, Hyperfine Interact 193, 97 (2009).
6. Y. Yan, W. Poonsawat, K. Khosonthongkee, C. Kobdaj, P. Suebka, “Kaonic hydrogen atoms with realistic potentials”, Phys. Rev. C 81, 065208 (2010).

$\pi\pi$ REACTION IN NON-RELATIVISTIC QUARK MODEL*

P. SUEBKA, C. KOBDAJ and Y. YAN

*School of Physics, Suranaree University of Technology,
111 University Avenue, Nakhon Ratchasima 30000, Thailand*

Received 31 May 2005

Revised 6 July 2005

The reaction $\pi^+\pi^- \rightarrow \pi^+\pi^-$ is studied in the non-relativistic quark model with the 3P_0 quark–antiquark dynamics. The cross section of the reaction $\pi^+\pi^- \rightarrow \pi^+\pi^-$ is well reproduced even for rather high energies.

Keywords: Pion–pion scattering; non-relativistic quark model.

1. Introduction

The study of the low and intermediate pion–pion scattering as well as other strong interaction processes lies within the domain of non-perturbative QCD. Due to the lack of effective methods in obtaining solutions to QCD in the non-perturbative confinement region, we have to resort to the development of effective models. Meson-exchange models, non-relativistic quark models and chiral perturbation theories are among the most successful approaches in studying the strong interaction at low and intermediate energies.

The meson-exchange models have made tremendous successes in the investigation of the nucleon–nucleon, meson–nucleon and meson–meson and nucleon–antinucleon interactions at low and intermediate energies,^{1–6} and even in the study of the elastic nucleon–nucleon scattering at high energies.^{7,8} The models, however, have many free parameters involved, which is the unavoidable shortcoming of the meson-exchange models.

The chiral perturbation theory, which is the effective field theory of the Standard Model below the scale of spontaneous chiral symmetry breaking, has become a well-established method for describing the low-energy interactions of the pseudoscalar octet. Elastic pion–pion scattering at low energies is a good example of mesonic chiral perturbation theory. A complete analytical calculation of the reaction $\pi\pi \rightarrow \pi\pi$ at the two-loop order has been performed.⁹ However, it is difficult to use the

*This work was supported in part by the Suranaree University of Technology grants SUT 1-105-46-12-44 and SUT 1-105-48-36-12.

method to describe reactions with higher energies, for example, for the reaction $\pi\pi \rightarrow \pi\pi$ at an energy around the $f_2(1270)$ threshold.

In the non-relativistic constituent quark model, quarks and antiquarks are kept as the relevant degrees of freedom whereas the interaction between the quarks, particularly the confinement, is described by effective, QCD inspired potentials. The advantage of the quark model over the meson exchange model is based on the fact that a large number of experimental observables can be understood qualitatively and quantitatively by a low number of free parameters. An overview of the various quark models with a detailed discussion can be found in Ref. 10. The processes of meson decays, baryon decays, meson–baryon reactions and baryon–antibaryon annihilations have been successfully described in the non-relativistic quark models^{11–17} in the 3P_0 quark–antiquark dynamics which has been proven to be the dominant $\bar{Q}Q$ dynamics in the non-relativistic quark models.

The reaction $\pi\pi \rightarrow \pi\pi$ at the isospin $I = 2$ channel has been successfully studied in the non-relativistic quark model,¹⁸ where the 3P_0 quark diagrams have no contribution. We will now study the $\pi\pi \rightarrow \pi\pi$ reaction in the non-relativistic quark model where the 3P_0 quark diagram dominates.

2. Reaction $\pi^+\pi^- \rightarrow \pi^+\pi^-$ in 3P_0

The success of the 3P_0 quark–antiquark dynamics in studying the reactions $e^+e^- \rightarrow \pi^+\pi^-$ and $e^+e^- \rightarrow \bar{N}N$ suggests that the reactions are completely dominated by the intermediate vector mesons.¹⁹ We may also expect that in the 3P_0 quark–antiquark dynamics, the processes shown in Fig. 1 would dominate the reaction $\pi^+\pi^- \rightarrow \pi^+\pi^-$, where a $\pi^+\pi^-$ pair annihilates into a virtual time-like meson, then the virtual meson decays into a $\pi^+\pi^-$ pair. The transition amplitude for the two step process takes the form

$$T = \langle \pi\pi | V_{67}^\dagger | \Psi_m \rangle \frac{1}{E - M} \langle \Psi_m | V_{23} | \pi\pi \rangle, \tag{1}$$

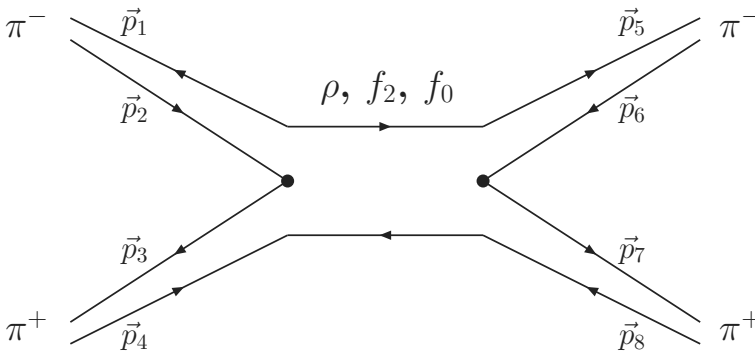


Fig. 1. $\pi^+\pi^- \rightarrow \pi^+\pi^-$ in the 3P_0 quark model.

where E is the center-of-mass energy of the two π system. Ψ_m and M are respectively the wave function and mass of the intermediate mesons. $\langle\pi\pi|V_{67}^\dagger|\Psi_m\rangle$ and $\langle\Psi_m|V_{23}|\pi\pi\rangle$ are respectively the transition amplitude of the intermediate meson annihilation into two pions and the one of two pions annihilation into a virtual time-like meson. V_{ij} is the quark–antiquark 3P_0 vertex defined as

$$\begin{aligned} V_{ij} &= \lambda \boldsymbol{\sigma}_{ij} \cdot (\mathbf{p}_i - \mathbf{p}_j) \hat{F}_{ij} \hat{C}_{ij} \delta(\mathbf{p}_i + \mathbf{p}_j) \\ &= \lambda \sum_{\mu} \sqrt{\frac{4\pi}{3}} (-1)^{\mu} \sigma_{ij}^{\mu} y_{1\mu}(\mathbf{p}_i - \mathbf{p}_j) \hat{F}_{ij} \hat{C}_{ij} \delta(\mathbf{p}_i + \mathbf{p}_j) \end{aligned} \quad (2)$$

where $y_{1\mu}(\mathbf{q}) = |\mathbf{q}|Y_{1\mu}(\hat{q})$, $\boldsymbol{\sigma}_{ij} = (\boldsymbol{\sigma}_i + \boldsymbol{\sigma}_j)/2$, \mathbf{p}_i and \mathbf{p}_j are the momenta of quark and antiquark created out of the vacuum. \hat{F}_{ij} and \hat{C}_{ij} are the flavor and color operators projecting a quark–antiquark pair to the respective vacuum quantum numbers. The derivation and interpretation of the quark–antiquark 3P_0 dynamics may be found in the literature.^{11,12}

The evaluation of the transition amplitudes of one meson to two mesons in the quark–antiquark 3P_0 dynamics is straightforward (see details in Appendix A). There are two free parameters, the size parameter of the mesons and the effective strength parameter λ in the quark–antiquark 3P_0 vertex. The size parameter b may be nailed down by the reaction $\rho^0 \rightarrow e^+e^-$, as done in Ref. 19, where we get $b = 3.847 \text{ GeV}^{-1}$.

The effective strength parameter λ may be determined by the reaction $\rho^0 \rightarrow \pi^+\pi^-$. The decay width of the reaction takes the form

$$\Gamma = \frac{\pi}{2} M_{\rho} k \left(\frac{M_{\pi}}{E_{\pi}} \right)^2 |T_{\rho \rightarrow \pi^+\pi^-}|^2, \quad (3)$$

where $T_{\rho \rightarrow \pi^+\pi^-}$ is the transition amplitude given in Eq. (A.5) in Appendix A. k is the momentum of the final pion mesons in the center-of-mass system. We consider the final pions to be rather relativistic. We associate each pion with a “minimal relativity” factor $(M_{\pi}/E_{\pi})^{1/2}$.² With the size parameter $b = 3.847 \text{ GeV}^{-1}$, determined from the reaction $\rho^0 \rightarrow e^+e^-$ in Ref. 19, the experimental value $\Gamma = 150 \text{ MeV}$ for the decay width of $\rho^0 \rightarrow \pi^+\pi^-$ requires the effective strength parameter λ to take the value $\lambda = 2.73$.

The differential cross section for the reaction $a + b \rightarrow c + d$ takes, in the center-of-mass system, the form²¹

$$\frac{d\sigma}{d\Omega} = \frac{v_f}{v_i} |M(\mathbf{p}, \mathbf{k})|^2, \quad (4)$$

with

$$M(\mathbf{p}, \mathbf{k}) = -(2\pi)^2 \frac{E_c E_d}{E_{cm}} T(\mathbf{p}, \mathbf{k}), \quad (5)$$

where $v_f \equiv E_f/dp$ and $v_i \equiv dE_i/dk$ are the final and initial speeds of the pions, respectively. \mathbf{p} and \mathbf{k} are the incoming and outgoing momenta, respectively. The

total cross section for the reaction $\pi^+\pi^- \rightarrow \pi^+\pi^-$, in terms of the partial wave transition amplitudes, is

$$\sigma = (2\pi)^4 \frac{E_{cm}^2}{16} \sum_L |T_L(k)|^2, \quad (6)$$

with the partial wave transition amplitudes $T_L(p, k)$ defined as

$$T_L(p, k) = 2\pi \int_0^\pi T(\mathbf{p}, \mathbf{k}) \sqrt{\frac{2l+1}{4\pi}} P_L(\cos\theta) \sin\theta d\theta, \quad (7)$$

where θ is the angle between the momenta \mathbf{k} and \mathbf{p} . For the reaction $\pi^+\pi^- \rightarrow \pi^+\pi^-$, the partial wave transition amplitudes T_L in Eq. (6) are linear combinations of the amplitudes in the isospin basis, that is

$$T_{2n} = \frac{2}{3}T_{2n}(I=0) + \frac{1}{3}T_{2n}(I=2), \quad (8)$$

$$T_{2n+1} = T_{2n+1}(I=1),$$

where I is the isospin of the $\pi\pi$ system.

Figure 2 shows the predictions for the cross section of the reaction $\pi^+\pi^- \rightarrow \pi^+\pi^-$ in the diagram in Fig. 1. The dashed line is the prediction for which only the ρ and $f_2(1270)$ mesons²⁰ are involved as the intermediate states. There is no free parameter in the calculation. The length parameter b of the ρ meson is fixed in the reaction $\rho \rightarrow e^+e^-$ and for simplicity we assign the meson $f_2(1270)$ the same length parameter. The effective strength parameter λ of the 3P_0 quark–antiquark

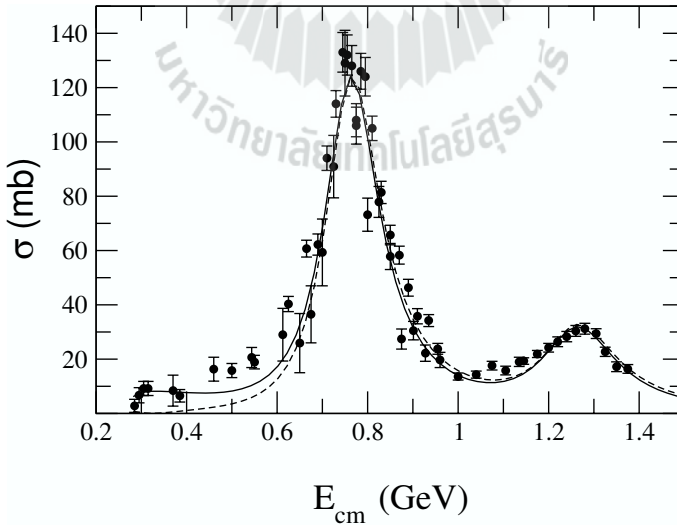


Fig. 2. Predictions for the cross section of the reaction $\pi^+\pi^- \rightarrow \pi^+\pi^-$ in the 3P_0 quark model with the ρ and $f_2(1270)$ mesons as the intermediate states (dashed line) and with the ρ , $f_2(1270)$ and $f_0(600)$ mesons as the intermediate states (solid line). Experimental data (solid circles) are taken from Refs. 22 and 23.

vertex is fixed in the reaction $\rho \rightarrow \pi\pi$. It is found that the prediction is reasonable at the resonance region of the reaction $\pi^+\pi^- \rightarrow \pi^+\pi^-$, that is the center-of-mass energies from 0.6 to 1.4 GeV. However, it is noticed that the prediction for the low energy region (lower than 0.6 GeV), with only the ρ and $f_2(1270)$ mesons involved as the intermediate states, is much lower than the experimental data.^{22,23}

The solid line in Fig. 2 stands for the model prediction where the ρ , $f_2(1270)$ and $f_0(600)$ mesons²⁰ are considered as the intermediate states in Fig. 1. In this work, all the three mesons are assigned the same length parameter $b = 3.847 \text{ GeV}^{-1}$, as determined in the process $\rho \rightarrow e^+e^-$. We employ the effective strength parameter $\lambda = 2.73$ for the processes $\pi^+\pi^- \rightarrow \rho \rightarrow \pi^+\pi^-$ and $\pi^+\pi^- \rightarrow f_2(1270) \rightarrow \pi^+\pi^-$, and $\lambda = 2.0$ for the process $\pi^+\pi^- \rightarrow f_0(600) \rightarrow \pi^+\pi^-$. It is noticed that the application of the same strength parameter $\lambda = 2.73$ to all the three processes leads to poor predictions for the low energy region. Although the contribution of the $f_0(600)$ intermediate state is negligible for the higher energy region (over 0.6 GeV), the involvement of the f_0 meson is very much necessary for understanding the reaction $\pi^+\pi^- \rightarrow \pi^+\pi^-$ at the low energy region (lower than 0.6 GeV).

3. Discussions and Conclusions

The cross section of the reaction $\pi^+\pi^- \rightarrow \pi^+\pi^-$ is well reproduced in the 3P_0 quark model in which there is only one free parameter involved. The reaction $\pi^+\pi^- \rightarrow \pi^+\pi^-$ at higher energies is dominated by the processes $\pi^+\pi^- \rightarrow \rho \rightarrow \pi^+\pi^-$ and $\pi^+\pi^- \rightarrow f_2(1270) \rightarrow \pi^+\pi^-$, while the process $\pi^+\pi^- \rightarrow f_0(600) \rightarrow \pi^+\pi^-$, is the dominant one at lower energies.

The parameters for the processes $\rho^0 \rightarrow e^+e^-$ and $\rho^0 \rightarrow \pi^+\pi^-$ work well with the meson f_2 but are not applicable to the meson $f_0(600)$. This may indicate that ρ and $f_2(1270)$ are mesons of the same kind while $f_0(600)$ is something else.

Appendix A. One Meson Annihilation Into Two Mesons in the 3P_0 Model

We study the reaction of one meson annihilation into two mesons shown in Fig. 3 in the quark–antiquark 3P_0 vertex of Eq. (2). The σ_{ij} in the vertex can be understood as an operator projecting a quark–antiquark pair onto a spin-1 state. It can be easily proven that

$$\langle 0, 0 | \sigma_{ij}^\mu | [\bar{\chi}_i \otimes \chi_j]_{JM} \rangle = (-1)^M \sqrt{2} \delta_{J,1} \delta_{M,-\mu}. \quad (\text{A.1})$$

Concerning SU(2) flavor a quark–antiquark pair which annihilates into the vacuum must have zero isospin. So the operator \hat{F}_{ij} has the similar property $\langle 0, 0 | \hat{F}_{ij} | T, T_z \rangle = \sqrt{2} \delta_{T,0} \delta_{T_z,0}$. For the color part, we simply have $\langle 0, 0 | \hat{C}_{ij} | q_\alpha^i \bar{q}_\beta^j \rangle = \delta_{\alpha\beta}$, where α and β are color indices. The transition amplitude for a meson decay into two mesons in the 3P_0 model is defined as $T = \langle \Psi_i | V_{45}^\dagger | \Psi_f \rangle$, where $|\Psi_i\rangle$ and $|\Psi_f\rangle$ are the initial and final states, respectively. The initial state is simply the one

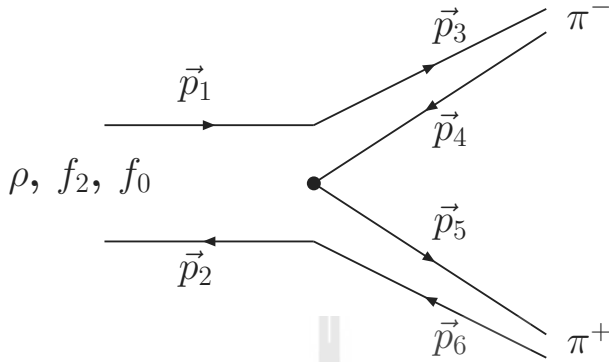


Fig. 3. A meson annihilation into a $\pi^+\pi^-$ pair in the 3P_0 quark model.

meson wave function (WF) having the form

$$|\Psi_i\rangle_S = N_S e^{-\frac{1}{8}b^2(\mathbf{p}_1-\mathbf{p}_2)^2} \left[\frac{1}{2}^{(1)} \otimes \frac{1}{2}^{(2)} \right]_{S_i} \left[\frac{1}{2}^{(1)} \otimes \frac{1}{2}^{(2)} \right]_{T_i}, \quad (\text{A.2})$$

for the S -wave meson (for example, the ρ meson), and

$$\begin{aligned} &|\Psi_i\rangle_P \\ &= N_P e^{-\frac{1}{8}b^2(\mathbf{p}_1-\mathbf{p}_2)^2} \left[y_{1\mu}(\mathbf{p}_1-\mathbf{p}_2) \otimes \left[\frac{1}{2}^{(1)} \otimes \frac{1}{2}^{(2)} \right]_{S'} \right]_{S_i} \left[\frac{1}{2}^{(1)} \otimes \frac{1}{2}^{(2)} \right]_{T_i}, \end{aligned} \quad (\text{A.3})$$

for the P -wave mesons (for example, the $f_2(1270)$ meson), where $y_{1\mu}(\mathbf{q}) = |\mathbf{q}|Y_{1\mu}(\hat{q})$.

We have spin $S_i = 1$ and isospin $T_i = 1$ for the ρ meson (the isospin projection $T_z = 0$ for ρ^0), spin $S_i = 2$ and isospin $T_i = 0$ for the $f_2(1270)$ meson, and spin $S_i = 0$ and isospin $T_i = 0$ for the $f_0(600)$ meson. Here we have employed the harmonic oscillator interaction between quark and antiquark. The final state $|\Psi_f\rangle$ is formed by coupling the WF's of the two final mesons. For two S -wave mesons we have

$$\begin{aligned} |\Psi_f\rangle &= N_s N_s e^{-\frac{1}{8}b^2(\mathbf{p}_3-\mathbf{p}_4)^2} e^{-\frac{1}{8}b^2(\mathbf{p}_5-\mathbf{p}_6)^2} \left[\left[\frac{1}{2}^{(3)} \otimes \frac{1}{2}^{(4)} \right]_{S_1} \otimes \left[\frac{1}{2}^{(5)} \otimes \frac{1}{2}^{(6)} \right]_{S_2} \right]_{S_f, M_f} \\ &\times \left[\left[\frac{1}{2}^{(3)} \otimes \frac{1}{2}^{(4)} \right]_{T_1} \otimes \left[\frac{1}{2}^{(5)} \otimes \frac{1}{2}^{(6)} \right]_{T_2} \right]_{T, T_z}. \end{aligned} \quad (\text{A.4})$$

The transition amplitude is derived as

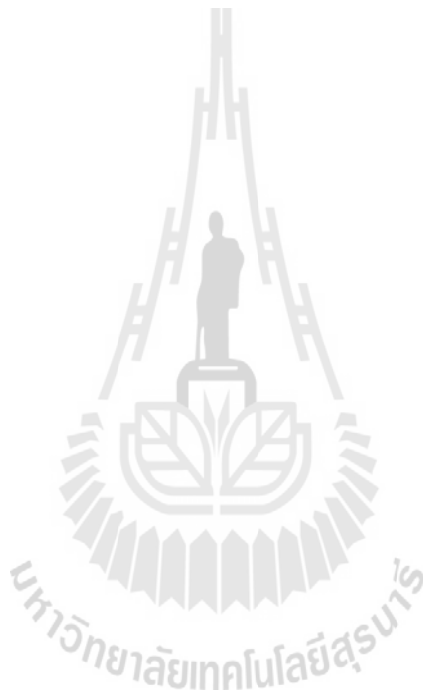
$$\begin{aligned}
 T_{\rho \rightarrow \pi^+ \pi^-} &= \lambda \frac{2^4}{3^3 \sqrt{3} \pi^{1/4}} b^{3/2} k e^{-\frac{1}{12} b^2 k^2} (-1)^m Y_{1m}(\hat{k}), \\
 T_{f_2(1270) \rightarrow \pi^+ \pi^-} &= \lambda \frac{2^4 \sqrt{3}}{3^4 \sqrt{5} \pi^{1/4}} b^{5/2} k^2 e^{-\frac{1}{12} b^2 k^2} (-1)^m Y_{2m}(\hat{k}), \\
 T_{f_0(600) \rightarrow \pi^+ \pi^-} &= \lambda \frac{2^3}{3^4 \pi^{1/4}} b^{1/2} e^{-\frac{1}{12} b^2 k^2} (2b^2 k^2 - 9),
 \end{aligned} \tag{A.5}$$

where \mathbf{k} is the momentum of the outgoing π mesons in the center-of-mass system. Note that we have, for simplicity, set the ρ , $f_2(1270)$, $f_0(600)$ and π mesons to have the same size parameter b , that is $N_S = (b^2/\pi)^{3/4}$ and $N_P = (2b^5/3\pi^{1/2})^{1/2}$.

References

1. W. N. Cottingham and R. V. Mau, *Phys. Rev.* **130** (1963) 735; W. N. Cottingham, M. Lacombe, B. Loiseau, J. M. Richard and R. V. Mau, *Phys. Rev. B* **8** (1973) 800; M. Lacombe *et al.*, *Phys. Rev. C* **21** (1980) 861.
2. R. Machleidt, K. Holinde and Ch. Elster, *Phys. Rep.* **149** (1987) 1.
3. D. Lohse, J. W. Durso, K. Holinde and J. Speth, *Nucl. Phys. A* **516** (1990) 513.
4. T. Hippchen J. Haidenbauer, K. Holinde and V. Mull, *Phys. Rev. C* **44** (1991) 1323; V. Mull, J. Haidenbauer, T. Hippchen and K. Holinde, *ibid.* **44** (1991) 1337; J. Haidenbauer, T. Hippchen and R. Tegen, *ibid.* **44** (1991) 1812.
5. J. Côte, M. Lacombe, B. Loiseau, B. Moussallam and R. V. Mau, *Phys. Rev. Lett.* **48** (1982) 1319; M. Lacombe, B. Loiseau, B. Moussallam and R. V. Mau, *Phys. Rev. C* **29** (1993) 1800.
6. Y. Yan and R. Tegen, *Phys. Rev. C* **54** (1996) 1441.
7. W. R. Gibbs and B. Loiseau, *Phys. Rev. C* **50** (1994) 2742.
8. Y. Yan, L. Pumsa-ard, R. Tegen, T. Gutsche, V. E. Lyubovitskij and A. Faessler, *IJMPE* **12** (2003) 367.
9. J. Bijnens, G. Colangelo, G. Ecker, J. Gasser and M. E. Sainio, *Phys. Lett. B* **374** (1996) 210.
10. C. B. Dover, T. Gutsche, M. Maruyama and A. Faessler, *Prog. Part. Nucl. Phys.* **29** (1992) 87.
11. A. Le Yaouanc *et al.*, *Phys. Rev. D* **8** (1973) 2223; *ibid.* **9** (1974) 1415; *ibid.* **11** (1975) 1272.
12. M. Maruyama, S. Furui and A. Faessler, *Nucl. Phys. A* **472** (1987) 643; M. Maruyama, S. Furui, A. Faessler and R. V. Mau, *ibid.* **473** (1987) 649; T. Gutsche, M. Maruyama and A. Faessler, *ibid.* **503** (1989) 737.
13. A. Muhn, T. Gutsche, R. Thierauf, Y. Yan and A. Faessler, *Nucl. Phys. A* **598** (1996) 285.
14. Y. Yan, R. Tegen, T. Gutsche and A. Faessler, *Phys. Rev. C* **56** (1997) 1596.
15. C. B. Dover, T. Gutsche and A. Faessler, *Phys. Rev. C* **43** (1991) 379.
16. T. Gutsche, R. D. Viollier and A. Faessler, *Phys. Lett. B* **331** (1994) 8.
17. Y. Yan, S. W. Huang and A. Faessler, *Phys. Lett. B* **354** (1995) 24.
18. T. Barnes and E. S. Swanson, *Phys. Rev. D* **46**, 131 (1992); *Phys. Rev. C* **63** (2001) 025204.
19. Y. Yan, C. Kobdaj, P. Suebka, Y. M. Zheng, A. Faessler, Th. Gutsche and V. E. Lyubovitskij, *Phys. Rev. C* **71** (2005) 025204.
20. S. Eidelman *et al.*, *Phys. Lett. B* **592** (2004) 1.

21. C. Joachain, *Quantum Collision Theory* (North-Holland Publishing Comp., 1975).
22. S. D. Protopopescu *et al.*, *Phys. Rev. D* **7** (1973) 1279.
23. E. A. Alekseeva *et al.*, *ZETF* **82** (1982) 1007.



Strong interactions in ponium*

Y. Yan^a, P. Suebka^a, C. Kobdaj^a and K. Khosonthongkee^a

^aSchool of Physics, Suranaree University of Technology,
111 University Avenue, Nakhon Ratchasima 30000, Thailand

Ponium is investigated in various pion-pion strong interactions which reproduce well the pion-pion scattering data. It is found that the ground-state ponium wave functions in those realistic pion-pion strong interactions are considerably different from the hydrogen-like one at small distance. One may suggest that some pion-pion interactions may need to be largely improved before applied to the pion-pion atomic system.

1. INTRODUCTION

Ponium is the $\pi^+\pi^-$ atomic state, bound mainly by the Coulomb force and effected by the strong interaction between the two pions. Ponium decays predominantly into $\pi^0\pi^0$ via strong interaction, which probes the low energy interactions of the pions, in particular, at zero energy. It has been believed that ponium might be employed to test more accurately the predictions of chiral perturbation theory. The investigation of ponium has recently become of particular interest due to the ponium DIRAC experiment. The preliminary result [1] of the ponium lifetime, based on part of the collected data, has been published as $\tau_{1s} = [2.91^{+0.49}_{-0.62}] \times 10^{-15}$ seconds.

The nonrelativistic formula of the ponium lifetime in the lowest order of electromagnetic interactions reads [2]

$$\Gamma_0 = \frac{2}{9} \frac{64\pi p}{M^3} |\psi(0)|^2 |a_0 - a_2|^2 \quad (1)$$

where M is the mass of the $\pi\pi$ system, p is the center-of-mass momentum of the π^0 in the ponium system, $\psi(0)$ is the $1s$ ponium function at the origin ($r = 0$), and a_0 and a_2 are the S-wave $\pi\pi$ scattering lengths for isospin $I = 0$ and 2, respectively.

Any reasonable prediction of the ponium lifetime in the potential model (or say, in the quantum mechanics regime) must be based on the accurate knowledge of the wave function of the ponium state. The evaluation of the ponium wave function has been a challenge to numerical methods. Required is an approach, which is able to overcome the longstanding problem, that is, accounting for both the strong short-range interaction and the long-range Coulomb force. In this work we apply the numerical approach, which has been successfully applied to the protonium problem [3], to study the ponium problem here. The aim of this work is to reveal whether the pion-pion interactions, which reproduce well the pion-pion scattering data, are applicable to ponium.

*Supported in part by SUT grants

2. STRONG INTERACTIONS IN PIONIUM

Since Pionium has a small $\pi^0\pi^0$ component, the coupling of the $\pi^+\pi^-$ and $\pi^0\pi^0$ configurations must be properly treated. The dynamical equations of the $(\pi^+\pi^-, \pi^0\pi^0)$ system may take the general form

$$E\Psi = (H_0 + \mathbf{V}_c + \mathbf{V}_s)\Psi \quad (2)$$

with

$$\Psi = \begin{pmatrix} \psi_{\pi^+\pi^-} \\ \psi_{\pi^0\pi^0} \end{pmatrix}, \quad H_0 = \begin{pmatrix} H_{\pi^+\pi^-}^0 & 0 \\ 0 & H_{\pi^0\pi^0}^0 \end{pmatrix}, \quad \mathbf{V}_c = \begin{pmatrix} V_c & 0 \\ 0 & 0 \end{pmatrix} \quad (3)$$

where V_c is the coulomb interaction between extended charges of pions. The charge distribution of π^+ and π^- is described by the form factor $F(q) = 1/(1 + q^2/a^2)$, with $a = 0.77$ GeV. The strong interaction matrix \mathbf{V}_s takes, for example, for S-wave pionium the form

$$\mathbf{V}_s = \begin{pmatrix} \frac{2}{3}V^0 + \frac{1}{3}V^2 & \frac{\sqrt{2}}{3}(V^2 - V^0) \\ \frac{\sqrt{2}}{3}(V^2 - V^0) & \frac{1}{3}V^0 + \frac{2}{3}V^2 \end{pmatrix} \quad (4)$$

where V^0 and V^2 are respectively the isospin 0 and 2 strong interactions of the $\pi\pi$ system. The binding energy of pionium is derived as $E_b = E - 2m_\pi$ with m_π the mass of π^\pm .

The pionium problem is more difficult than other exotic problems, for example, the protonium problem in term of evaluating their wave functions since the Bohr radius of pionium is much larger than the one of protonium. Here we solve the pionium dynamical equation in eq. (1) by expanding the pionium wave function Ψ in the complete basis of Sturmian functions [4].

Table 1
Energy shift of the 1s pionium compared to the pure Coulomb interaction level.

	Model B	Model C	Model D	Model E	Data
$\Delta E(eV)$	-1.36	-2.97	-3.93	-2.87	–
$\tau(10^{-15}s)$	1.10	2.68	2.59	2.24	$2.91_{-0.62}^{+0.49}$

Studied first in the work is the pion-pion interactions in the work [5], which are worked out in the meson-exchange model and reproduce well the pion-pion phase shift data. The work considers the contributions of the ρ -exchange in the t -channel and the exchanges of ρ , f_2 and ε (a scalar meson) in the s -channel for the very low energy pion-pion scattering. For the ε -exchange both the scalar coupling and the gradient coupling are studied. For our convenience, we may call the interaction with the ε scalar coupling Model A and the one with the ε gradient coupling Model B. It is found that the pion-pion potential in Model A supports a number of pion-pion deep bound states which have never been observed. The deep bound states stem mainly from the large contribution of the ε scalar coupling at zero energy. The predictions for the energy shift and the pionium lifetime in

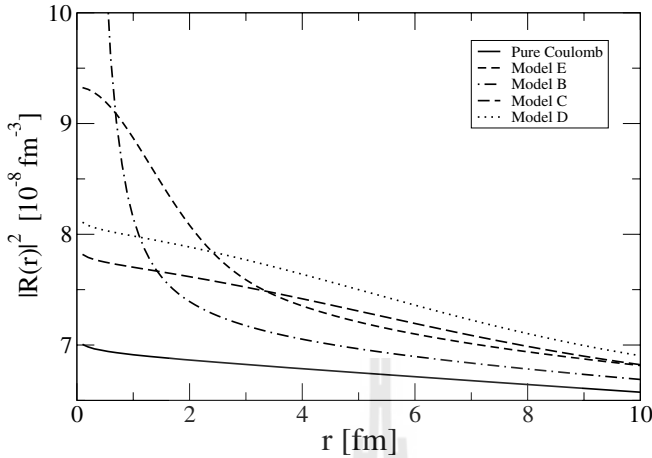


Figure 1. Squared $1s$ radial wave functions for the $\pi^+\pi^-$ component of pionium. For comparison the pure Coulomb interaction wave function is also plotted. All the wave functions have been multiplied by a factor 10^8 .

Model B are shown in Table 1 while the $1s$ radial wave function for the $\pi^+\pi^-$ component of pionium is plotted in Fig. 1 as the dash-dotted curve. The lifetime in Model B and also in other models below is evaluated using eq. (1) with the scattering length a_0 and a_2 taken from [6]. Although Model B does not support any deep bound state, it is obvious that the interaction in the model is also too strong at zero energy. The main contributor to the pion-pion interaction at zero energy in Model B is the t -channel ρ -exchange. The pion-pion potentials in both Model A and B reproduce very well the pion-pion scattering data, but both of them fail to give reasonable predictions for the pionium properties.

The pion-pion interaction has been studied intensively in the chiral perturbation theory (ChPT) and considerable successes have been achieved in the regime. However, the ChPT success in reproducing pion-pion experimental data does not necessarily guarantee a practical potential which is applicable to multi-pion systems where the off-shell effects play important roles. In this work we study the pionium system in the pion-pion potentials derived in the chiral Lagrangian [7]. In analogy to the works [8], where meson-meson potentials provided by the lowest order chiral Lagrangian combined with Lippmann-Schwinger equations are applied to study the reactions of $\gamma\gamma$ to two mesons and two mesons to two mesons, and the derivation of the nucleon-nucleon interaction in chiral perturbation theory [9], we impose a cutoff of the momentum on the pion-pion potentials derived in the chiral perturbation theory. Devoted to Model C is the potential derived from the tree diagram of the leading order Lagrangian \mathcal{L}_2 in [7] with the cutoff $\Lambda = 0.1$ GeV for all momenta and to Model D is the potential derived from the tree diagrams of the chiral Lagrangian $\mathcal{L}_{eff} = \mathcal{L}_2 + \mathcal{L}_4 + \mathcal{L}_6$ in [7] with the same cutoff. Shown in Table 1 are the predictions of Model C and D for the energy shifts and lifetimes of pionium, and the long dashed and dotted curves in Fig. 1 are the $1s$ radial wave functions for the $\pi^+\pi^-$

component of pionium. All the parameters of the potentials are taken from the works [7]. It is found that the predictions of Model C and D are fair good with a reasonable cutoff $\Lambda = 0.1$ GeV, hence it is possible to construct a pion-pion potential in the framework of the chiral perturbation theory. Of course, to get a practical pion-pion potential one needs to reproduce not only the pionium data but also the pion-pion scattering data by solving Lippmann-Schwinger equations for both bound and scattering problems.

The last model interaction we study here is a simple, local potential which has been widely employed for studying the influence of the hadronic interaction on pionium wave functions [10]. The potential is independent of both the energy of the pionium system and pion masses, and reproduce very well the phase shifts given by two-loop chiral perturbation theory [7]. For convenience, we may call the pion-pion interaction here Model E. In consistence with the works [10], we solve for the $(\pi^+\pi^-, \pi^0\pi^0)$ system here the coupled Schrödinger equations employed in the works [10].

The predictions of Model E for the energy shift and lifetime of the $1s$ pionium state are listed in Table 1 while the evaluated $1s$ radial wave functions for the $\pi^+\pi^-$ component of pionium is plotted in Fig. 1 as the dashed curve. It is clear that the ground state pionium wave function in Model E is considerably different from the hydrogen-like one at small distances, and the $1s$ pionium lifetime is much shorter than the experimental value.

3. SUMMARY AND CONCLUSIONS

The pionium system has been studied in various strong interactions, which may lead us to some points. The interaction in the meson-exchange model with the scalar coupling for the ε -exchange is unreasonably strong for the pionium system. The pionium system strongly favors the gradient coupling for the ε -exchange, and demands a much weaker coupling for the t -channel ρ -exchange. A practical pion-pion potential may be derived from the chiral perturbation theory, which can reproduce both the pionium and pion-pion scattering data and is applicable to other multi-pion systems, for example, the pion gas probably produced in high-energy heavy-ion collisions. The local pion-pion potential, which has been widely applied to the pionium system, is indeed too strong at zero energy though it reproduces well the pion-pion phase shift data.

REFERENCES

1. B. Adeva *et al.*, Phys. Lett. B 619 50 (2005) 50.
2. T. L. Trueman, Nucl. Phys. 26 (1961) 57.
3. Y. Yan, R. Tegen, T. Gutsche and A. Faessler, Phys. Rev. C 56 (1997) 1596.
4. M. Rotenberg, Adv. At. Mol. Phys. 6 (1970) 233.
5. D. Lohse, J.W. Durso, K. Holinde and J. Speth, Nucl. Phys. A 516 (1990) 513.
6. S. Pislak *et al.*, Phys. Rev. Lett. 87 (2001) 221801.
7. J. Bijmans, G. Colangelo, G. Ecker, J. Gasser, M. E. Sainio, Nucl. Phys. B 508 (1997) 263.
8. J. A. Oller, E. Oset, Nucl. Phys. A 620 (1997) 438; A 629 (1998) 739.
9. D. R. Entem and R. Machleidt, Phys. Lett. B 524 (2002) 93.
10. A. Gashi, G. Rasche and W. S. Woolcock, Phys. Lett. B 513 (2001) 269; A. Gashi, G. C. Oades, G. Rasche, W. S. Woolcock, Nucl. Phys. A 699 (2002) 732.

$\bar{p}D$ atoms in realistic potentials

Y. Yan^{a,*}, K. Khosonthongkee^a, C. Kobdaj^a, P. Suebka^a, Th. Gutsche^b, Amand Faessler^b,
V.E. Lyubovitskij^b

^a School of Physics, Suranaree University of Technology, 111 University Avenue, Nakhon Ratchasima 30000, Thailand

^b Institute for Theoretical Physics, Tübingen University, Auf der Morgenstelle 4, D-72076 Tübingen, Germany

Received 2 November 2007; received in revised form 22 November 2007; accepted 29 November 2007

Available online 5 December 2007

Editor: J.-P. Blaizot

Abstract

The $\bar{p}D$ atoms are studied in various realistic, popular $\bar{N}N$ potentials. The small energy shifts and decay widths of the atoms, which stem from the short-ranged strong interactions between the antiproton and deuteron, are evaluated in a well-established, accurate approach based on the Sturmian functions. The investigation reveals that none of the employed potentials, which reproduce the $\bar{N}N$ scattering data quite well, is able to reproduce the experimental data of the energy shifts of the $2p$ $\bar{p}D$ atomic states. The energy shifts of the $2p$ $\bar{p}D$ atomic states are very sensitive to the $\bar{N}N$ strong interactions, hence the investigation of the $\bar{p}D$ atoms is expected to provide a good platform for refining the $\bar{N}N$ interaction, especially at zero energy.

© 2007 Elsevier B.V. All rights reserved.

PACS: 36.10.Gv; 13.75.Cs; 03.65.Ge

Keywords: $\bar{p}D$ atom; $\bar{N}N$ interaction; Sturmian function; Accurate numerical approach

1. Introduction

The second simplest antiprotonic atom is the antiprotonic deuteron atom $\bar{p}D$, consisting of an antiproton and a deuteron bound mainly by the Coulomb interaction but distorted by the short range strong interaction. The study of the $\bar{p}D$ atom is much later and less successful than for other exotic atoms like the protonium and ponium. Experiments were carried out at LEAR just in very recent years to study the properties of the $\bar{p}D$ atom [1,2]. Even prior to the experiments some theoretical works [3–5] had been carried out to study the $\bar{p}D$ atomic states in simplified $\bar{p}D$ interactions. Recently, a theoretical work [6] proposed a mechanism explaining the unexpected behavior, of the scattering lengths of $\bar{N}N$ and $\bar{p}D$ system, that the imaginary part of the scattering length does not increase with the size of the nucleus.

In the theoretical sector, one needs to overcome at least two difficulties in the study of the $\bar{p}D$ atom. First, the interaction between the antiproton and the deuteron core should be derived from realistic $\bar{N}N$ interactions, for example, the Paris $\bar{N}N$ potentials [7–9], the Dover–Richard $\bar{N}N$ potentials I (DR1) and II (DR2) [10,11], and the Kohnno–Weise $\bar{N}N$ potential [12]. Even if a reliable $\bar{p}D$ interaction is in hands, the accurate evaluation of the energy shifts and decay widths (stemming from the strong $\bar{p}D$ interactions) and especially of the nuclear force distorted wave function of the atom is still a challenge. It should be pointed out that the methods employed in the works [3–5] are not accurate enough for evaluating the wave functions of the $\bar{p}D$ atoms.

In the present work we study the $\bar{p}D$ atom problem employing a properly adapted numerical method based on Sturmian functions [13]. The method accounts for both the strong *short* range nuclear potential (local and non-local) and the *long* range Coulomb force and provides directly the wave function of the $\bar{p}D$ system with complex eigenvalues $E = E_R - i\frac{\Gamma}{2}$. The protonium and ponium problems have been successfully investigated [14,15] in the numerical approach. The numerical method

* Corresponding author.

E-mail address: yupeng@sut.ac.th (Y. Yan).

is much more powerful, accurate and much easier to use than all other methods applied to the exotic atom problem in history. The $\bar{p}D$ interactions in the work are derived from various realistic $\bar{N}N$ potential, which is state-dependent. The work is organized as follows. The $\bar{p}D$ interactions are expressed in Section 2 in terms of the $\bar{N}N$ interactions. In Section 3 the energy shifts and decay widths of the $1s$ and $2p$ $\bar{p}D$ atomic states are evaluated. Discussions and conclusions are given in Section 3, too.

2. $\bar{p}D$ interactions in terms of $\bar{N}N$ potentials

We start from the Schrödinger equation of the antiproton–deuteron system in coordinate space

$$\left(\frac{P_\rho^2}{2M_\rho} + \frac{P_\lambda^2}{2M_\lambda} + V_{12}(\vec{r}_2 - \vec{r}_1) + V_{13}(\vec{r}_3 - \vec{r}_1) + V_{23}(\vec{r}_3 - \vec{r}_2) \right) \Psi(\vec{\lambda}, \vec{\rho}) = E\Psi(\vec{\lambda}, \vec{\rho}) \quad (1)$$

where $\vec{\lambda}$ and $\vec{\rho}$ are the Jacobi coordinates of the system, defined as

$$\vec{\lambda} = \vec{r}_3 - \frac{\vec{r}_1 + \vec{r}_2}{2}, \quad \vec{\rho} = \vec{r}_2 - \vec{r}_1, \quad (2)$$

$M_\rho = M/2$ and $M_\lambda = 2M/3$ are the reduced masses. Here we have assigned, for simplicity, the proton and neutron the same mass M . Eq. (1) can be expressed in the form, where the strong interaction is expressed in the isospin basis,

$$\left(\frac{P_\rho^2}{2M_\rho} + \frac{P_\lambda^2}{2M_\lambda} + V_S + V_C \right) \Psi(\vec{\lambda}, \vec{\rho}) = E\Psi(\vec{\lambda}, \vec{\rho}) \quad (3)$$

where V_S and V_C stand for the nuclear interaction and Coulomb force, respectively, and take the forms

$$V_S = V_{\bar{N}N}^0(\vec{r}_2 - \vec{r}_1) + \frac{1}{4} [V_{\bar{N}N}^0(\vec{r}_3 - \vec{r}_1) + V_{\bar{N}N}^0(\vec{r}_3 - \vec{r}_2)] + \frac{3}{4} [V_{\bar{N}N}^1(\vec{r}_3 - \vec{r}_1) + V_{\bar{N}N}^1(\vec{r}_3 - \vec{r}_2)], \quad (4)$$

$$V_C = \frac{1}{2} [V_C(\vec{r}_3 - \vec{r}_1) + V_C(\vec{r}_3 - \vec{r}_2)] \quad (5)$$

V^0 and V^1 in Eq. (4) are the isospin 0 and 1 nuclear interactions, respectively. Note that we have assigned \vec{r}_{12} as the relative coordinate of the deuteron core.

One may express the interactions V_C and V_S in Eqs. (4) and (5) in terms of the interactions of certain $\bar{N}N$ states. In the $|JMLS\rangle$ basis of the $\bar{p}D$ states

$$|JMLS\rangle = |(L_\rho \otimes L_\lambda)_L \otimes (S_{12} \otimes S_3)_S\rangle_{JM} \quad (6)$$

we derive

$$(H_0 + W_C(\lambda, \rho) + V_{\bar{N}N}^0(\rho) + W_S(\lambda, \rho))\Psi(\lambda, \rho) = E\Psi(\lambda, \rho) \quad (7)$$

with

$$H_0 = \frac{P_\rho^2}{2M_\rho} + \frac{P_\lambda^2}{2M_\lambda} \quad (8)$$

W_C and W_S in Eq. (7) are respectively the Coulomb force and strong interaction between the antiproton and deuteron, and $V_{\bar{N}N}^0$ the interaction between the proton and neutron in the deuteron core. W_C and W_S are derived explicitly as

$$W_C(\lambda, \rho) = \frac{1}{2} \int_{-1}^1 dx V_C(r_{13}), \quad (9)$$

$$W_S(\lambda, \rho) = \frac{1}{2} \int_{-1}^1 dx \sum_{Q, Q'} \langle P|Q\rangle \langle Q|V_{\bar{N}N}(\vec{r}_{13})|Q'\rangle \langle Q'|P'\rangle \quad (10)$$

with

$$V_{\bar{N}N}(\vec{r}_{13}) = \frac{1}{2} V_{\bar{N}N}^0(\vec{r}_{13}) + \frac{3}{2} V_{\bar{N}N}^1(\vec{r}_{13}), \quad (11)$$

$$r_{13} \equiv |\vec{r}_1 - \vec{r}_3| = \left(\lambda^2 + \frac{\rho^2}{4} - \lambda\rho x \right)^{1/2} \quad (12)$$

where $x = \cos\theta$ with θ being the angle between $\vec{\lambda}$ and $\vec{\rho}$. In Eq. (10) $|P\rangle \equiv |JMLS\rangle$ and $|P'\rangle \equiv |JML'S\rangle$ are as defined in Eq. (6) while the states $|Q\rangle$ and $|Q'\rangle$ are

$$|Q\rangle = |(L_\sigma \otimes S_{13})_{J_\sigma} \otimes (L_\gamma \otimes S_2)_{J_\gamma}\rangle_{JM}, \quad (13)$$

$$|Q'\rangle = |(L'_\sigma \otimes S_{13})_{J_\sigma} \otimes (L_\gamma \otimes S_2)_{J_\gamma}\rangle_{JM}. \quad (14)$$

Here $\vec{\sigma}$ and $\vec{\gamma}$ are also the Jacobi coordinates of the system, defined as

$$\vec{\gamma} = \vec{r}_2 - \frac{\vec{r}_1 + \vec{r}_3}{2}, \quad \vec{\sigma} = \vec{r}_3 - \vec{r}_1. \quad (15)$$

So defined the states $|Q\rangle$ and $|Q'\rangle$ is based on the consideration that the $\bar{N}N$ interactions can be easily expressed in the $|J_\sigma M_\sigma L_\sigma S_{13}\rangle$ basis of the $\bar{N}N$ states. Note that $\langle P|Q\rangle$ depends on not only the quantum numbers of the states $|P\rangle$ and $|Q\rangle$, but also λ , ρ and the angle θ between $\vec{\lambda}$ and $\vec{\rho}$ resulting from the projection of the orbital angular momenta between different Jacobi coordinates. We listed the integral kernels in Eq. (10), $\sum_{Q, Q'} \langle P|Q\rangle \langle Q|V(\vec{r}_{13})|Q'\rangle \langle Q'|P'\rangle$, for the lowest $\bar{p}D$ states in the approximation that the deuteron core is assumed in the S-state, as follows:

$$|P\rangle = |P'\rangle = |^2S_{1/2}\rangle: \quad \frac{3}{4} V_{\bar{N}N}^1(^1S_0) + \frac{1}{4} V_{\bar{N}N}^1(^3S_1),$$

$$|P\rangle = |P'\rangle = |^4S_{3/2}\rangle: \quad V_{\bar{N}N}^1(^3S_1),$$

$$|P\rangle = |P'\rangle = |^2P_{1/2}\rangle:$$

$$F_1^2 \cdot \left[\frac{1}{12} V_{\bar{N}N}^1(^3P_0) + \frac{3}{4} V_{\bar{N}N}^1(^1P_1) + \frac{1}{6} V_{\bar{N}N}^1(^3P_1) \right],$$

$$|P\rangle = |P'\rangle = |^4P_{1/2}\rangle: \quad F_1^2 \cdot \left[\frac{2}{3} V_{\bar{N}N}^1(^3P_0) + \frac{1}{3} V_{\bar{N}N}^1(^3P_1) \right],$$

$$|P\rangle = |P'\rangle = |^2P_{3/2}\rangle:$$

$$F_1^2 \cdot \left[\frac{3}{4} V_{\bar{N}N}^1(^1P_1) + \frac{1}{24} V_{\bar{N}N}^1(^3P_1) + \frac{5}{24} V_{\bar{N}N}^1(^3P_2) \right],$$

$$|P\rangle = |P'\rangle = |^4P_{3/2}\rangle: \quad F_1^2 \cdot \left[\frac{5}{6} V_{\bar{N}N}^1(^3P_1) + \frac{1}{6} V_{\bar{N}N}^1(^3P_2) \right],$$

Table 1

The energy shifts ΔE and decay widths of the $1s$ and $2p$ antiproton–deuteron atomic states in the approximation of undistorted deuteron core. The minus sign of the energy shifts means that the strong interaction is repulsive. The units are eV and meV for $1s$ and $2p$ states, respectively

	Paris98		DR2		KW		Data	
	ΔE	Γ	ΔE	Γ	ΔE	Γ	ΔE	Γ
$^2S_{1/2}$	–2445	1781	–2673	2380	–2478	2450		
$^4SD_{3/2}$	–2680	2822	–2668	2390	–2503	2469		
$^2P_{1/2}$	–186	584	17	896	99	657		
$^4P_{1/2}$	265	402	47	846	101	785		
$^2P_{3/2}$	–128	515	14	897	98	643		
$^4PF_{3/2}$	282	477	21	887	97	648		
$^4PF_{5/2}$	244	814	21	877	101	660		
$\Delta\bar{E}_{1s}, \bar{\Gamma}_{1s}$	–2602	2475	–2670	2387	–2494	2463	–1050 ± 250 [1]	1100 ± 750 [1]
								2270 ± 260 [2]
$\Delta\bar{E}_{2p}, \bar{\Gamma}_{2p}$	124	602	22	883	99	668	–243 ± 26 [2]	489 ± 30 [2]

$$\begin{aligned}
|P\rangle = |P'\rangle &= |^4P_{5/2}\rangle: F_1^2 \cdot V_{\bar{N}N}(^3P_2), \\
|P\rangle = |P'\rangle &= |^4D_{3/2}\rangle: F_3^2 \cdot \left[\frac{1}{2}V_{\bar{N}N}(^3D_1) + \frac{1}{2}V_{\bar{N}N}(^3D_2) \right], \\
|P\rangle = |P'\rangle &= |^2F_{3/2}\rangle: F_2^2 \cdot V_{\bar{N}N}(^3F_2), \\
|P\rangle = |P'\rangle &= |^4F_{5/2}\rangle: F_2^2 \cdot \left[\frac{4}{9}V_{\bar{N}N}(^3F_2) + \frac{5}{9}V_{\bar{N}N}(^3F_3) \right], \\
|P\rangle = |^4P_{3/2}\rangle, |P'\rangle &= |^4F_{3/2}\rangle: F_1F_2 \cdot \frac{1}{\sqrt{6}}V_{\bar{N}N}(^3PF_2), \\
|P\rangle = |^4P_{5/2}\rangle, |P'\rangle &= |^4F_{5/2}\rangle: F_1F_2 \cdot \frac{2}{3}V_{\bar{N}N}(^3PF_2), \\
|P\rangle = |^4S_{3/2}\rangle, |P'\rangle &= |^4D_{3/2}\rangle: \\
F_3 \cdot \left[\frac{1}{\sqrt{2}}V_{\bar{N}N}(^3SD_1) + \frac{1}{\sqrt{2}}V_{\bar{N}N}(^3SD_2) \right] & \quad (16)
\end{aligned}$$

where $|P\rangle \equiv |JMLS\rangle$ and $|P'\rangle \equiv |JML'S\rangle$ are the $\bar{p}D$ atomic states. Both the $\bar{p}D$ and $\bar{N}N$ states in Eq. (16) are labelled as $^{2S+1}L_J$ with S , L and J being respectively the total spin, total orbital angular momentum and total angular momentum. The potentials $V_{\bar{N}N}$, being functions of $r_{13} = \sqrt{\lambda^2 + \rho^2/4} - \rho\lambda x$, stand for the $\bar{N}N$ interactions for various $\bar{N}N$ states as indicated in the brackets.

The F_1 , F_2 and F_3 in Eq. (16) are functions of only λ and ρ , taking the forms

$$F_1 = \begin{cases} 1 - \frac{1}{12} \frac{\rho^2}{\lambda^2}, & \rho < 2\lambda, \\ \frac{4\lambda}{3\rho}, & \rho > 2\lambda, \end{cases} \quad (17)$$

$$F_2 = \begin{cases} (1 - \frac{\rho^2}{4\lambda^2})^2, & \rho < 2\lambda, \\ 0, & \rho > 2\lambda, \end{cases} \quad (18)$$

$$F_3 = \begin{cases} 2F^1(1, -\frac{3}{2}, \frac{3}{2}, \frac{\rho^2}{4\lambda^2}), & \rho < 2\lambda, \\ \frac{5}{8} - \frac{3\rho^2}{32\lambda^2} + \text{Arctanh}(\frac{2\lambda}{\rho})[\frac{3\lambda}{4\rho} - \frac{3\rho}{8\lambda} + \frac{3\rho^3}{64\lambda^3}], & \rho > 2\lambda, \end{cases} \quad (19)$$

where ${}_2F^1(\alpha, \beta, \gamma, x)$ is the hypergeometric function and $\text{Arctanh}(x)$ the inverses hyperbolic tangent function.

3. Energy shifts and decay widths of $\bar{p}D$ atoms

It is not a simple problem to accurately evaluate the energy shifts and decay widths, especially wave functions of exotic atoms like protonium, pionium and antiproton–deuteron atoms, which are mainly bound by the Coulomb force, but also effected by the short range strong interaction. In this work we study the $\bar{p}D$ atoms in the Sturmian function approach which has been successfully applied to our previous works [14,15]. Employed for the $\bar{N}N$ interactions are various realistic $\bar{N}N$ potentials, namely, the Paris $\bar{N}N$ potentials of the 1994 version (Paris84), 1998 version (Paris98) and 2004 version (Paris04), the Dover–Richard $\bar{N}N$ potentials I (DR1) and II (DR2), and the Kohno–Weise $\bar{N}N$ potential (KW). In this preliminary work, we just limit our study to the approximation of undistorted deuteron core. However, one may see that the main conclusions of the work are free of this approximation.

Shown in Table 1 are the energy shifts and decay widths, which stem from the Paris98, DR2 and KW $\bar{N}N$ interactions, in the approximation of undistorted deuteron core. The theoretical results for other interactions like Paris84, Paris04 and DR1 are quite similar to the ones listed in Table 1. The wave function of the undistorted deuteron core is evaluated in the Bonn OBEPQ potential [16]. It is found that the theoretical results for the $1s$ $\bar{p}D$ atomic states are more or less the same by all the employed $\bar{N}N$ potentials. The predicted energy shifts are roughly as twice large as the experimental data. However, one may expect that the predictions of the potentials in question could be improved to some extent by solving the $\bar{p}D$ dynamical equation in Eq. (7) without any approximation. A better treatment of the deuteron core will yield lower $1s$ $\bar{p}D$ atomic states, hence smaller energy shifts. The theoretical results for the decay widths of the $1s$ $\bar{p}D$ atoms are also larger than the experimental data though not as far from the data as for the energy shifts. The predictions for the decay widths are also expected to be improved by treating the deuteron core more properly.

The theoretical predictions for the energy shifts of the $2p$ $\bar{p}D$ atomic states are totally out of line for all the $\bar{N}N$ potentials employed. The experimental data show that the averaged energy level of the $2p$ $\bar{p}D$ atoms is pushed up by the strong

interaction, the same as for the $1s \bar{p}D$ atoms, but the theoretical results uniquely show the averaged energy level shifting down. It is unlikely to improve, by treating the deuteron core more accurately, the theoretical predictions of the $\bar{N}N$ potentials in question for the $2p \bar{p}D$ energy shifts since a more accurate treatment of the deuteron core will lead to deeper $2p \bar{p}D$ atomic states.

All the $\bar{N}N$ potentials employed in the work reproduce $\bar{N}N$ scattering data reasonably, but badly fail to reproduce the energy shifts of the $2p \bar{p}D$ atoms. The investigation of the $\bar{p}D$ atoms may provide a good platform for refining the $\bar{N}N$ interaction, especially at zero energy since the energy shifts of the $2p \bar{p}D$ atomic states are very sensitive to the $\bar{N}N$ strong interactions.

The research here is just a preliminary work, where a frozen, S-state deuteron is employed. The work may be improved at two steps, considering that the numerical evaluation is time-consuming. One may, at the first step, solve the $\bar{p}D$ dynamical equation in Eq. (7) by expanding the $\bar{p}D$ wave function in a bi-wave basis of the Sturmian functions, where a realistic nucleon–nucleon potential is employed but the deuteron core is assumed to be at the S-state. Such an evaluation is still manageable at a personnel computer but it may take a week or longer. We may compare the results of the improved work with the results here to figure out how important an unfrozen deuteron core is.

One may also consider, at the second step, to solve the $\bar{p}D$ dynamical equation in Eq. (7) by expanding the $\bar{p}D$ wave function in a bi-wave basis of the Sturmian functions without any approximation, where realistic nucleon–nucleon and nucleon–antinucleon potentials are employed and the deuteron core is

allowed to be at both the S- and D-waves. It is certain that the numerical calculation will take longer time but, anyway, we will do it after we complete the first-step improvement.

Acknowledgements

This work is supported in part by the National Research Council of Thailand through Suranaree University of Technology and the Commission on Higher Education, Thailand (CHERES-RG Theoretical Physics).

References

- [1] M. Augsburg, et al., Phys. Lett. B 461 (1999) 417.
- [2] D. Gotta, et al., Nucl. Phys. A 660 (1999) 283.
- [3] S. Wycech, A.M. Green, J.A. Niskanen, Phys. Lett. B 152 (1985) 308.
- [4] G.P. Latta, P.C. Tandy, Phys. Rev. C 42 (1990) R1207.
- [5] G.Q. Liu, J.-M. Richard, S. Wycech, Phys. Lett. B 2602 (1991) 15.
- [6] V.A. Karmanov, K.V. Protasov, A.Yu. Voronin, Eur. Phys. J. A 8 (2000) 429.
- [7] M. Pignone, M. Lacombe, B. Loiseau, R. Vinh Mau, Phys. Rev. C 50 (1994) 2710.
- [8] B. El-Bennich, M. Lacombe, B. Loiseau, R. Vinh Mau, Phys. Rev. C 59 (1998) 2313.
- [9] S. Wycech, B. Loiseau, AIP Conf. Proc. 796 (2005) 131.
- [10] C.B. Dover, J.M. Richard, Phys. Rev. C 21 (1980) 1466.
- [11] J.M. Richard, M.E. Sainio, Phys. Lett. B 110 (1982) 349.
- [12] M. Kohno, W. Weise, Nucl. Phys. A 454 (1986) 429.
- [13] M. Rotenberg, Adv. At. Mol. Phys. 6 (1970) 233.
- [14] Y. Yan, R. Tegen, T. Gutsche, A. Faessler, Phys. Rev. C 56 (1997) 1596.
- [15] P. Suebka, Y. Yan, Phys. Rev. C 70 (2004) 034006.
- [16] R. Machleidt, K. Holinde, Ch. Elster, Phys. Rep. 149 (1987) 1.

ACCURATE EVALUATION OF WAVE FUNCTIONS OF PIONIUM AND KAONIUM

Y. YAN*, C. NUALCHIMPLEE, P. SUEBKA, C. KOBDAJ and K. KHOSONTHOGKEE

*School of Physics, Suranaree University of Technology,
111 University Avenue, Nakhon Ratchasima 30000, Thailand*

**yupeng@sut.ac.th*

Pionium and kaonium are studied in an accurate numerical approach based on Sturmian functions. It is found that the ground-state wave functions of the exotic atoms in realistic strong interactions, particularly for kaonium, are considerably different from the hydrogen-like ones at small distances. The kaon-kaon scattering length derived from the $1s$ energy shift of kaonium by applying the Deser-Trueman formula is strongly inconsistent with the one derived directly by solving the Schrödinger equation. The theoretical results indicate that it is arguable to treat kaonium perturbatively.

Keywords: Pionium; kaonium; Sturmian functions; low energy strong interaction.

PACS Nos.: 36.10.-k, 13.75.Lb

1. Introduction

Hadronic exotic atoms are bound mainly by the Coulomb force, but the strong interaction also plays a role, leading to an energy shift from the pure Coulomb energy and distorting the hydrogen-like wave function at short distance (a few fm). Pionium and kaonium are among the simplest hadronic exotic atoms since they couple to only few other channels. Pionium decays into only the $\pi^0\pi^0$ pair via the strong interaction while kaonium decays to the $\pi\pi$ and $\eta\pi$ channels. One may link, after a simple calculation in the quantum field theory, the decay branching ratio of pionium and kaonium to the corresponding scattering amplitude. For pionium decaying to the $\pi^0\pi^0$ pair, for example, we have

$$\Gamma = \frac{64\pi}{M^3 p} \left| \int \frac{d\vec{k}}{(2\pi)^3} \psi_{1s}(\vec{k}) f_0(k, p) \right|^2 \quad (1)$$

where M is the mass of the exotic atom, p is the momentum of the final π_0 , f_0 is the S-wave scattering amplitude of the process $\pi^+\pi^- \rightarrow \pi^0\pi^0$ at zero energy, and $\psi_{1s}(\vec{k})$ is the $1s$ wave function of pionium in momentum space and normalized according to $\int \frac{d\vec{k}}{(2\pi)^3} |\psi_{1s}(\vec{k})|^2 = 1$. In the approximation that the scattering amplitude $f_0(k, p)$

is estimated by its on-shell form $f_0(0, p)$, one derives

$$\Gamma = \frac{64\pi}{M^3} p |\psi_{1s}(0)|^2 |f(0, p)|^2 \quad (2)$$

where $\psi_{1s}(0)$ is the $1s$ pionium wave function at the origin. The above equation is just the widely referred Trueman formula.¹

It is clear that the wave function of hadronic exotic atoms plays a crucial role in linking the life time of the atoms to the scattering lengths of the corresponding systems. For pionium, its wave function might be reasonably approximated by the hydrogen-like one since the pion-pion strong interaction is believed to be relatively weak, compared to other hadron-hadron interactions. But for kaonium, it could be another story since the kaon-kaon strong interaction can be strong enough to support deep bound states. It is arguable that the wave function of kaonium can be well approximated by the hydrogen-like one.

The evaluation of wave functions of exotic atoms has been a challenge to numerical methods. Required is an approach, which is able to account accurately for both the strong short-range interaction and the long-range Coulomb force. The numerical approach based on Sturmian functions has been found effective and accurate. In this work we use the numerical method which has been carefully studied and discussed in the work² to study pionium and kaonium. The paper is arranged as follows: Pionium and kaonium are studied in Section 2 and 3, respectively. Discussion and conclusions are given in Section 4.

2. Pionium

Pionium is mainly a Coulomb bound state of π^+ and π^- , coupled strongly with $\pi^0\pi^0$ due to the strong interaction at small distance. The strong interaction between the two pions leads to an energy shift from the Coulomb energy ($E = -1.86$ keV) and a distortion to the hydrogen-like wave function at short distance (a few fm). Pionium decays predominantly into $\pi^0\pi^0$ via strong interaction, which probes the low energy interactions of the pions, especially at zero-energy.

Among all hadronic exotic atoms, pionium is the simplest and has been studied the best up to now. The DIRAC experiment at CERN has been commissioned since 1998 to measure the pionium lifetime and the first results have been published recently based on part of the collected data. The result of the pionium lifetime is $\tau_{1S} = 2.91_{-0.62}^{+0.49} \times 10^{-15}$ seconds.³ In the theoretical sector, pionium has been studied extensively in various models. As expected, the results of the chiral perturbation theory is in line with the experimental data.

In the approximation of the pionium wave function ψ_{1s} in Eq. (2) to the hydrogen-like wave function, one derives the chiral perturbation result at leading order

$$\Gamma = \frac{2}{9} \alpha^3 p |a_0 - a_2|^2 \quad (3)$$

where α is the fine structure constant, and a_0 and a_2 are respectively the isospin $I = 0$ and $I = 2$ S-wave scattering lengths of the pion-pion reaction. The chiral perturbation theory has a NLO prediction for the pionium lifetime,

$$\Gamma = \frac{2}{9}\alpha^3 p |a_0 - a_2|^2 (1 + \delta), \quad (4)$$

with $\delta = 0.058 \pm 0.012$.⁴ Inserting into Eq. (4) $|a_0 - a_2| = 0.265 \pm 0.004$, the $O(p^6)$ result of the chiral perturbation theory,⁵ one gets the pionium lifetime $\tau = (2.9 \pm 0.1) \cdot 10^{-15}$ s.

That the chiral perturbation theory reproduces the pionium lifetime data perfectly implies that a pion-pion strong interaction applicable to the pion-pion dynamics equation in the quantum mechanism regime must give a pionium wave function which differs not much from the hydrogen-like one. In another word, the pion-pion strong interaction is rather weak, compared with strong interactions for other hadronic systems, for example, the $\overline{N}N$ system.

As mentioned in the works,^{6,7} the evaluation of pionium wave functions is not an easy task. It is more difficult than other exotic problems, for example, the protonium problem since the Bohr radius of pionium is much larger than the one of protonium. Employed here is a numerical approach based on Sturmian functions.⁸ The numerical method is much more powerful, accurate and much easier to use than all other methods applied to exotic atom problems in the quantum mechanism regime in history. For the details of the numerical method and the accuracy in the hadronic exotic atom problem, we refer to the works.^{2,8,9}

In this work we have no intention to study various versions of pion-pion strong interactions, but instead just to demonstrate the problem with one of the simplest forms of pion-pion strong interactions. The investigation of pionium with various pion-pion strong interaction models, in both local and nonlocal forms, may be found in the work.¹⁰ Employed here for the purpose of demonstration is the pion-pion strong interaction which has been widely employed for calculating of the electromagnetic corrections in low energy pion-nucleon scattering and for studying the influence of the hadronic interaction on pionium wave functions.⁶ The potential is independent of both the energy of the pionium system and pion masses, and reproduce very well the phase shifts given by two-loop chiral perturbation theory.

Shown in Fig. 1 as the solid line is the $1s$ radial wave function for the $\pi^+\pi^-$ component of the pionium in the pion-pion strong interaction taken from the works.⁶ In the calculation we have employed the non-relativistic Schrödinger equation for the $(\pi^+\pi^-, \pi^0\pi^0)$ system where the mass difference has been considered between the $\pi^+\pi^-$ pair and the $\pi^0\pi^0$ pair. It is found that the difference is not much between the full pionium wave function (solid line) and the hydrogen-like one (dashed line). The energy shift is derived as $\Delta E_{1s} = 3.04$ eV, indicating that the energy level is pulled down by the strong interaction, compared to the pure Coulomb interaction. The lifetime of the pionium is estimated in the potential model to be 3.15×10^{-15} and 2.35×10^{-15} seconds, where the hydrogen-like and full pionium wave functions

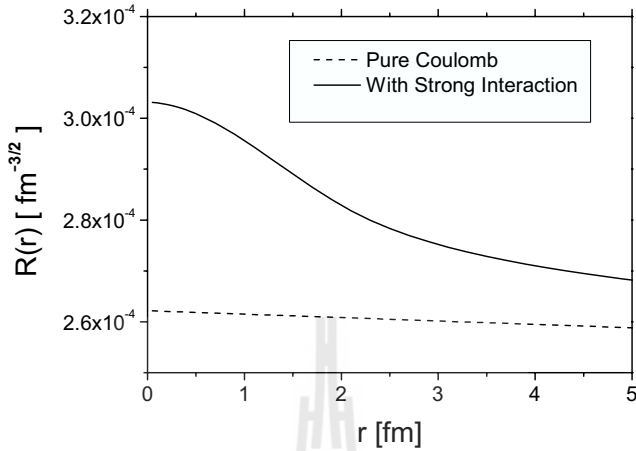


Fig. 1. $\pi^+\pi^-$ component of full and pure-Coulomb $1s$ radial pionium wave functions.

are applied to Eq. (3), respectively. The theoretical results of the pionium lifetime shows the importance of the pionium wave function in potential models or quantum mechanics regime. It is believed that the application of Eq. (1) with the full pionium wave function and full scattering amplitude in the pion-pion interaction⁶ will lead to a pionium lifetime close to the DIRAC data.

3. Kaonium

Kaonium is the hadronic atom of K^+ and K^- mixed with the $\overline{K^0}K^0$ component at small distance. It is bound mainly by the Coulomb force, but affected by the strong interaction at small distance. The kaonium can not decay into a $K^0\overline{K^0}$ pair due to the kinetic reason, but may decay into $\pi\pi$ and $\eta\pi$ via strong interaction. Unlike the pionium, there are few works^{12–15} on this exotic atom.

We study the kaonium first in the K^-K^+ interaction taken from the work.¹⁴ The interaction is derived under the assumption that K^+K^- forms quasi-bound states in $I = 0$ and $I = 1$, which correspond to $f_0(980)$ and $a_0(980)$, respectively. Since the interaction gives two molecular states $f_0(980)$ and $a_0(980)$, it must be much stronger than the pion-pion strong interaction. Shown in Fig. 2 (left panel) are both the real and imaginary parts of the K^-K^+ component of the kaonium in the interaction¹⁴ (Model A). It is found that the K^+K^- real part of the kaonium wave function differs considerably from the hydrogen-like one at small distance, and also has a node at $r \approx 1.5$ fm since there exist deep bound states. At small distance the imaginary part of the pionium wave function is not negligible.

Recently there has been a work studying kaonium in the strong interaction generated by vector meson exchange within the framework of the standard $SU(3)_V \otimes SU(3)_A$ invariant effective Lagrangian.¹⁵ Since the imaginary part of the interaction is in the δ -function form which is not suitable for quantum mechanics

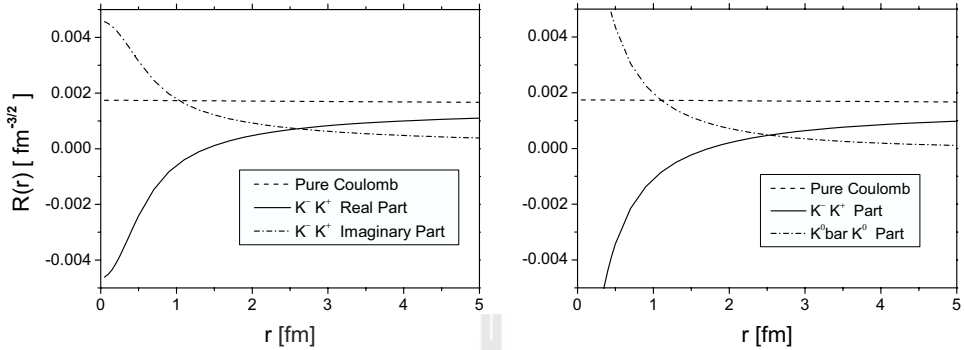


Fig. 2. 1s radial wave functions of kaonium in Model A (left panel) and Model B (right panel).

calculations, we apply only the real part of the interaction to evaluate the kaonium wave function. Shown in Fig. 2 (right panel) are the derived kaonium wave functions, with the K^+K^- component largely different from the hydrogen-like one and having a node at $r \approx 1.5$ fm and the K^0K^0 part also rather large.

To see further how safe it is to approximate the kaonium wave function to the hydrogen-like one, we compare the scattering length evaluated directly by solving the Schrödinger equation with the one derived from the kaonium energy shifts by applying the Deser-Trueman formula,^{1,11}

$$-\Delta E_{1s} + i \frac{\Gamma_{1s}}{2} = 2\alpha^3 \mu^2 f_0^{K^+K^-}(0) \quad (5)$$

where μ is the reduced mass of the K^-K^+ pair, ΔE_{1s} and Γ_{1s} are respectively the energy shift and decay width of the 1s kaonium state due to strong interaction, and $f_0^{K^+K^-}(0)$ is the S-wave K^-K^+ scattering amplitude at zero energy.

Shown in Table 1 are the energy shifts (the second column) evaluated with only the real part of the interactions in both Model A and B, the scattering lengths (the third column) derived from the energy shifts listed in the second column by applying the Deser-Trueman formula, and the scattering lengths (the fourth column) derived directly^{14,15} by solving the Schrödinger equation. The negative energy shifts in Table 1 mean that the 1s energy level is pushed up by the strong interactions. It is found that in the same interaction the scattering length derived directly by solving the Schrödinger equation is considerably different from the one derived from the 1s energy shift of the kaonium by applying the Deser-Trueman formula.

Table 1. 1s kaonium energy shifts and kaon-kaon scattering lengths in unit of M_K^{-1} .

	$\Delta E_{1s}(eV)$	$a^{K^+K^-}(M_K^{-1})$	$a^{K^+K^-}(M_K^{-1})$
Model A	-548	5.7	7.8
Model B	-354	3.69	2.72

4. Discussion and Conclusions

Pionium and kaonium are studied in an accurate numerical approach based on Sturmian functions. It is found that the ground-state wave functions of the exotic atoms in realistic strong interactions, particularly for the kaonium, are considerably different from the hydrogen-like ones at small distances. The kaon-kaon scattering length derived from the $1s$ kaonium energy shift by applying the Deser-Trueman formula is strongly inconsistent with the one derived directly by solving the Schrödinger equation. The theoretical results indicate that it might not be safe to treat the kaonium perturbatively.

Acknowledgments

This work is supported in part by the Commission on Higher Education, Thailand (CHE-RES-RG Theoretical Physics).

References

1. T. L. Trueman, Nucl. Phys. **26**, 57 (1961).
2. Y. Yan, R. Tegen, T. Gutsche and A. Faessler, Phys. Rev. C **56**, 596 (1997).
3. B. Adeva, *et al.* [DIRAC Collaboration], Phys. Lett. B **619**, 50 (2005).
4. J. Gasser, V. E. Lyubovitskij, A. Rusetsky and A. Gall, Phys. Rev. D **64**, 016008 (2001).
5. G. Colangelo, J. Gasser and H. Leutwyler, Nucl. Phys. B **603**, 125 (2001).
6. A. Gashi, G. Rasche and W.S. Woolcock, Phys. Lett. B **513**, 269 (2001).
7. I. Amirkhanov, I. Puzynin, A. Tarasov, O. Voskresenskaya and O. Zeinalova, Phys. Lett. B **452**, 155 (1999).
8. M. Rotenberg, Adv. At. Mol. Phys. **6**, 233 (1970).
9. P. Suebka, Y. Yan, Phys. Rev. C **70**, 034006 (2004)
10. Y. Yan, P. Suebka, C. Kobdaj, K. Khosonthongkee, Nucl. Phys. A **790**, 402c, (2007).
11. S. Deser, M. L. Goldberger, K. Baumann and W. Thirring, Phys. Rev. **96**, 774 (1954).
12. S. Wycech, and A.M. Green, Nucl. Phys. A **562**, 446 (1993).
13. S.V. Bashinsky, and B.O. Kerbikov, Phys. At. Nucl. **59**, 1979 (1996).
14. D. Jido, Y. Kanada-En'yo, arXiv:0806.3601 [nucl-th]; Private Communications.
15. S. Krewald, R. H. Lemmer, and F. P. Sassen, Phys. Rev. D **69**, 016003 (2004).

Accurate evaluation of the $1s$ wave functions of kaonic hydrogen

C. Nualchimplee · P. Suebka · Y. Yan · Amand Faessler

Published online: 27 August 2009
© Springer Science + Business Media B.V. 2009

Abstract Kaonic hydrogen is studied with realistic potentials in an accurate numerical approach based on Sturmian functions. It is found that the ground-state wave function of the exotic atom with realistic strong interactions is considerably different from the hydrogen-like ones at small distances. The K^-p scattering length extracted from the $1s$ energy shift of the kaonic hydrogen by applying the Deser-Trueman formula is severely inconsistent with the one derived directly by solving the Schrödinger equation. We pay special attention to the recent measurement of the energy shift and decay width of the $1s$ kaonic hydrogen state by the DEAR Collaboration. Our work strongly supports the argument that the DEAR data of the K^-p scattering length extracted with the Deser-Trueman formula from the measured $1s$ energy shift and decay width are not accurate, if not to say, unreliable.

Keywords Kaonic hydrogen · Pionium · Sturmian functions

PACS 36.10.-k · 13.75.Lb

C. Nualchimplee (✉) · P. Suebka · Y. Yan
School of Physics, Institute of Science, Suranaree University of Technology,
111 University Avenue, Nakhon Ratchasima 30000, Thailand
e-mail: nchakrit@hotmail.com

Y. Yan
e-mail: yupeng@sut.ac.th

A. Faessler
Institute for Theoretical Physics, Tübingen University,
Auf der Morgenstelle 4, 72076 Tübingen, Germany
e-mail: amand.faessler@uni-tuebingen.de

1 Introduction

Kaonic hydrogen is mainly the Coulomb bound state of a K^- and a proton but is affected by the strong interaction at small distances. Furthermore, the strong interaction couples the K^-p state to the \bar{K}^0n , $\pi\Sigma$, $\pi\Lambda$, $\eta\Sigma$ and $\eta\Lambda$ channels and results in the $\pi\Sigma$ and $\pi\Lambda$ decaying modes. It is believed that the study of kaonic hydrogen effectively probes the low-energy, especially zero energy strong kaon-nucleon interaction. Inspired by the recent precise determination of the energy and decay width by the DEAR Collaboration [1, 2], kaonic hydrogen has been extensively studied in the theoretical sector, mainly in effective field theory [3–7].

One may link, after a simple calculation in quantum field theory, the decay branching ratios of kaonic hydrogen to the $\pi\Sigma$ and $\pi\Lambda$ channels to the corresponding scattering amplitudes. In the rest frame of kaonic hydrogen, one has the decay branching ratios defined as

$$\Gamma = \frac{64\pi}{M^3} p \left| \int \frac{d\mathbf{k}}{(2\pi)^3} \psi_{1s}(\mathbf{k}) f_0(k, p) \right|^2, \quad (1)$$

where M is the mass of the kaonic hydrogen atom, p is the relative momentum of the final state particles, f_0 is the S-wave scattering amplitude of the processes $K^-p \rightarrow \pi\Sigma$ and $K^-p \rightarrow \pi\Lambda$ at zero energy, and $\psi_{1s}(\mathbf{k})$ is the $1s$ wave function of kaonic hydrogen in momentum space and normalized according to $\int \frac{d\mathbf{k}}{(2\pi)^3} |\psi_{1s}(\mathbf{k})|^2 = 1$. In the approximation that the scattering amplitude $f_0(k, p)$ is estimated by its on-shell form $f_0(0, p)$, one derives

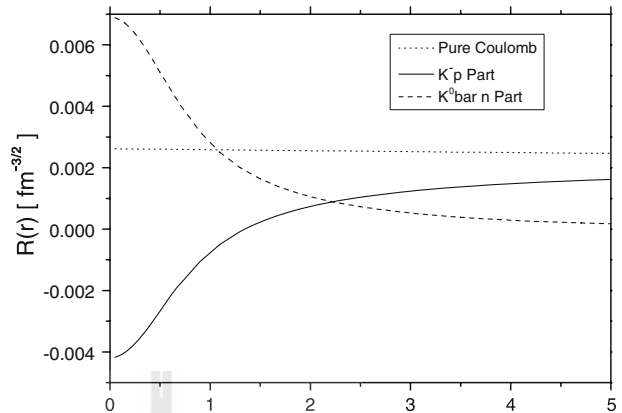
$$\Gamma = \frac{64\pi}{M^3} p |\psi_{1s}(0)|^2 |f(0, p)|^2, \quad (2)$$

where $\psi_{1s}(0)$ is the $1s$ kaonic hydrogen wave function at the origin. The above equation is widely referred as the Trueman formula [8].

It is clear that the wave function of kaonic hydrogen plays a crucial role in linking the lifetime or decay branching ratios of the atom to the scattering lengths of the corresponding system. For pionium its wave function might be reasonably approximated by the hydrogen-like one since the strong pion-pion interaction is believed to be relatively weak, compared to other hadron-hadron interactions. But for kaonic hydrogen it could be another story since the strong kaon-nucleon interaction can possibly support at least one deep bound state, the $\Lambda(1405)$ near threshold. In this case it is arguable that the wave function of kaonic hydrogen can be well approximated by the hydrogen-like one.

The evaluation of wave functions of exotic atoms has been a challenge to numerical methods [9, 10]. An approach is required, which is able to account accurately for both the strong short-range interaction and the long-range Coulomb force. The numerical approach based on Sturmian functions [11] has been found effective and accurate. In this work we use the numerical method which has been carefully studied and discussed in [11–14] to further study kaonic hydrogen. The paper is arranged as follows: kaonic hydrogen is studied with realistic potentials in Section 2. The discussion and conclusions are given in Section 3.

Fig. 1 1s radial wave functions of kaonic hydrogen with the interaction of [15]. The pure-Coulomb kaonic hydrogen wave function is plotted as a dotted curve



2 Kaonic hydrogen with realistic interactions

We study kaonic hydrogen first with the interaction taken from the work [15]. The interaction is constructed by fitting the free $\bar{K}N$ scattering data [16], the KpX data of kaonic hydrogen by the KEK Collaboration [17] and the binding energy and decay width of $\Lambda(1405)$, which is regarded as an isospin $I = 0$ bound state of $\bar{K}N$. Since the interaction gives one molecular state $\Lambda(1405)$, it must be much stronger than the strong pion-pion interaction.

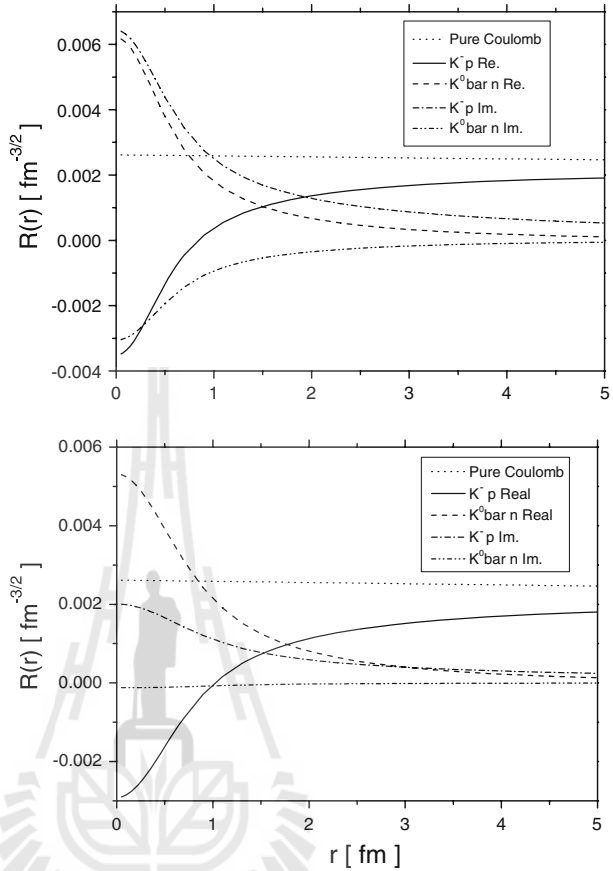
Shown in Fig. 1 are both the K^-p and \bar{K}^0n components of the kaonic hydrogen with the interaction [15]. It is found that the K^-p part of the kaonic hydrogen wave function differs considerably from the hydrogen-like one at small distances, and also has a node at $r \approx 1.5$ fm because there exists one deep bound state. Also at small distances the \bar{K}^0n part of the kaonic hydrogen wave function is not negligible.

Based on the coupled-channel interaction [15], equivalent single-channel $\bar{K}N$ potentials are derived with imaginary parts in energy-independent forms [18]. With this single-channel interaction, the kaonic hydrogen is investigated in the present work. In Fig. 2 (lower panel) we plot the various components of the kaonic hydrogen wave function with the complex $\bar{K}N$ potentials [18]. One finds again that the K^-p component differs considerably from the hydrogen-like kaonic hydrogen wave function at small distances and, again, the \bar{K}^0n component is not negligible.

The kaonic hydrogen is also studied in various versions of effective local potential [19], which is constructed such as to reproduce the full scattering amplitude of the chiral SU(3) coupled-channel framework. It is found that the different versions of the potential [19] give quite similar results. The wave functions derived with the effective potentials [19] are also similar to the one derived with the interaction of Ref. [18]. As an example, in Fig. 2 (upper panel), we plot the various components of the kaonic hydrogen wave function evaluated with the equivalent local HN_{JH} potential of [19]. In summary, the kaonic hydrogen wave function derived with the interactions of [15, 18, 19] has a main feature that the K^-p component is largely different from the hydrogen-like one and has a node in the region from 1 to 2 fm, and the \bar{K}^0n component is also rather large at small distances.

To further see how safe it is to approximate the kaonic wave function to the hydrogen-like one, we compare the scattering length evaluated directly by solving

Fig. 2 1s radial wave functions of kaonic hydrogen: *Upper panel* with the HNJJH potential of [19] and *left panel* with the interaction [18]. The pure-Coulomb kaonic hydrogen wave function is plotted as a *dotted curve*



the Schrödinger equation with the one extracted from the kaonic energy shifts by applying the Deser-Trueman formula [8, 20]:

$$\Delta E_{1s} + i \frac{\Gamma_{1s}}{2} = 2\alpha^3 \mu^2 a_{K^-p}. \tag{3}$$

In the above expression μ is the reduced mass of the K^-p system, ΔE_{1s} and Γ_{1s} are the energy shift and decay width of the 1s kaonic hydrogen due to the strong interaction, and a_{K^-p} stands for the S-wave K^-p scattering length.

The theoretical results are shown in the first and second rows of Table 1 for the single-channel $\bar{K}N$ potential [18] and the equivalent local HNJJH potential of [19], respectively. The K^-p scattering lengths a_{K^-p} in the first and second rows of Table 1 are taken from the works [18, 19] where the isospin symmetry limited is applied. For consistence, we have also evaluated the energy shift ΔE_{1s} and decay width Γ of the 1s kaonic hydrogen in the isospin symmetry limit where the mass of proton is applied for both the proton and neutron and the mass of K^- for both the K^- and \bar{K}^0 . The negative energy shifts in Table 1 mean that the 1s energy level is pushed up by the strong interaction since there exists one deep bound state, the $\Lambda(1405)$. Listed in the last column of Table 1 are the K^-p scattering length (\tilde{a}_{K^-p}) which are extracted

Table 1 ΔE_{1s} and Γ evaluated in the work with the strong interactions from [18] (first row) and [19] (second row) and taken from [1, 2] (third row)

ΔE_{1s} [eV]	$\Gamma_{1s}/2$ [eV]	a_{K^-p} [fm]	\tilde{a}_{K^-p} [fm]
-268	173	$-0.678 + 0.506i$	$-0.650 + 0.420i$
-248	292	$-0.608 + 0.835i$	$-0.602 + 0.709i$
-194 ± 40	125 ± 56	$-0.78 \pm 0.15 + i(0.49 \pm 0.28)$	$-0.468 \pm 0.090 + i(0.302 \pm 0.135)$

a_{K^-p} taken from [18] (first row), [19] (second row) and [16] (third row). \tilde{a}_{K^-p} extracted from the energy shifts and decay widths in Column 1 and 2 by applying the Deser-Trueman formula of (3)

from the energy shifts and decay widths in Column 1 and 2 by applying the Deser-Trueman formula of (3). For comparison, experimental data [1, 2, 16] are shown in the third row of Table 1, with the energy shift and decay width determined by the DEAR experiment [1, 2] and the K^-p scattering length a_{K^-p} by Martin [16]. The scattering length \tilde{a}_{K^-p} in the third row is extracted by the DEAR Collaboration [1, 2] from the measured energy shift and decay width of kaonic hydrogen by applying the Deser-Trueman formula of (3).

It is clear that with the same interaction [18, 19] the scattering length derived directly by solving the Schrödinger equation is rather different from the one extracted from the $1s$ energy shift of kaonic hydrogen by applying the Deser-Trueman formula. From Table 1 one finds that the error for the imaginary part of the extracted scattering lengths is almost 20%, compared to the directly-derived scattering lengths with the interactions of [18, 19].

3 Discussion and conclusions

Kaonic hydrogen is studied with various versions of realistic interaction potentials, which are directly evaluated in the framework of a Schrödinger equation involving in addition the Coulomb interaction. The ground-state wave function of kaonic hydrogen, derived for various $\bar{K}N$ interactions, is shown to be largely different from the hydrogen-like one at small distances. The K^-p scattering length extracted from the $1s$ energy shift of kaonic hydrogen by applying the Deser-Trueman formula is strongly inconsistent with the one derived directly by solving the Schrödinger equation. Our work strongly supports the argument [6, 7] that the DEAR data of the K^-p scattering length, which are extracted with a Deser-Trueman formula from the measured $1s$ energy shift and decay width, are not accurate.

Acknowledgements This work is supported in part by the Commission on Higher Education, Thailand (CHE-RES-RG Theoretical Physics) and the International Graduiertenkolleg GRK683 of the Deutsche Forschungsgemeinschaft (DFG), Germany. Y. Y would like to thank Prof. Th. Gutsche (Institute for Theoretical Physics, Tübingen University) for fruitful discussions.

References

1. Beer, G., et al. [DEAR Collaboration]: Measurement of the kaonic hydrogen x-ray spectrum. Phys. Rev. Lett. **94**, 212302 (2005)
2. Gargnelli, M., et al. [DEAR Collaboration]: Kaonic hydrogen measurement with DEAR at DAΦNE. Int. J. Mod. Phys. A **20**, 341–348 (2005)

3. Meißner, U.-G., Raha, U., Rusetsky, A.: Spectrum and decays of kaonic hydrogen. *Eur. Phys. J. C* **35**, 349–357 (2004)
4. Ivanov, A.N., Cargnelli, M., Faber, M., Marton, J., Troitskaya, N.I., Zmeskal, J.: On kaonic hydrogen. Quantum field theoretic and relativistic covariant approach. *Eur. Phys. J. A* **21**, 11–28 (2004)
5. Borasoy, B., Nißler, R., Weise, W.: Kaonic hydrogen and k-p scattering. *Phys. Rev. Lett.* **94**, 213401 (2005)
6. Oller, J.A., Prades, J., Verbeni, M.: Surprises in threshold antikaon-nucleon physics. *Phys. Rev. Lett.* **95**, 172502 (2005)
7. Borasoy, B., Meißner, U.-G., Nißler, R.: K-p scattering length from scattering experiments. *Phys. Rev. C* **74**, 055201 (2006)
8. Trueman, T.L.: Energy level shifts in atomic states of strongly-interacting particles. *Nucl. Phys.* **26**, 57–67 (1961)
9. Gashi, A., Rasche, G., Woolcock, W.S.: The influence of the hadronic interaction on the pionium wave functions. *Phys. Lett. B* **513**, 269–272 (2001)
10. Amirkhanov, I., Puzynin, I., Tarasov, A., Voskresenskaya, O., Zeinalova, O.: The influence of strong interaction on the pionium wave functions at small distances. *Phys. Lett. B* **452**, 155–158 (1999)
11. Rotenberg, M.: Theory and application of Sturmian functions. *Adv. At. Mol. Phys.* **6**, 233–268 (1970)
12. Yan, Y., Tegen, R., Gutsche, T., Faessler, A.: Sturmian function approach and $\bar{N}N$ bound states. *Phys. Rev. C* **56**, 1596–1604 (1997)
13. Suebka, P., Yan, Y.: Accurate evaluation of pionium wave functions. *Phys. Rev. C* **70**, 034006 (2004)
14. Yan, Y., Suebka, P., Kobdaj, C., Khosonthongkee, K.: Strong interactions in pionium. *Nucl. Phys. A* **790**, 402c–405c (2007)
15. Akaishi, Y., Yamazaki, T.: Nuclear \bar{K} bound states in light nuclei. *Phys. Rev. C* **65**, 044005 (2002)
16. Martin, A.D.: Kaon-nucleon parameters. *Nucl. Phys. B* **179**, 33–48 (1981)
17. Iwasaki, M., et al. [KEK Collaboration]: Observation of kaonic hydrogen $K_{\alpha}X$ rays. *Phys. Rev. Lett.* **78**, 3067–3069 (1997)
18. Yamazaki, T., Akaishi, Y.: The basic K nuclear cluster $K^{-}pp$ and its enhanced formation in the $p + p \rightarrow K^{+} + X$ reaction. [arXiv:0709.0630](https://arxiv.org/abs/0709.0630) [nucl-th]
19. Hyodo, T., Weise, W.: Effective $\bar{K}N$ interaction based on chiral SU(3) dynamics. *Phys. Rev. C* **77**, 035204 (2008)
20. Deser, S., Goldberger, M.L., Baumann, K., Thirring, W.: Energy level displacements in pi-mesonic atoms. *Phys. Rev.* **96**, 774–776 (1954)

Kaonic hydrogen atoms with realistic potentials

Y. Yan,^{1,2,*} W. Poonsawat,^{1,2} K. Khosonthongkee,^{1,2} C. Kobdaj,^{1,2} and P. Suebka^{1,2}

¹*School of Physics, Institute of Science, Suranaree University of Technology, Nakhon Ratchasima, Thailand*

²*Center of Excellence in Physics, Ministry of Education, Bangkok, Thailand*

(Received 2 June 2009; revised manuscript received 25 November 2009; published 23 June 2010)

Kaonic hydrogen is studied with various realistic potentials in an accurate numerical approach based on Sturmian functions. It is found that the mass difference between the K^-p and \bar{K}^0n channels has a considerable effect on theoretical results of the energy shift and decay width of kaonic hydrogen. On average, the theoretical result in the isospin symmetry limit is smaller by a factor of about 20% than the full result where the mass difference between the K^-p and \bar{K}^0n channels is properly treated. The theoretical results based on realistic local potentials, which reproduce well scattering data, are inconsistent with the recent measurement of the energy shift and decay width of the $1s$ kaonic hydrogen state by the DEAR Collaboration.

DOI: [10.1103/PhysRevC.81.065208](https://doi.org/10.1103/PhysRevC.81.065208)

PACS number(s): 36.10.Gv, 13.75.Jz

Kaonic hydrogen is mainly the Coulomb bound state of a K^- and a proton, but is affected by the strong interaction at small distances. The strong interaction couples the K^-p state to the \bar{K}^0n , $\pi\Sigma$, $\pi\Lambda$, $\eta\Sigma$, and $\eta\Lambda$ channels and results in the $\pi\Sigma$ and $\pi\Lambda$ decaying modes. It is believed that the study of kaonic hydrogen effectively probes the low-energy, and especially zero-energy, strong kaon-nucleon interaction. Inspired by the recent precise determination of the energy and decay width by the DEAR Collaboration [1], kaonic hydrogen has been extensively studied in the theoretical sector, mainly in effective field theory [2–10].

The success of the effective field theory applied to kaonic hydrogen makes it possible to construct equivalent local $\bar{K}N$ potentials, which may be conveniently applied to computations of K -nuclear few-body systems and hyper-nucleus productions [11]. The solution of the Schrödinger or Lippmann-Schwinger equation with such an equivalent potential should approximate as closely as possible the scattering amplitude derived from the full coupled-channel calculation of the effective field theory.

In this work, we study kaonic hydrogen with local potentials, which are purely phenomenological or based on chiral SU(3) models. The $1s$ kaonic hydrogen energy shift and decay width are derived by solving the dynamical equation

$$\left[-\frac{1}{r^2} \frac{d}{dr} \left(r^2 \frac{d}{dr} \right) + \frac{l(l+1)}{r^2} - \mathbf{Q}^2 + \mathbf{fV} \right] \mathbf{R}(r), \quad (1)$$

with

$$\mathbf{Q}^2 = \begin{pmatrix} q_c^2 & 0 \\ 0 & q_0^2 \end{pmatrix}, \quad \mathbf{f} = \begin{pmatrix} f_c & 0 \\ 0 & f_0 \end{pmatrix}, \quad (2)$$

$$\mathbf{V} = \mathbf{V}^{\text{em}} + \mathbf{V}^h, \quad (3)$$

$$\mathbf{V}^{\text{em}} = \begin{pmatrix} V^{\text{em}} & 0 \\ 0 & 0 \end{pmatrix}, \quad (4)$$

$$\mathbf{V}^h = \begin{pmatrix} \frac{1}{2}(V_1^h + V_0^h) & \frac{1}{2}(V_1^h - V_0^h) \\ \frac{1}{2}(V_1^h - V_0^h) & \frac{1}{2}(V_1^h + V_0^h) \end{pmatrix}, \quad (5)$$

$$\mathbf{R}(r) = \begin{pmatrix} R_{K^-p}(r) \\ R_{\bar{K}^0n}(r) \end{pmatrix}, \quad (6)$$

$$q_c^2 = \frac{[E^2 - (M_p - M_{K^-})^2][E^2 - (M_p + M_{K^-})^2]}{4E^2}, \quad (7)$$

$$q_0^2 = \frac{[E^2 - (M_n - M_{\bar{K}^0})^2][E^2 - (M_n + M_{\bar{K}^0})^2]}{4E^2}, \quad (8)$$

$$f_c = \frac{E^2 - M_p^2 - M_{K^-}^2}{E}, \quad (9)$$

$$f_0 = \frac{E^2 - M_n^2 - M_{\bar{K}^0}^2}{E}, \quad (10)$$

where V^{em} is the electromagnetic potential, V_0^h and V_1^h are respectively the isospin $I = 0$ and 1 strong interactions of the $\bar{K}N$ system, and $R_{K^-p}(r)$ and $R_{\bar{K}^0n}(r)$ are respectively the K^-p and \bar{K}^0n components of the radial wave function of the $\bar{K}N$ system. Equation (1) embeds into the Schrödinger equation the relativistic effect and the mass difference between the K^-p and \bar{K}^0n components. The relativistic modification of the Schrödinger equation to Eq. (1) has been discussed in Refs. [12–17].

The local potentials considered herein are the phenomenological $\bar{K}N$ potential taken from Refs. [18,19] and the various effective potentials which are worked out in Ref. [20]. The interaction [18,19] is constructed by fitting the free $\bar{K}N$ scattering data [21], the KpX data of kaonic hydrogen by the KEK Collaboration [22] and the binding energy and decay width of $\Lambda(1405)$, which is regarded as an isospin $I = 0$ bound state of $\bar{K}N$.

In Ref. [20], an effective local potential in coordinate space is constructed such as the solution of the Schrödinger or Lippmann-Schwinger equation with such a potential approximates as closely as possible the scattering amplitude derived from the full chiral coupled-channel calculation. Four versions of effective potentials referred to as ORB, HNJH, BNW, BMN have been constructed in Ref. [20], based respectively on the chiral SU(3) models [3,4,8,10].

The accurate evaluation of energy shifts, decay widths, and especially wave functions of exotic atoms has been a challenge to numerical methods [16,23]. An approach is required which is able to account accurately for both the strong short-range

* yupeng@sut.ac.th

TABLE I. $1s$ kaonic hydrogen energy shift ΔE_{1s} (ΔE_{1s}^0) and decay width Γ_{1s} (Γ_{1s}^0) derived by directly solving Eq. (1) with (without) the mass difference between the K^-p and \bar{K}^0n states considered.

	ΔE_{1s}^0 [eV]	Γ_{1s}^0 [eV]	ΔE_{1s} [eV]	Γ_{1s} [eV]
AY [19]	-268	312	-384	288
ORB [20]	-255	534	-348	646
HNJH [20]	-248	527	-336	648
BNW [20]	-220	544	-288	674
BMN [20]	-197	517	-297	622

interaction and the long-range Coulomb force. The numerical approach based on Sturmian functions [24] has been found effective and accurate. In this work, we use the numerical method which has been carefully studied and discussed in Refs. [24–26] to study kaonic hydrogen.

The $1s$ kaonic hydrogen energy shift ΔE_{1s} and decay width Γ_{1s} shown in Table I are derived by solving Eq. (1) in the above-mentioned Sturmian function approach [24–26], with the mass difference between the K^-p and \bar{K}^0n channels treated as shown in Eqs. (1) to (10). The negative energy shift in Table I means that the $1s$ energy level is effectively pushed up by the strong interaction since there exists one deep bound state, the $\Lambda(1405)$. Shown in Table I are also the energy shift ΔE_{1s}^0 and decay width Γ_{1s}^0 in the isospin symmetry limit, where the mass of proton is applied for both the proton and neutron and the mass of K^- for both the K^- and \bar{K}^0 .

It is found from Table I that the theoretical results in the approximation of the isospin symmetry limit are rather different from the full results where the mass difference between the K^-p and \bar{K}^0n channels is properly treated, as shown in Eqs. (1) to (10). Except for the decay width for the phenomenological $\bar{K}N$ potential [18,19], the isospin symmetry approximation largely underestimates both the energy shift and decay width of the $1s$ kaonic hydrogen. On average, the theoretical result for the energy shift in the isospin symmetry limit is smaller by a factor of about 28% than the full result. For the equivalent local potentials referred to as ORB, HNJH, BNW, BMN in Table I, which are constructed in Ref. [20], based respectively on the chiral SU(3) models [3,4,8,10], the isospin symmetry approximation for the decay width of the $1s$ kaonic hydrogen is about 18% smaller than the result where the mass difference between the K^-p and \bar{K}^0n channels is considered.

The most recent experimental values on the energy shift and decay width of the ground state of kaonic hydrogen are, respectively,

$$\Delta E_{1s} = -193 \pm 37 \text{ (stat)} \pm 6 \text{ (syst)} \text{ eV} \quad (11)$$

and

$$\Gamma_{1s} = 249 \pm 111 \text{ (stat)} \pm 30 \text{ (syst)} \text{ eV} \quad (12)$$

obtained by the DEAR Collaboration [1]. These values are smaller by a factor of almost 2 than the experimental values measured by the KEK Collaboration [22], which are,

TABLE II. K^-p scattering lengths a_{K^-p} derived with local single-channel potentials [19,20] compared with the K^-p scattering lengths \tilde{a}_{K^-p} (taken from Refs. [18,20]) derived with the multichannel effective interactions [3,4,8,10,18].

	a_{K^-p} [fm]	\tilde{a}_{K^-p} [fm]
AY [19]	$-0.678 + i0.506$	$-0.70 + i0.53$
ORB [3]	$-0.586 + i0.844$	$-0.617 + i0.861$
HNJH [4]	$-0.566 + i0.829$	$-0.608 + i0.835$
BNW [8]	$-0.487 + i0.838$	$-0.532 + i0.833$
BMN [10]	$-0.426 + i0.788$	$-0.410 + i0.824$

respectively,

$$\Delta E_{1s} = -323 \pm 63 \text{ (stat)} \pm 11 \text{ (syst)} \text{ eV} \quad (13)$$

and

$$\Gamma_{1s} = 407 \pm 208 \text{ (stat)} \pm 100 \text{ (syst)} \text{ eV}. \quad (14)$$

It is clear that except for the decay width derived with the phenomenological $\bar{K}N$ potential referred to as AY in Table I, all other theoretical values are much larger than the DEAR data. However, the theoretical results shown in Table I for both the pure phenomenological potential and the chiral SU(3) symmetry-based potentials are fairly consistent with the KEK measurements, considering the large error of the KEK values of the $1s$ kaonic hydrogen decay width.

It is difficult to conclude whether the equivalent potentials based on chiral SU(3) models are reasonable since the KEK and DEAR data are so inconsistent with each other. One may have to wait for the more accurate measurement of the $1s$ kaonic hydrogen by the SIDDHARTA Collaboration.

One may argue that the theoretical results of the $1s$ kaonic hydrogen energy shifts and decay widths derived in the work with the local, equivalent single-channel potentials may not reflect well the original equivalent interactions. To clear this issue, we compare the K^-p scattering lengths derived with the effective multichannel interactions [3,4,8,10,18] with the ones evaluated with the local single-channel potentials [19,20] using

$$a_{K^-p} = \frac{1}{2}(a_{I=0} + a_{I=1}) \quad (15)$$

in the isospin-symmetry limit, where the mass of proton is applied for both the proton and neutron and the mass of K^- for both the K^- and \bar{K}^0 . Shown in Table II are the K^-p scattering lengths a_{K^-p} derived with the local single-channel potentials [19,20], which are employed here in this work to evaluate the energy shifts and decay widths of the $1s$ kaonic hydrogen and the K^-p scattering lengths \tilde{a}_{K^-p} derived with the multichannel effective interactions [3,4,8,10,18]. It is found that the average discrepancy between a_{K^-p} and \tilde{a}_{K^-p} is less than 5%, much smaller than the effect resulted from the mass difference between the K^-p and \bar{K}^0n channels. One may conclude that the local single-channel potentials [19,20] applied to the KN system well approximate the original multichannel effective interactions.

ACKNOWLEDGMENTS

The author would like to thank Th. Gutsche (Institute for Theoretical Physics, Tübingen University), M. Lutz (GSI)

and T. Hyodo (Department of Physics, Tokyo Institute of Technology) for fruitful discussions. This work is supported

in part by the Commission on Higher Education, Thailand (CHE-RES-RG Theoretical Physics).

-
- [1] G. Beer *et al.* (DEAR Collaboration), *Phys. Rev. Lett.* **94**, 212302 (2005); M. Gargnelli *et al.* (DEAR Collaboration), *Int. J. Mod. Phys. A* **20**, 341 (2005).
- [2] J. A. Oller and U.-G. Meißner, *Phys. Lett. B* **500**, 263 (2001).
- [3] E. Oset, A. Ramos, and C. Bennhold, *Phys. Lett. B* **527**, 99 (2002).
- [4] T. Hyodo, S. I. Nam, D. Jido, and A. Hosaka, *Phys. Rev. C* **68**, 018201 (2003).
- [5] U. -G. Meißner, U. Raha, and A. Rusetsky, *Eur. Phys. J. C* **35**, 349 (2004); **41**, 213 (2005); **47**, 473 (2006).
- [6] A. N. Ivanov, M. Cargnelli, M. Faber, J. Marton, N. I. Troitskaya, and J. Zmeskal, *Eur. Phys. J. A* **21**, 11 (2004).
- [7] A. N. Ivanov, M. Cargnelli, M. Faber, H. Fuhrmann, V. A. Ivanova, J. Marton, N. I. Troitskaya, and J. Zmeskal, *Eur. Phys. J. A* **25**, 329 (2005).
- [8] B. Borasoy, R. Nißler, and W. Weise, *Phys. Rev. Lett.* **94**, 213401 (2005); *Eur. Phys. J. A* **25**, 79 (2005).
- [9] J. A. Oller, J. Prades, and M. Verbeni, *Phys. Rev. Lett.* **95**, 172502 (2005).
- [10] B. Borasoy, U.-G. Meißner, and R. Nißler, *Phys. Rev. C* **74**, 055201 (2006).
- [11] A. Limphirat, C. Kobdaj, M. Bleicher, Y. Yan, and H. Stoecker, *J. Phys. G: Nucl. Part. Phys.* **36**, 064049 (2009).
- [12] P. R. Auvil, *Phys. Rev. D* **4**, 240 (1971).
- [13] B. C. Pearce and B. K. Jennings, *Nucl. Phys. A* **528**, 655 (1991).
- [14] W. R. Gibbs, Li Ai, and W. B. Kaufmann, *Phys. Rev. C* **57**, 784 (1998).
- [15] A. Gashi, E. Matsinos, G. C. Oades, G. Rasche, and W. S. Woolcock, *Nucl. Phys. A* **686**, 463 (2001).
- [16] A. Gashi, G. Rasche, and W. S. Woolcock, *Phys. Lett. B* **513**, 269 (2001).
- [17] A. Gashi, G. C. Oades, G. Rasche, and W. S. Woolcock, *Nucl. Phys. A* **699**, 732 (2002).
- [18] Y. Akaishi and T. Yamazaki, *Phys. Rev. C* **65**, 044005 (2002).
- [19] T. Yamazaki and Y. Akaishi, *Phys. Rev. C* **76**, 045201 (2007).
- [20] T. Hyodo and W. Weise, *Phys. Rev. C* **77**, 035204 (2008).
- [21] A. D. Martin, *Nucl. Phys. B* **179**, 33 (1981).
- [22] M. Iwasaki *et al.* (KEK Collaboration), *Phys. Rev. Lett.* **78**, 3067 (1997).
- [23] I. Amirkhanov, I. Puzynin, A. Tarasov, O. Voskresenskaya, and O. Zeinalova, *Phys. Lett. B* **452**, 155 (1999).
- [24] M. Rotenberg, *Adv. At. Mol. Phys.* **6**, 233 (1970).
- [25] Y. Yan, R. Tegen, T. Gutsche, and A. Faessler, *Phys. Rev. C* **56**, 1596 (1997).
- [26] P. Suebka and Y. Yan, *Phys. Rev. C* **70**, 034006 (2004).

